

Functional gradients in the human lateral prefrontal cortex revealed by a comprehensive coordinate-based meta-analysis

Majd Abdallah^{1,2,*}, Gaston Zanitti^{1,2}, Valentin Iovene^{1,2}, and Demian Wassermann^{1,2,*}

¹Team Parietal, Inria, CEA, Université Paris-Saclay, Palaiseau, 91120, France

²NeuroSpin, CEA, Université Paris-Saclay, Gif-sur-Yvette, 91190, France

*Corresponding authors

January 20, 2022

Abstract

The human lateral prefrontal cortex (LPFC) enables flexible goal-directed behavior. Yet, its organizing principles remain actively debated despite decades of research. Meta-analysis efforts to map the LPFC have either been restricted in scope or suffered from limited expressivity in meta-analysis tools. The latter shortcoming hinders the complexity of questions that can be expressed in a meta-analysis and hence limits the specificity of structure-function associations. Here, we adopt NeuroLang, a novel approach to meta-analysis based on first-order probabilistic logic programming, to infer the organizing principles of the LPFC with greater specificity from 14,371 neuroimaging publications. Our results reveal a rostrocaudal and a dorsoventral gradient, respectively explaining the most and second-most variance in whole-brain meta-analytic connectivity in the LPFC. Moreover, we find a cross-study agreement on a spectrum of increasing abstraction from caudal to rostral LPFC both in specific network connectivity and structure-function associations that supports a domain-general role for the mid-LPFC. Furthermore, meta-analyzing inter-hemispheric asymmetries along the rostrocaudal gradient reveals specific associations with topics of language, memory, response inhibition, and error processing. Overall, we provide a comprehensive mapping of the organizing principles of task-dependent activity in the LPFC, grounding future hypothesis generation on a quantitative overview of past findings.

Keywords— Lateral prefrontal cortex, rostrocaudal gradient, meta-analysis, probabilistic logic programming, neuroinformatics

1 Introduction

2 The human lateral prefrontal cortex (LPFC) supports a wide variety of cognitive processes
3 that are considered hallmark features of the human brain [1, 2]. Understanding the functional
4 organization of the LPFC is thus important to the study of adaptive human behavior. Yet, the
5 overarching organizing principle of the LPFC is still actively debated, with a variety of proposals
6 on whether it is unitary, hierarchical, or houses a set of separable networks subserving distinct
7 functions [3, 4, 5, 6, 7, 8]. There have been a few large-scale attempts to map the entire LPFC,
8 but these mappings often lack specificity, partly due to the limited breadth of queries that
9 common meta-analysis methods can express. In this study, we adopt a novel approach to meta-
10 analysis based on symbolic artificial intelligence to infer the organizing principles of the LPFC
11 from thousands of neuroimaging studies with greater expressivity and specificity.

12 The versatility of the LPFC suggests that it is far from unitary [5, 6, 9, 10, 11]. An
13 influential class of hypotheses emerging from the domain of abstraction and hierarchical control
14 proposes a rostrocaudal gradient in the LPFC, wherein caudal regions respond to immediate
15 sensory stimuli, middle regions select actions based upon a prevailing context, and rostral regions
16 integrate concrete representations into more abstract rules and goals to enable temporal control
17 of behavior [1, 2, 3, 6, 11, 12, 13, 14, 15, 16]. A second class of hypotheses holds that a
18 dorsoventral gradient segregating regions involved in distinct stimulus domains, such as spatial
19 vs. non-spatial, also governs the distribution of functions in the LPFC [2, 17, 18]. Further results
20 reveal that the ventral, dorsal, and middle LPFC are each organized along their rostrocaudal
21 axes according to the level of abstraction in task representations [2, 19, 20].

22 Contemporary evidence from systems neuroscience proposes that the LPFC is spanned by
23 distinct functional networks, such as the attention, default mode, and most importantly the
24 salience (SN) and frontoparietal control (FPCN) networks [10, 21, 22, 23, 24]. These networks
25 are globally situated upon a brain-wide intrinsic connectivity gradient, wherein the transmodal
26 regions of the default mode network are maximally distant from sensorimotor unimodal regions
27 [25, 26], with multimodal regions of the SN and FPCN occupying intermediate zones. One
28 proposal holds that this spatial principle ascribes the LPFC with a role in integrating both con-
29 crete and abstract representations, suggesting an external/present-oriented to internal/future-
30 oriented gradient extending outwardly from the motor cortex towards the anterior of the brain
31 [8]. However, recent studies that rely on causal evidence argue against a linear unidimen-
32 sional gradient in the LPFC, and rather support the hypothesis of separable networks dy-
33 namically interacting within global and local hierarchies to support adaptive human behavior
34 [6, 7, 9, 10, 27, 28] (also see [29] for a comprehensive review). Within this systems-based frame-
35 work, the middle LPFC not the rostral LPFC is believed to act as a focal point, integrating
36 concrete and abstract representations from disparate networks, with increasingly rostral and
37 caudal LPFC regions acting in a domain-specific manner [8, 28, 29].

38 Further, inter-hemispheric functional asymmetries in the LPFC are widely reported, most
39 notably for language [22, 30] and inhibitory control processes [31, 32]. Functional asymmetries
40 between hemispheres are believed to arise from dynamic patterns of inter- and intra-hemispheric
41 connectivity that represent organizing principles of functional specializations whose putative
42 function is to promote efficient control of behavior [33, 34]. Thus, mapping the LPFC should
43 take into account differences across hemispheres, especially in the distribution of lateralized
44 topic associations. While there is a preponderance of research on the organization of the left
45 LPFC in the fields of hierarchical control and language [8], a comprehensive comparison is yet to
46 draw firm conclusions regarding the specific functional associations of both LPFC hemispheres.

47 The multitude of proposals on the LPFC may arise from the diversity of protocols and
48 researcher’s degrees-of-freedom in individual studies whose idiosyncrasies (task type, timing,
49 magnitude of stimuli/responses, data analysis methods, and publication bias) can limit general-
50 izeability [35, 36]. And besides concerns of small sample sizes [37], each individual study probes

1 a narrow scope of the broad range of functions that putatively engage the LPFC, which poses
2 the risk of interpreting the results based on a small set of task contrasts. Therefore, it remains
3 unclear to what extent the functional boundaries derived from each individual study correspond
4 to the global organization of activity observed in the LPFC during a wider variety of behaviors.
5 Ultimately, a quantitative meta-analysis is needed to make inferences on the global organization
6 of the LPFC. Unlike individual studies, meta-analysis offers an overarching perspective on task-
7 dependent activity and maps a wide range of mental functions onto the LPFC by synthesizing
8 thousands of published findings into a single statistical framework [38, 39, 40].

9 The few existing meta-analyses on the LPFC, although informative, have been limited in
10 scope, assumptions, and most importantly, tools. These limitations preclude a reliable distinc-
11 tion of closely related LPFC regions in terms of their relative specificity to networks and mental
12 functions. On one hand, due to the difficulty of manual compilation of activation peaks from the
13 literature, most meta-analyses on the LPFC have been restricted to particular regions [e.g. right
14 inferior frontal gyrus 33] or functions [e.g. working memory 41]. On the other hand, large-scale
15 automated meta-analyses [e.g. 9] have assumed that LPFC regions are clusters of piece-wise
16 constant coactivation, ignoring overlaps between them and not specifying an organizing spatial
17 schema of functional transitions from one region to another. Finally, commonly-used tools,
18 such as Neurosynth [40], are not expressive enough to represent complex hypotheses of specific
19 functional associations in the LPFC. For example, it is arguably difficult and arduous to query
20 a meta-analytic database on the probability that a topic is associated with a study given acti-
21 vation in one region and the simultaneous absence of activation in any spatially-anterior region
22 (similarly posterior, superior or homologous). The expressivity limitation becomes challenging
23 when performing a comprehensive meta-analysis with tens of topics at a time as well as regions
24 that are consistently coactivated by several tasks.

25 Here, we overcome these challenges using a recently-introduced query language, called Neu-
26 roLang [42] to perform a comprehensive coordinate-based meta-analysis on 14,371 articles from
27 the Neurosynth database [40], along with a gradient-mapping technique [26] to identify the
28 organizing principles of activity in the LPFC. NeuroLang puts forth first-order probabilistic
29 logic programming as a structured and more expressive formalism to represent neuroscience
30 hypotheses and solve complex queries on large databases [42]. For instance, we can succinctly
31 express queries of functional specificity in the likes of: “*What is the probability that empathy is*
32 *present given activation in the rostral LPFC and there does not exist any activation reported in*
33 *caudal or middle LPFC?*”. NeuroLang also brings the power of probabilistic reasoning to deal
34 with elements of uncertainty in heterogeneous data, such as in peak locations, between-regions
35 coactivation, and the presence of terms, all in a single unifying framework. Most importantly,
36 however, a meta-analysis performed using NeuroLang is highly reproducible, that is, the same
37 queries used by one study can be used by future studies to validate the results as more data
38 becomes available.

39 By leveraging the expressivity of NeuroLang to perform this meta-analysis, we identify a
40 principal rostrocaudal gradient and a subsidiary dorsoventral gradient that respectively ex-
41 plain the most and second-most variance in meta-analytic connectivity in the LPFC in both
42 hemispheres. Moreover, we find that the principal gradient captures a spectrum of increas-
43 ing abstraction in patterns of network connectivity and specific topic associations from caudal
44 to rostral LPFC, while supporting a proposed domain-general role for middle LPFC regions.
45 Finally, a gradient-based meta-analysis of inter-hemispheric asymmetries reveals the relative
46 dominance of language and memory in the left LPFC as well as the relative dominance of
47 inhibitory control and error processing in the right LPFC.

2 Results

2.1 Principal rostrocaudal and secondary dorsoventral gradients explain most of the variance in meta-analytic connectivity in the LPFC

In the first analysis, we infer the extent to which LPFC regions agree in the spatial distribution of meta-analytic connectivity patterns across thousands of studies found in the Neurosynth database. In other words, our goal is to identify the main profiles of variation (i.e. gradients) in whole-brain meta-analytic connectivity within the LPFC [25, 26].

Towards achieving this goal, we need to reduce the high-dimensionality of voxel-level data to increase interpretability of our findings and alleviate computational burdens. To do this, we project voxel-level data onto 1024 functional regions from the Dictionaries of Functional Modes (DiFuMo) probabilistic atlases covering the entire brain [43]. The DiFuMo is a set of continuously-valued brain atlases derived from thousands of subjects across 27 studies, including a total of 2192 task-based and resting-state functional magnetic resonance imaging (fMRI) sessions publicly available on OpenNeuro [44]. Unlike spatially-constrained clusters, a DiFuMo atlas does not ignore the overlap among neuronal populations, allowing voxels to be grouped into multiple functional regions with varying weights. To this end, we write NeuroLang logic program (Program available here) that infers the conditional probability of a brain region to be reported active given activation in a LPFC region, as well as the conditional probability that the brain region is active given no activation in the LPFC region. The program then computes the logarithm with base 10 of the odds ratio (LOR) of these two hypotheses for every LPFC-brain region pairs, creating a $N \times M$ meta-analytic connectivity matrix, where N denotes the number of regions in the LPFC and M the number of regions in the entire brain. The LOR captures the amount of evidence in favor of specific coactivation between each LPFC region and brain regions, as compared to the evidence favoring independent activation of each.

After constructing the coactivation matrix, we apply an unsupervised non-linear dimensionality reduction method known as diffusion embedding [26, 45] to the resultant meta-analytic connectivity matrix in each hemisphere, separately, using the BrainSpace toolbox [46]. The resultant low-dimensional embedding identifies the position of each LPFC region along unidimensional axes, known as gradients, each representing a direction of variation in meta-analytic connectivity. The axis that accounts for the greatest amount of variance in meta-analytic connectivity is called the principal gradient, which will be the focus of the next analyses. Technical details on formulating the NeuroLang logic program that infers the meta-analytic connectivity matrix along with details on diffusion embedding are found in the Materials and Methods section.

The results of this analysis are shown in Figure 1 and Figure 2. Figure 1A depicts the principal gradient of coactivation which explains the greatest percentage of variance in the meta-analytic connectivity in both LPFC hemispheres (see Figure 1C and Figure 1D). This gradient is anchored at one end by caudal LPFC regions and at the other end by rostral LPFC regions, supporting a dominant rostrocaudal organization in the LPFC across the literature. The spatial layout of the principal gradient is expressed in terms of the posterior-to-anterior and inferior-to-superior positions of regions distributed along successive twenty-percentile gradient segments (i.e. quintile bins; see Figure 2). On the other hand, Figure 1B shows the gradient that explains the second-most percentage of variance in connectivity, extending along the dorsoventral axis of the LPFC. This gradient is anchored at on end by ventral LPFC regions and at the other end by dorsal LPFC regions. Collectively, the topographic profiles of the first two gradients of meta-analytic connectivity support and integrate the views that the LPFC is organized along its rostrocaudal and dorsoventral axes. Although the topography of the proposed gradients has been previously described [e.g. 2, 6, 19], the relative extent to which they explain the

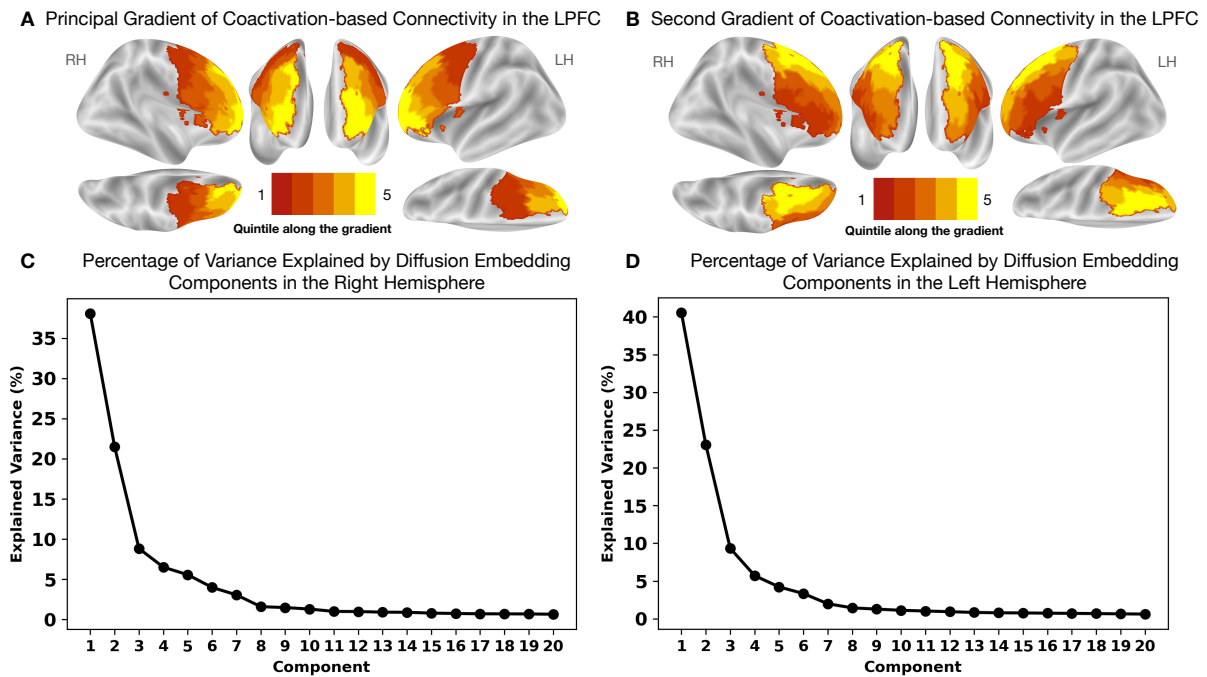


Figure 1: Principal rostrocaudal and secondary dorsoventral gradients explain the greatest amount of variance in meta-analytic connectivity in the LPFC. (A) The principal gradient in both hemispheres echoes a widely proposed rostrocaudal organization in the LPFC. This gradient represents the dominant direction of gradual variations in coactivation, and hence function, in the LPFC. **(B)** The gradient that explains the second-most variance in meta-analytic coactivation-based connectivity echoes a dorsoventral organization in the LPFC extending from ventrolateral to dorsolateral PFC regions. **(C)** and **(D)** The amount of variance explained by diffusion embedding components in the right and left LPFC, respectively.

1 distribution of activations in the LPFC across a wide variety of brain states have remained
 2 unclear. Thus, we contribute by revealing a dominant rostrocaudal gradient representing the
 3 overarching organizing principle of task-dependent activation in the LPFC in the literature.

4 **2.2 Varying coactivation patterns along the rostrocaudal gradient** 5 **capture a spectrum of increasing abstraction in large-scale net-** 6 **work connectivity**

7 In the second analysis, we characterize the rostrocaudal gradient in both LPFC hemispheres
 8 in terms of varying coactivation patterns of successive twenty-percentile gradient segments (i.e.
 9 quintile bins) and their overlap with canonical large-scale brain networks (Figure 3). For this
 10 purpose, we write a NeuroLang logic program (Program available here) that first performs a
 11 multilevel kernel density analysis [47] using a uniform kernel of 10 mm radius at the study level,
 12 and then projects the resulting binary activation maps (1 map per study) onto 1024 functional
 13 regions. This yields a mapping between brain regions and each study in the database, wherein
 14 each region has a probability of being reported by a study, which depends on the location of the
 15 reported voxels (further details are provided in Materials and Methods). However, this is not
 16 the case for quintile bins along the principal gradient, which are labels and not continuously
 17 valued regions. Therefore, we set the program to consider activation reported in a quintile bin
 18 if at least one peak is reported within it or within its near vicinity ($< 3mm$). Consequently,
 19 for each quintile bin along the principal gradient, the program infers the logarithmic ratio of

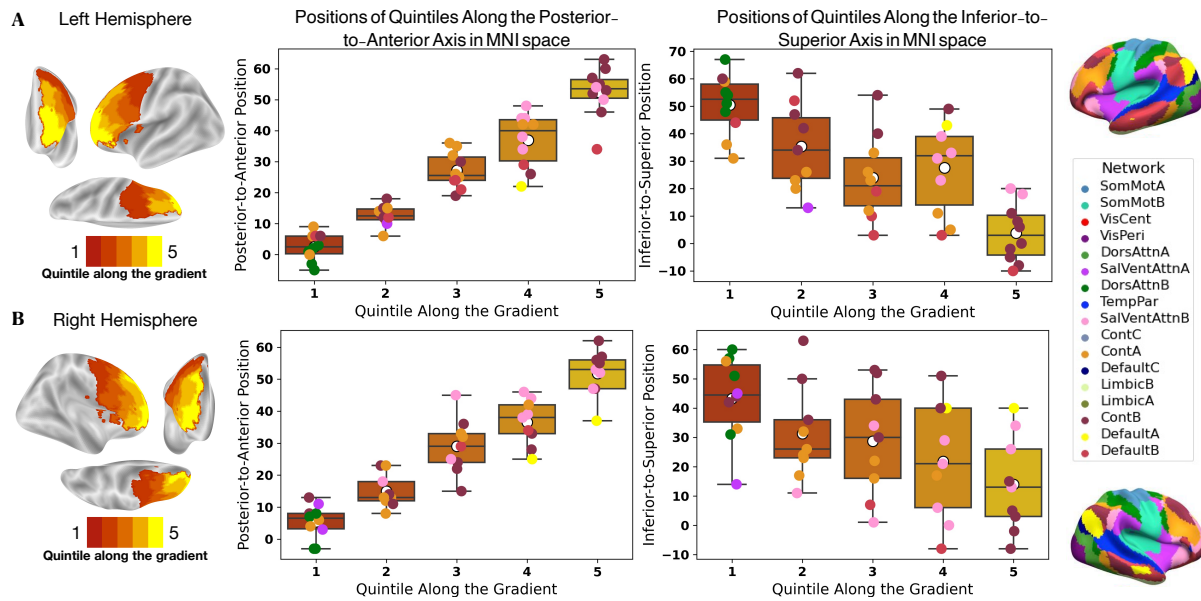


Figure 2: The posterior-to-anterior and inferior-to-superior positions in MNI space of regions grouped into quintile bins along the principal gradient reflect a rostro-caudal organization. (A) Positions of regions in the left hemisphere. (B) Positions of regions in the right hemisphere. Each colored sphere represents a region in the LPFC, with the color reflecting its network membership within the 17-Networks atlas shown at the left of the figure [24]. **SomMot**: Somatomotor, **VisCent/Peri**: Visual Central/Peripheral, **SalVentAttn**: Salience/Ventral Attention, **DorsAttn**: Dorsal Attention, **TempPar**: Temporo-parietal, **Cont**: Executive Control, **Default**: Default Mode

1 odds for a brain region to be reported active given activation in a quintile bin to the odds of
 2 the region activation given no bin activation. This ratio represents the amount of evidence for a
 3 specific coactivation between a brain region and a given quintile bin along the principal gradient
 4 of the LPFC.

5 The results of this analysis are shown in Figure 3. A cortical coactivation map is constructed
 6 by recovering regions that exhibit at least threefold the odds (or $LOR > 0.5$) of being reported
 7 active give activation is reported in a bin compared to being active given otherwise. The
 8 “Network Overlap” panel in Figure 3A and Figure 3B depicts the large-scale brain networks
 9 defined by the 17-Network parcellation [24] that overlap with each bin’s coactivation pattern.
 10 The relative proportion of overlap between the coactivation pattern and each network is reflected
 11 by the level of color transparency in the brain plot. Increasingly opaque colors indicate that
 12 more volume of the coactivation pattern overlaps with a given network, with the most opaque
 13 colors signifying predominant networks.

14 This analysis reveals a structured ordering of network connectivity profiles along the rostro-
 15 caudal LPFC gradient in both hemispheres, from a pattern mostly dominated by networks in-
 16 volved in external processing to a pattern dominated by networks involved in internally-oriented
 17 cognition. Almost all bins coactivate with the salience and frontoparietal control networks (i.e.
 18 SalVentAttnB, ContA and ContB) to varying degrees, with ContA mostly dominating the coac-
 19 tivation pattern of caudal-to-middle zones of the gradient. Moreover, while middle zones’ coac-
 20 tivation patterns mostly overlap with the salience and control networks, they also overlap with
 21 both externally and internally focused networks in a rostrocaudal fashion. That is, bin 2 in both
 22 hemispheres coactivates more with the dorsal attention networks, while bin 3 coactivates with
 23 the default mode network. This result may support contemporary accounts of domain-general

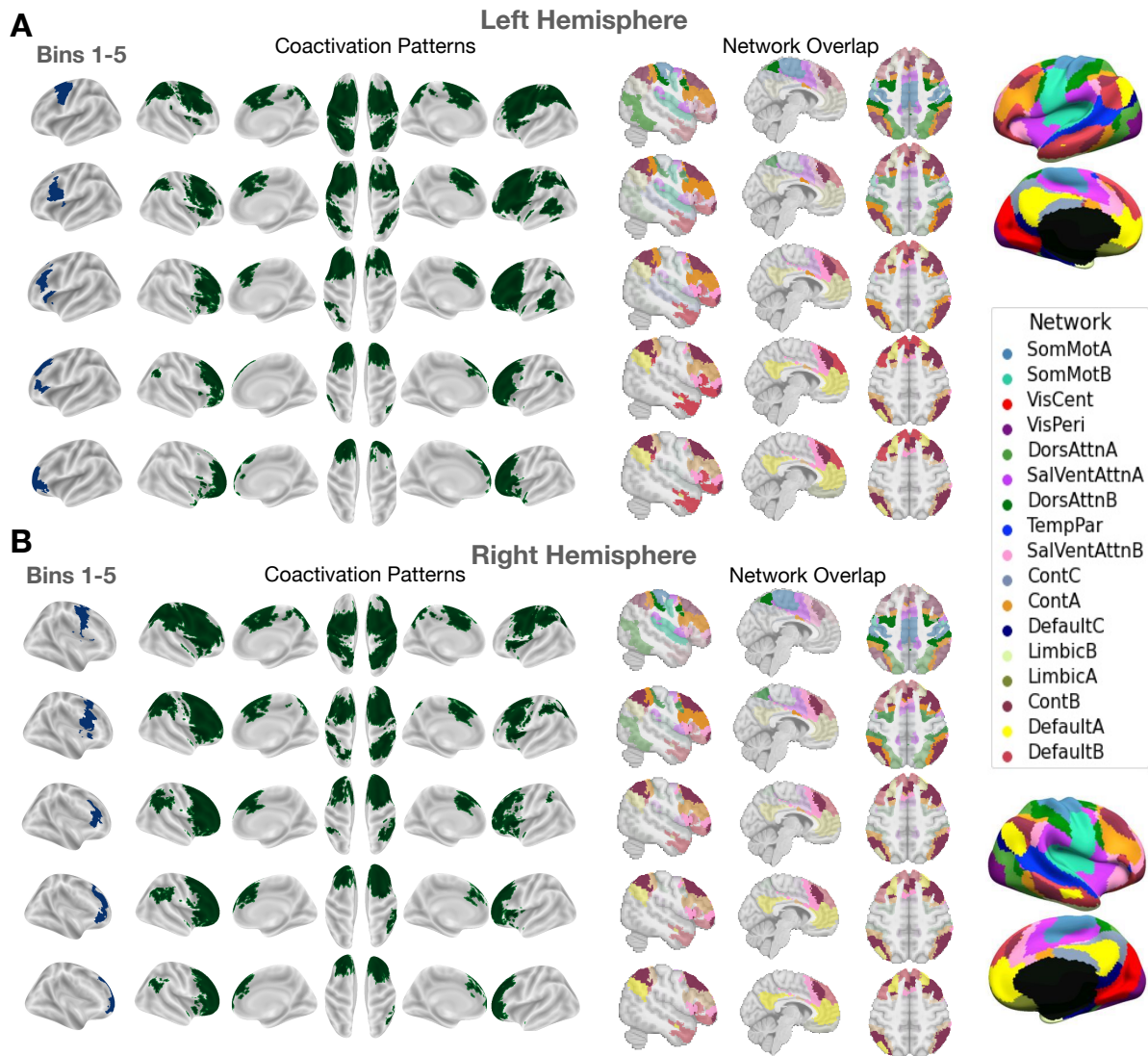


Figure 3: The meta-analytic coactivation patterns of quintile bins along the principal gradient in the LPFC capture a spatial layout of increasing abstraction in canonical network connectivity. (A) Coactivation patterns along the principal gradient in the left LPFC. (B) Coactivation patterns along the principal gradient in the right LPFC. Each coactivation map shows the regions that have a least three times the odds of being reported active given activation reported in a bin relative to being reported active when no activation is reported in the bin. Note that cerebellar and sub-cortical regions although included in the analysis are not shown in the figures. The **Network Overlap panel shows the brain networks from the 17-Networks atlas [24] that overlap with the coactivation pattern of each quintile bin. The transparency of the color reflects the relative proportion of volume in the coactivation pattern the overlaps with each brain network. **SomMot**: Somatomotor, **VisCent/Peri**: Visual Central/Peripheral, **SalVentAttn**: Saliency/Ventral Attention, **DorsAttn**: Dorsal Attention, **TempPar**: Temporo-parietal, **Cont**: Control, **Default**: Default Mode**

- 1 integrative processing in the mid-LPFC regions as opposed to more domain-specificity at the
- 2 extremities of the rostrocaudal LPFC gradient.

2.3 Mapping specific topic associations in the LPFC supports the hypothesis of increasing abstract representations extending along the principal rostrocaudal gradient

In the third analysis, we infer specific functional associations of coactivation patterns among quintile bins along the principal gradient of the LPFC in both hemispheres using what we call “segregation queries”. A segregation query infers the probability “that a topic is present in a study given coactivation in a set of regions and the simultaneous absence of coactivation in another set of regions”. This type of queries is arguably difficult to express in other automated meta-analysis tools especially as the number of topics and regions increases, but can be readily represented in NeuroLang. Expressing segregation queries using NeuroLang enables the inference of specific structure-functions associations that are otherwise blurred by the coactivation of regions across tasks. The reason for this blurring is that typical fMRI task contrasts rarely isolate regions underlying distinct but related processes, which likely need to be probed across multiple tasks to ensure the independence of regions [48].

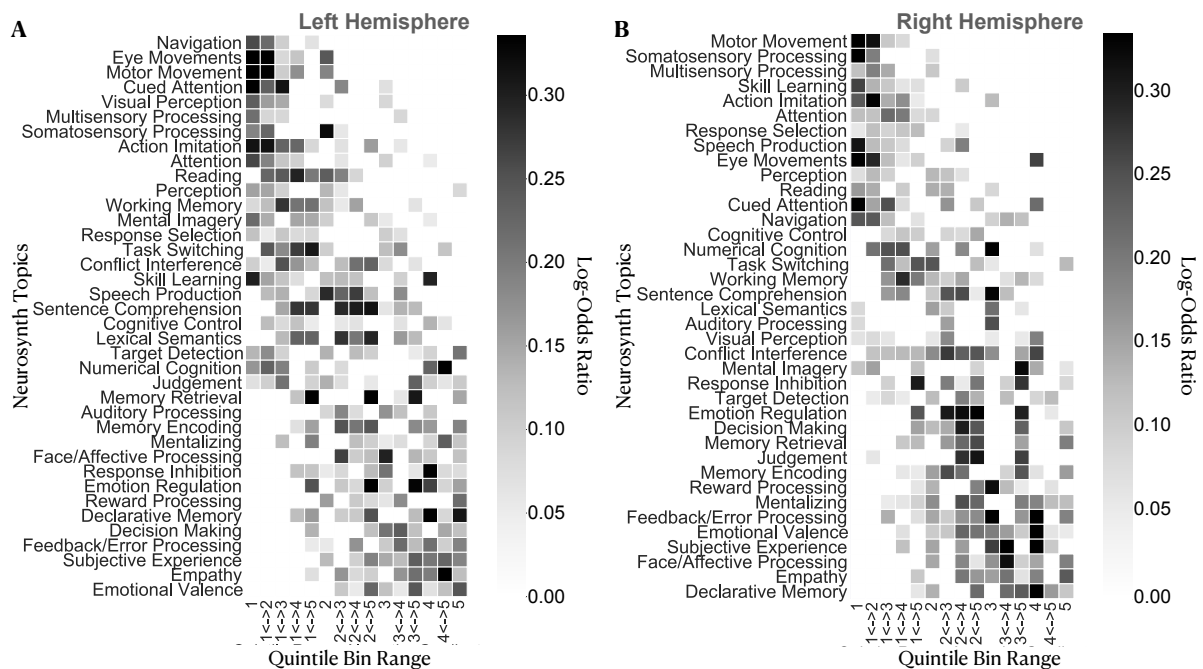


Figure 4: Segregation-based meta-analysis of topic-bin associations using 38 topics reveals a systematic shift in function from caudal to rostral LPFC regions characterized by increasing abstraction. (A) and (B) show specific topic associations in the left and right hemispheres, respectively. Topics are ordered by the weighted mean of their location along the principal gradient. A two-headed arrow along the horizontal axis signifies a coactivation among quintile bins in a given range and potentially any region within but not outside the range. Note that the exact order of topics varies between hemispheres, but the general profile of topic distribution is comparable.

We conduct this segregation-based meta-analysis using 38 topics expertly-chosen from an original set of 100 topics (version-5 of topic modelling) from Neurosynth [49]. These topics cover broad cognitive and behavioral domains mainly studied in cognitive neuroscience. We set the NeuroLang logic program (Program available here) to infer the probability that a topic is present given activation in bin a ($a \in [1, 5]$) and bin b ($b \in [1, 5]$) and there exists no activation in any bin outside the range $[a, b]$. For instance, in the event where $a = 1$ and $b = 4$, the program

1 queries the database on the probability that a topic is present in a study given coactivation of
2 bins 1 and 4 (and potentially any region in between) and there exists no activation in any bin
3 outside the quintile range [1, 4]. In the event where $a = b$, the program queries the database
4 on the presence of a topic given activation constrained in only one quintile bin at a time. We
5 illustrate this visually in Figure 4, for example, the coactivation of bins 1 and 4 (and potentially
6 any bins in between) is represented by the “1 < - > 4” notation on the horizontal axis, and
7 the sole activation of bin 3 is represented by the “3” notation. Concurrently, the program
8 infers the probability of the opposite event by selecting the studies that do not match a criteria
9 imposed by a given segregation query. By computing the LOR of the two opposing hypotheses,
10 we obtain a measure of the evidence in favor of specific associations between each topic and
11 spatially-constrained activation patterns along the principal gradient of the LPFC.

12 Results of this analysis are depicted in Figure 4A and Figure 4B for the left and right
13 hemispheres, respectively. Topics are ordered by the weighted mean of their location along the
14 gradient, revealing a systematic shift in topic associations from external processing at the caudal
15 end to more abstract cognitive, affective and memory-related topics at the rostral end of the
16 principal gradient. Between these extremities, we observe domain-general executive functions
17 and topics related to language and semantic processing. This pattern of topic-bin associations
18 suggests that as activation patterns extend away from caudal LPFC (bins 1 and 2) towards
19 the rostral LPFC (bins 4 and 5), task representations become more abstracted from direct
20 perception/action cycles.

21 **2.4 Gradient-based meta-analysis of inter-hemispheric asymmetries** 22 **reveals lateralized associations with topics of language, memory,** 23 **inhibitory control, and error processing**

24 Our final analysis aims at contrasting the two hemispheres in terms of specific topic associations
25 in a gradient-like fashion. More precisely, we compare homologous quintile bins in both hemi-
26 spheres in terms of their specific topic associations given unilateral activation. For this purpose,
27 we write a NeuroLang logic program (Program available here) that solves inter-hemispheric seg-
28regation queries to infer the probability “*that a topic is present in a study given activation in a*
29 *right LPFC quintile bin and there exists no reported activation in the entire left LPFC*”. The
30 program also infers the probability of the opposite hypothesis; “*the probability that a Neu-*
31 *rosynth topic is present in a study given activation in a left LPFC quintile bin and there exists*
32 *no reported activation in the entire right LPFC*”. The LOR of these two hypotheses represents
33 the amount of evidence for topic association given unilateral activation in the right hemisphere
34 relative to a unilateral activation in the left hemisphere of the LPFC in a gradient-like fashion.

35 The results of this analysis are depicted in Figure 5. In general, we do not observe any
36 systematic variation in the degree and nature of hemispheric asymmetries moving along the
37 principal gradient in the LPFC. That is, the amount of evidence for hemispheric dominance
38 as well as the domains of lateralized topic associations in the LPFC are comparable between
39 caudal and rostral LPFC regions, especially in the left hemisphere (see Figure 5). In this
40 context, we find that the left LPFC exhibits greater amount of evidence for topic associations
41 than the right LPFC when given unilateral activations. This result is consistent with findings
42 that the left hemisphere shows a tendency to interact more exclusively with itself than the right
43 hemisphere [50]. Specifically, we find that language-related topics, such as “lexical semantics”,
44 “sentence comprehension”, and “reading” show more than threefold the evidence ($LOR > 0.5$)
45 for left-hemispheric dominance along the entire principal LPFC gradient. Likewise, we find that
46 memory-related topics, “memory retrieval” and “declarative memory”, also show a comparable
47 amount of evidence for left-hemispheric dominance across multiple quintile bins of the principal
48 LPFC gradient as language-related topics. In contrast, topics such as “response inhibition” (in
49 bins 2 and 3), “feedback/error processing” (in bins 2 and 3), and “somatosensory processing”

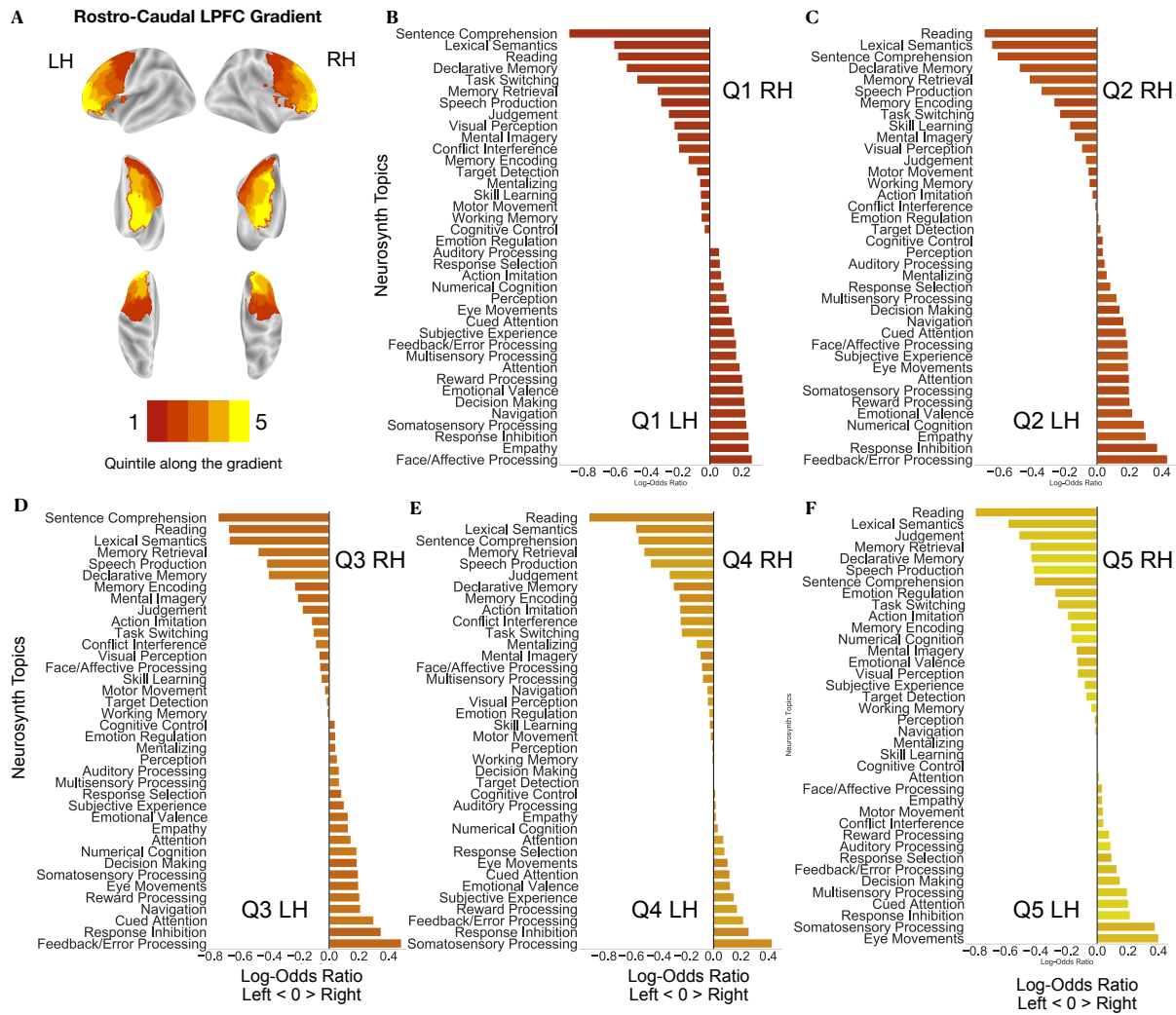


Figure 5: Gradient-based meta-analysis of functional asymmetries reveals the left-hemispheric dominance of language and memory and the right-hemispheric dominance of response inhibition, error processing, and somatosensory processing in the LPFC. Horizontal bar graphs show the topics that are mostly predicted by the presence of unilateral activation in each quintile bin in the right LPFC versus its homologous bin in the left LPFC. Positive log-odds ratios (LORs) indicate evidence in favor of right hemispheric-dominance of a topic in any given bin, whereas negative LORs indicate evidence in favor of left dominance of a topic in any given bin. Topics are ordered from most-left dominant to most-right dominant in each case. **Q**: Quintile, **LH**: Left Hemisphere, **RH**: Right Hemisphere

- 1 (bins 4 and 5) show weaker evidence ($LOR < 0.5$) for right-hemispheric dominance in the LPFC.
- 2 Together, these results reassert the views on hemispheric asymmetries in the LPFC, with the
- 3 left LPFC involved in language and semantic memory processes [22, 30, 33, 51] and the right
- 4 LPFC involved in stimulus-driven action control and monitoring processes [31, 32, 52, 53].

5 **3 Discussion**

6 In this study, we infer the main gradients of organization in the LPFC, a principal rostrocaudal
7 and subsidiary dorsoventral gradient, from a large corpus of literature. These gradients explain
8 most of the variance in meta-analytic connectivity patterns in the LPFC, respectively. We find

1 an agreement in the literature on a spectrum of increasing abstraction both in the spatial dis-
2 tribution of large-scale networks and specific topic associations along the principal gradient in
3 both hemispheres. Finally, when assessing inter-hemispheric asymmetries, we do not observe
4 a systematic transition in the degree of hemispheric-dominance in topic associations along the
5 principal gradient, especially in the left LPFC. Rather we find a pattern of diffusely lateralized
6 topic associations consistent with previous findings on language, memory, and response inhi-
7 bition. This comprehensive and expressive meta-analysis is enabled by a recently-introduced
8 domain-specific query language, called NeuroLang, that formalizes meta-analysis and expands
9 the scope of hypotheses that can be tested against an ever expanding literature. Overall, the
10 findings of this study can serve to ground new hypothesis generation in future studies on a
11 quantitative overview of previously published results.

12 **3.1 The principal gradient of meta-analytic connectivity in the LPFC** 13 **echoes a rostrocaudal organization characterized by domain-** 14 **generality in the intermediate zone and domain-specificity at** 15 **the extremities**

16 The principal gradient of meta-analytic coactivation in the LPFC echoes a rostrocaudal orga-
17 nization in the sense that successive twenty-percentile bins along the gradient show a linear
18 increase in their posterior—to-anterior position from the premotor cortex towards the anterior
19 of the brain. Thus, this gradient places caudal LPFC regions at the farthest point from rostral
20 LPFC regions on a spectrum of similarity in meta-analytic connectivity patterns. This result
21 agrees with a popular class of hypotheses emerging from abstraction and hierarchical control
22 studies on a rostrocaudal gradient in the LPFC [3, 9, 11, 13, 54]. Yet, a question that remains
23 open concerns the properties of different zones along the gradient in terms of domain-generality
24 and domain-specificity.

25 Early fMRI studies on the organization of the LPFC ascribe the rostral LPFC with the
26 role of integrating concrete information from more caudal regions into more abstract forms and
27 relaying back top-down control signals [2, 11, 13, 54]. However, recent accounts relying on
28 causal evidence argue against a linear gradient, and rather place the mid-LPFC as the nexus
29 of both concrete and abstract representations, with the rostral and caudal LPFC involved in
30 distinct specific domains [6, 8, 29]. Here, we cannot infer such integrative processing by means
31 of causality, nevertheless, we find that the mid-LPFC regions previously described as integrative
32 in [6, 28] overlap with the middle zones (bins 2 and 3) of the principal LPFC gradient. This
33 means that the meta-analytic connectivity profile of mid-LPFC is not completely similar nor
34 dissimilar to those of rostral and caudal LPFC, but rather overlaps with them. Moreover, we
35 find that the coactivation patterns of middle zones (bins 2 and 3) in Figure 3 extends along the
36 LPFC in each hemisphere to include regions of caudal and rostral LPFC, a pattern not observed
37 for the extremities of the gradient (bins 1 and 5). Furthermore, we find that those middle zones
38 predominantly coactivate with the salience (SalVentAttnB) and control networks (ContA and
39 ContB), but to a lesser extent with the attention (DorsAttnA and DorsAttnB) and default
40 mode networks (DefaultA and DefaultB). The salience and control networks are integrative
41 networks believed to mediate the interaction of the default and attention networks to control
42 the transition between internally and externally focused processing according to context [55].
43 Likewise, this coactivation pattern is not observed for the two extremities of the gradient, where
44 networks involved either in external processing (SomMotA, DorsAttnA, and SalVentAttnA)
45 or internal cognition (DefaultA and DefaultB) are relatively more dominant. Finally, given
46 coactivation restricted within the caudal-to-middle zones of the gradient (bins 1 to 4), we
47 observe associations with topics related to action execution and perception (see Figure 4). In
48 contrast, when coactivation is restricted within middle-to-rostral zones, we observe associations

1 with topics of self-reference, memory, emotion and social cognition. These patterns of network
2 and function associations may indicate domain-general (i.e. internally and externally oriented
3 processing) in mid-LPFC regions and more domain-specificity (i.e. either internally or externally
4 oriented processing) in caudal and rostral LPFC regions. Thus, the rostrocaudal gradient of
5 meta-analytic connectivity in the LPFC is consistent with the revised view of distinct LPFC
6 hierarchies converging in mid-LPFC [6].

7 **3.2 The principal gradient of LPFC meta-analytic connectivity con-** 8 **forms with the principal gradient of brain-wide intrinsic connec-** 9 **tivity in both the spatial layout of networks and distribution of** 10 **functions**

11 The topography of the principal LPFC gradient of meta-analytic connectivity resembles the
12 general layout of the principal brain-wide gradient described in [26], which represents the dom-
13 inant spatial principle governing the topography of resting-state connectivity throughout the
14 entire cerebral cortex. This spatial principle conceptualizes higher-order cognition as emerging
15 from dynamic interactions of large-scale networks, systematically organized along an axis of ab-
16 straction that extends from unimodal sensorimotor regions to transmodal default mode regions
17 [25, 26, 56]. Importantly, it incorporates the seemingly isolated local processing streams across
18 the cortex within a global continuous framework. In this sense, the spatial location of a brain
19 region is not arbitrary; a region’s position along the principal gradient is a major determinant
20 of its connectivity profile, its network membership and consequently its functional role. Specif-
21 ically, it has been found that the longer the spatial distance between a region and the primary
22 cortices, the more distant are its functional connections and the more it is dispositioned to
23 subserve abstract mental functions [57]. The default mode network occupies the top end of
24 the principal intrinsic connectivity gradient and exhibits the greatest geodesic distance from
25 the sensorimotor cortices, allowing it to process highly internalized information abstracted from
26 immediate sensory input [26, 58].

27 In this study, we find that the rostrocaudal gradient in the LPFC captures systematic tran-
28 sitions in large-scale functional networks (Figure 3), such that caudal regions mainly coactivate
29 with sensorimotor/attention networks, middle regions mainly coactivate with salience/executive
30 control networks, and most rostral regions coactivate with the default mode network. Moreover,
31 inferring specific topic associations using NeuroLang’s segregation queries supports the notion
32 of increasing abstraction along the principal LPFC gradient Figure 4. In particular, we find
33 that activations reported only in the caudal end (bins 1 and 2) predict topics of acting and
34 perceiving, while activations restricted to the rostral end (bins 4 and 5) predict topics related
35 to emotion, social cognition, and memory—functions that rely on abstract representations un-
36 tethered from immediate environmental demands [59]. Interestingly, the presence of the topics
37 “memory retrieval” and “emotion regulation” in both LPFC hemispheres and “response inhi-
38 bition” in the right LPFC is best predicted by the coactivation between most rostral regions
39 (i.e. quintile bin 5) and more caudal regions (bins 1 to 3, see Figure 4). This result supports
40 a prominent role for the rostral LPFC in retrieving past memories as well as future plans and
41 goals to enable temporal control of behavior and emotions [60]. Ultimately, the rostrocaudal
42 LPFC gradient described herein represents a literature-inferred map of an external/present ori-
43 ented to internal/temporally-remote organizing spatial principle, wherein globally interacting
44 networks interface locally in the LPFC to support adaptive behavior within dynamic contexts
45 [6, 29].

1 **3.3 Segregation-based meta-analysis of inter-hemispheric asymme-** 2 **tries reasserts the left-hemispheric dominance of language and** 3 **memory and the right-hemispheric dominance of inhibition and** 4 **feedback/error processing in the LPFC**

5 Segregation-based meta-analysis of inter-hemispheric asymmetries reveals hemisphere-specific
6 associations with language, memory, response inhibition, error-processing, and somatosensory
7 processing in the LPFC. The importance of segregation queries in this case is in inferring the
8 structure-function associations whose presence is predicted by unilateral activation in the LPFC.
9 Previously, the lateralization of function in the brain has been well documented for certain
10 functions, notably language [22, 30] and response inhibition [32]. More recently, an effort to map
11 hemisphere-specific functions across the whole brain [61] has revealed four global dimensions of
12 laterlization: symbolic communication, perception and action, emotion, and decision making.
13 However, a comprehensive comparison of hemisphere-specific functional associations within the
14 LPFC remains lacking, especially when taking into account the principal organizing gradient in
15 each hemisphere. The analysis carried out in this study is one step forward towards filling this
16 gap.

17 This analysis, however, does not reveal systematic variations in the degree and nature of
18 lateralized structure-function associations along the principal LPFC gradient (Figure 5). That
19 is, unilateral structure-function association patterns seem to be comparable both in topics and
20 strength throughout the gradient, especially in the left hemisphere. The greatest observed
21 evidence for left-hemispheric dominance in the LPFC is attributed to language and memory-
22 related topics, which is consistent with a long line of research on the linguistic and semantic
23 selectivity of the left hemisphere compared to the right hemisphere [34]. In contrast, the greatest
24 amount of evidence for right-hemispheric dominance in the LPFC is attributed to “response
25 inhibition” and “feedback/error processing”, and to a lesser extent “somatosensory processing”
26 and “eye movements”. Surprisingly, we observe relatively weaker evidence ($LOR < 0.3$, see
27 Figure 5) for right-hemispheric dominance of attention-related topics, such as “attention”, “cued
28 attention” and “navigation”, although these are often attributed to the right brain hemisphere
29 [52, 53]. While there may be more than one explanation for these observations, a plausible one
30 is related to the data-driven nature of topics. More specifically, topics are “bags” of words that
31 frequently co-occur in the abstracts of articles, making them at best proxies to the actual mental
32 functions. This means that topics can be noisy and not specific enough to capture finely-grained
33 cognitive constructs. Nonetheless, topics are relatively better representatives of psychological
34 domains than individual terms that pose the risk of being interpreted out of context. Overall,
35 these results support the preferential roles of the left LPFC in language/semantic representations
36 and the right LPFC in sensory monitoring and the cued inhibition of behavior.

37 **3.4 Limitations**

38 While the present results provide a relatively unbiased mapping of the organizing gradients in
39 the LPFC through meta-analysis, several limitations are worth noting. First, we make sim-
40 plifying assumptions in order to improve interpretability and alleviate computational burdens,
41 notably the use of 1024 functional regions from the DiFuMo atlases [43] and the choice of twenty-
42 percentile bins along the gradient as units of analysis. These assumptions might impose a fixed
43 dimensionality on the brain and forces voxels to be grouped in static regions, which ignores
44 dynamics in brain activity observed at multiple timescales within individuals [62]. Another
45 simplifying assumption is the use of topics that represent broad concepts built upon the fre-
46 quency with which terms co-occur in studies, ignoring more finely-grained cognitive structures.
47 Integrating ontologies, such as the Cognitive Atlas [48], will arguably improve the ability of au-
48 tomated meta-analyses to differentiate fine-grained cognitive constructs. In fact, NeuroLang is

1 well equipped to integrate ontologies into meta-analyses, and this will be our next step towards
2 improving the precision of meta-analytic queries.

3 A second limitation is that our meta-analysis is based on an automatically-generated coordinate-
4 based dataset. Coordinate-based meta-analytic datasets suffer from information loss due to the
5 relative sparseness of reported results [63], with peak activations being sensitive to statistical
6 methods adopted in each study, notably thresholding [47]. Moreover, with small sample sizes
7 per study, potential “publication bias”, or the tendency of authors and journals to only pub-
8 lish positive or “statistically significant” results [36], might impact the reliability of the current
9 findings. Even though spatial smoothing priors and probabilistic brain atlases may alleviate
10 some bias, future meta-analyses will rely on complete data like unthresholded statistical images
11 stored in large repositories, such as NeuroVault [64], to validate the results.

12 Finally, an important limitation, not specific to this meta-analysis, is that our current
13 knowledge of task-dependent activation in the brain is as good as the task paradigms that
14 induce these activations [65]. More broadly, an ongoing endeavor in cognitive neuroscience is
15 developing the appropriate paradigms that isolate cognitive processes of closely related brain
16 regions [65]. Studies in the domain of abstraction and hierarchical control use nested tasks
17 classed by different levels of abstraction, which can reveal functional gradients in the LPFC
18 (e.g. [6, 11]). However, these studies are not common in the literature and are limited to small
19 range of functions. In contrast, the bulk of tasks included in the Neurosynth database, while
20 not hierarchical, captures a much wider variety of brain states, but at the expense of losing
21 some level of specificity.

22 **3.5 Conclusion**

23 In conclusion, the present study provides quantitative meta-analytic evidence for organizing gra-
24 dients in the LPFC of humans. The LPFC appears to be organised along two spatial gradients,
25 rostrocaudal and dorsoventral, that respectively explain the most and second-most variance in
26 meta-analytic connectivity. We also reveal that the dominant gradient captures a spectrum
27 of increasing abstraction in network connectivity and specific structure-function associations,
28 grounding a popular class of hypotheses on comprehensive empirical evidence and supporting
29 recent revised views on the functional properties of different LPFC regions. Importantly, we
30 overcome the limitations of previous large-scale attempts using a novel domain-specific query
31 language, called NeuroLang, to formulate expressive queries on the largest coordinate-based
32 meta-analysis database to date. As more studies are aggregated into future databases, the
33 analyses carried out in this study can be reproduced using the same queries as well as extended
34 to explore other brain regions.

35 **4 Materials and Methods**

36 **4.1 Data and Software**

37 We use the latest version of the Neurosynth database [40] last updated in July 2018 to in-
38 clude 14,371 publications with more than 500,000 activation coordinates covering the whole
39 brain. Each study in the database is represented by a PubMed ID, peak activation coord-
40 inates and weighted topic associations. Activation coordinates are either reported in MNI
41 space or are transformed from Talairach space before analysis. To examine the structure-
42 function associations in the LPFC, we use the set of 100 Neurosynth topic terms (version 5)
43 previously generated by applying latent Dirichlet allocation to the abstracts of articles in the
44 database [49]. Out of the 100 topics, we include 38 topics that we believe represent coher-
45 ent cognitive functions, excluding those that correspond to subject populations (e.g. brain
46 disorders, age, sex), brain anatomy, imaging modalities and analysis techniques. Finally,

1 all analyses and visualizations are implemented in python. In particular, we use the Neu-
2 roLang (<https://github.com/NeuroLang/NeuroLang>) package to perform all meta-analysis
3 steps and the BrainSpace package (<https://github.com/MICA-MNI/BrainSpace>) to estimate
4 a low-dimensional embedding of meta-analytic connectivity patterns in the LPFC [46]. All
5 python notebooks and data files used in this study will be publicly available to be openly
6 accessed and used on <https://osf.io/ur7ej/quickfiles>.

7 **4.2 The lateral prefrontal cortex mask**

8 To facilitate the selection of regions in the LPFC for meta-analysis, a spatial mask of the LPFC
9 is needed. We rely on a previously created mask of the lateral frontal lobe created from [9].
10 However, we exclude voxels with less than 25% probability of falling in the grey matter as well
11 as voxels located at $x < 18$ or $x > -18$ from the midline of the brain to ensure that regions in
12 the anterior and superior parts of the medial prefrontal cortex are not included. We also exclude
13 voxels in the orbitofrontal cortex and anterior insula, while making sure to include voxels of
14 the lateral orbitofrontal cortex. Finally, to focus our analysis on the association regions of the
15 lateral frontal lobe (i.e, the LPFC), we exclude voxels in the motor cortex as defined by the
16 somatomotor networks of the 17-Networks atlas [24]. The LPFC mask is shown in Figure 6A.

17 **4.3 The 1024 functional regions dictionary from DiFuMo**

18 To increase the interpretability of our findings and alleviate computational burdens, we reduce
19 voxel-level data to region-level data. In particular, we adopt the 1024 functional regions dictio-
20 nary from the Dictionaries of Functional Modes (DiFuMo) atlases [43]. The DiFuMo is a set
21 of multi-scale functional atlases estimated via massive online dictionary learning [66] applied
22 to functional brain volumes of thousands of subjects across 27 large-scale studies, forming a
23 total of 2192 task-based and resting-state MRI sessions. Reducing voxel data to 1024 func-
24 tional regions has been argued to capture the functional neuroanatomy of the brain equally
25 well as voxel-level analysis while reducing computational burdens Dadi et al. [43]. Unlike other
26 dimensionality-reduction techniques, massive online dictionary learning assigns non-negative
27 continuous loadings to each voxel designating its relative weight on each region. Voxels that
28 have a loading value equal to 0 on any given region are considered to not belong in this region.
29 Finally, to identify the regions in the LPFC, we recover those that have at least 50% of their
30 volume fall within the LPFC mask described earlier (see the next section on Representing het-
31 erogeneous data in a single framework with NeuroLang). Note that we do not mask out voxels
32 of regions that are outside the LPFC mask—we either include or exclude entire regions without
33 breaking continuity. This means that some functional regions can include voxels outside the
34 LPFC mask. The reason for this crossover is that functionally-defined regions seldom conform
35 to anatomical landmarks in the brain. Comprehensive details on DiFuMo can be found in the
36 original study by Dadi et al. [43].

37 **4.4 Representing heterogeneous data in a single framework with** 38 **NeuroLang**

39 The goal behind developing NeuroLang is to create a universal language that reduces the likeli-
40 hood of miscommunication within the cognitive neuroscience community by enabling databases,
41 hypotheses, and questions to be defined in a formal, shareable and reproducible manner. This
42 is believed to be a critical step towards advancing the field of cognitive neuroscience [65].

43 In this study, we represent various data types coming from heterogeneous sources, such as
44 peak coordinates, topic models, anatomical masks, and brain atlases in a single framework.
45 More precisely, these data and the relationships among them can be represented as facts and

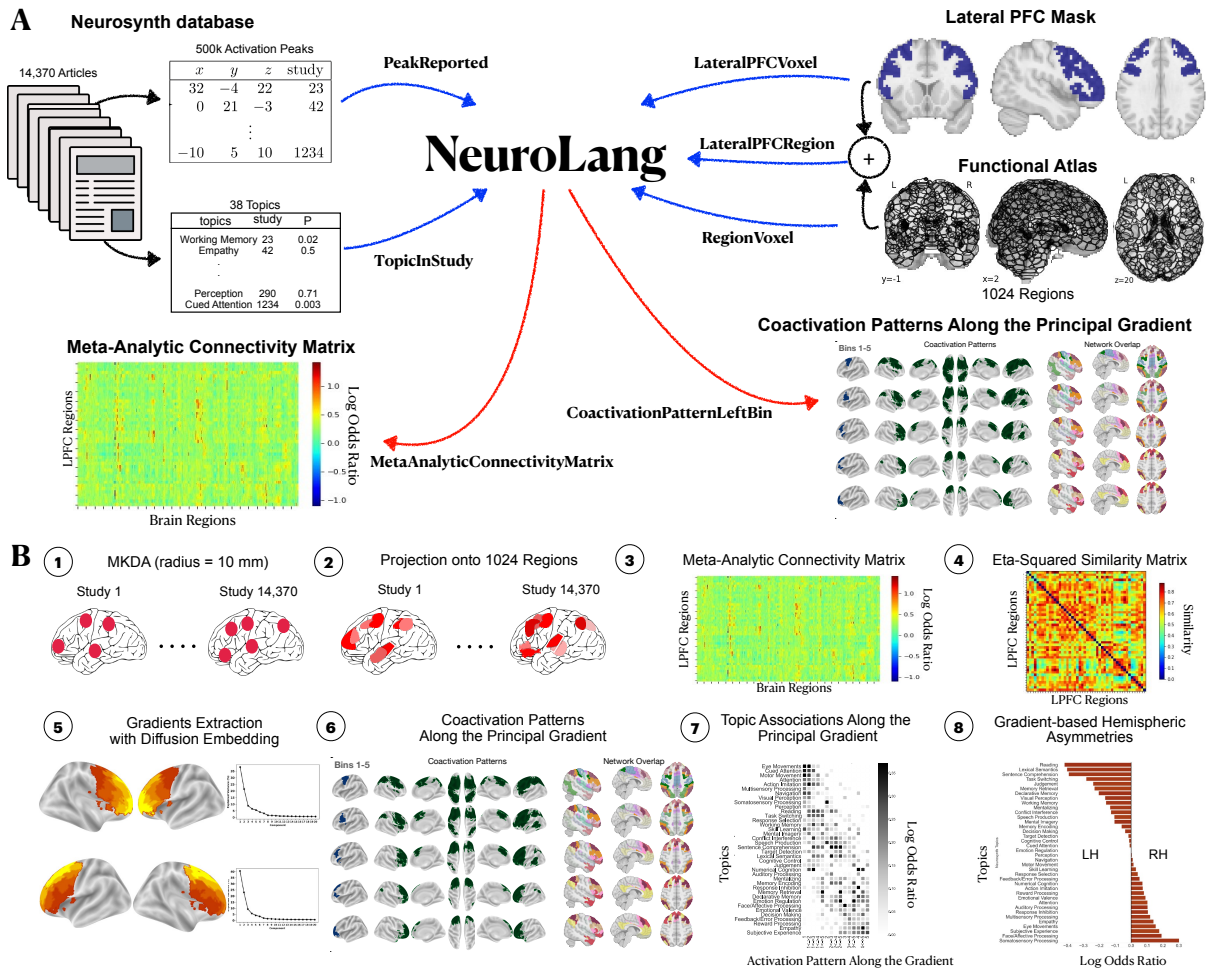


Figure 6: Schematic overview of our analysis pipeline. **(A)** Inputs and outputs of NeuroLang. Inputs are represented using blue arrows and include: Peak activations and topics from the Neurosynth database, the lateral PFC mask, and the 1024 regions from the DiFuMo atlases are represented in a unifying framework within NeuroLang. Two examples of outputs are shown here and represented using red arrows. **(B)** The main steps of the meta-analysis carried out in this study. (1) Multilevel Kernel Density Analysis (MKDA) selects voxels within 10 mm radius of each peak activation in each study for meta-analysis. (2) The binary activation map of each study is projected onto 1024 functional regions. Varying shades of red signify that regions have different probabilities of being reported by a study depending on the location of reported voxels with respect to each region. (3) The meta-analytic connectivity matrix is inferred, and it encodes the log-odds ratios of coactivation between each region in the LPFC and every region in the brain. (4) The degree of similarity between LPFC regions in their meta-analytic connectivity profiles is estimated via eta-squared similarity metric. (5) The gradients of meta-analytic connectivity in each hemisphere are derived from the affinity matrix using Diffusion Embedding. (6) Coactivation patterns of successive quintile bins along the gradient are inferred, as well as their overlap with large-scale networks. (7) Specific topic associations along the principal gradient are inferred using segregation queries. (8) Finally, gradient-based meta-analysis of hemispheric asymmetries is performed using segregation queries between homologous quintile bins.

1 rules using declarative logic-based statements such that the user only has to specify what is
 2 to be found rather than how to find it. Facts and rules in NeuroLang are tuple-sets or tables

1 structured in rows. Each row is a sequence of k elements representing a piece of data, such as
2 the MNI coordinates of a reported peak in a study, and can be implicitly assigned a probability
3 that quantifies the level of uncertainty in this data. Fact tables represent explicit information
4 present in the data, while rule tables represent inferred relationships among the different data
5 elements. The goal is to declare these tables as **predicates** in a probabilistic logic program
6 that solves complex queries on them. For a survey on probabilistic databases and probabilistic
7 programming the reader is referred to [67].

8 To concretely showcase how we represent data in NeuroLang, we start with the Neurosynth
9 database. the database includes studies that report peak activations coordinates in standard
10 space (Figure 6A). In NeuroLang, we represent these peaks in a fact table called `PeakReported`.
11 This table contains a row `(x, y, z, study)` for each peak with coordinates `(x, y, z)` that
12 has been reported active by a `study`. Also, the studies themselves are represented in a fact
13 table called `Study` that contains a row for each study containing a single element, `(study)`,
14 representing its PubMed identifier. Similarly to Neurosynth, we assume each study within
15 the database to be an *independent equiprobable sample* of neuroscientific knowledge [40]. This
16 assumption is represented by another fact table we call `SelectedStudy`, which simply assigns
17 a uniform probability ($1/N$, $N = 14,370$) for each study to be selected in any possible world
18 of events. In other words, this assumption allows the studies to have a similar weight in the
19 meta-analysis [40, 42].

20 Further, the spatial uncertainty surrounding the reported location of each peak in a given
21 study can be represented in a rule table, named `VoxelReported`. In this rule, a multilevel kernel
22 density analysis (MKDA) [47] assumes each peak's 10mm neighboring voxels to be equivalently
23 reported [47]. Then, the `VoxelReported` table contains a row `(x, y, z, study)` for each voxel
24 at location `(x, y, z)` and falls within 10 mm Euclidean distance from a peak reported by a
25 `study`. Being based on Datalog [68], a fully declarative logic programming language designed
26 to solve queries on large databases, the NeuroLang program that computes `VoxelReported` is
27 written as follows:

```
VoxelReported(x, y, z, study) :-  
    GreyMatterVoxel(x, y, z) & PeakReported(x2, y2, z2, study)  
    & distance = EUCLIDEAN(x, y, z, x2, y2, z2) & distance < 10  
  
ans(x, y, z, study) :- VoxelReported(x, y, z, study)
```

28 The answer states that "a voxel at location `(x, y, z)` in grey matter is considered active
29 in a `study` if it is situated within 10 mm radius from a peak reported by `study` at location
30 `(x2, y2, z2)`". Here, `GreyMatterVoxel` is also a fact table representing a grey matter mask
31 in MNI space. This table contains a row `(x, y, z)` for each brain voxel having at least 25%
32 chance of being found in grey matter. The `distance` variable is estimated using the built-in
33 function `EUCLIDEAN`, which computes the distance between two locations in standard space.

34 The Neurosynth database also includes topics that have been derived using latent Dirichlet
35 allocation applied to the abstracts of the articles [65]. Each study in the database has a loading
36 value on each topic, which can be considered as a proxy to the probability that a topic is
37 present in a study. This weighted topic-study association is represented in a probabilistic fact
38 table named `TopicInStudy`. This table contains a row `(topic, study)` for each `topic` present
39 in a `study`, and the study has a non-zero loading on the topic. The reason for calling this
40 table probabilistic is that the study-on-topic loading is implicitly embedded as a measure of
41 uncertainty in the presence of a topic in a given study.

42 Anatomical masks and functional atlases can also be represented in NeuroLang. For in-
43 stance, we represent the LPFC mask described previously in a fact table called `LateralPFCVoxel`.
44 This table contains a row `(x, y, z)` for each voxel belonging to the LPFC mask. Moreover, we
45 represent the 1024 functional regions from DiFuMo in a fact table called `RegionVoxelWeighted`,

1 which contains a row (\mathbf{r} , x , y , z , w) for each voxel at location (x,y,z) in MNI space hav-
2 ing a non-zero weight w on a DiFuMo region \mathbf{r} . Similar to case of topic-study association, the
3 voxel-on-region weight can be used as a measure of uncertainty in a voxel belonging to a region.
4 This is achieved by first scaling the weight of every voxel in each region to the maximum weight
5 value in that region. In this sense, the voxel with the maximum loading on a region will have a
6 probability of 1 of belonging to it. This creates a probabilistic fact table `RegionVoxel`, named
7 this way as it does not contain the weight variable explicitly, but implicitly. This probabilis-
8 tic table can be used by a NeuroLang program to infer other probabilistic tables. This will
9 be concretely shown in the following sections. Finally, regions belonging to the LPFC can be
10 represented in a rule table called `LateralPFCRegion`. This table contains a row (\mathbf{r}), where \mathbf{r}
11 is a brain region that have at least 50% of its volume overlapping with the LPFC mask. The
12 following NeuroLang program, written in Datalog syntax, infers this table:

```
RegionVolume( $\mathbf{r}$ , count( $x$ ,  $y$ ,  $z$ )) :- RegionVoxelWeighted( $\mathbf{r}$ ,  $x$ ,  $y$ ,  $z$ ,  $w$ )

VolumeOfOverlapWithMask( $\mathbf{r}$ , count( $x$ ,  $y$ ,  $z$ )) :-
    RegionVoxelWeighted( $\mathbf{r}$ ,  $x$ ,  $y$ ,  $z$ ,  $w$ ) & LateralPFCVoxel( $x$ ,  $y$ ,  $z$ )

LateralPFCRegion( $\mathbf{r}$ ) :-
    RegionVolume( $\mathbf{r}$ ,  $v0$ ) & VolumeOfOverlapWithMask( $\mathbf{r}$ ,  $v$ ) & ( $v/v0 > 0.5$ )

ans( $\mathbf{r}$ ) :- LateralPFCRegion( $\mathbf{r}$ )
```

13 We start by declaring the predicates to be used in solving the query. These predicates are the
14 `RegionVolume` and `VolumeOfOverlapWithMask`. These encode the total volume and the volume
15 of overlap with the LPFC mask of each brain region \mathbf{r} , respectively. The `LateralPFCRegion`
16 is the final answer of this program and states that : “A brain region \mathbf{r} belongs to the LPFC
17 if its volume of overlap, v , with an LPFC mask makes up more than 50% of its total volume,
18 $v0$ ”. Volume variables v and $v0$ are estimated by the built-in function `count(x , y , z)`, which
19 simply counts the number of voxels in a brain region.

20 4.5 Inferring the meta-analytic connectivity matrix using NeuroLang

21 To infer a whole-brain meta-analytic connectivity profile for each LPFC region, we query the
22 database on the probability that a brain region is reported active given the presence as well as
23 when given the absence of activation in a LPFC region. This gives us a measure of specificity
24 in the meta-analytic connectivity between each LPFC region and every brain region.

25 To infer these probabilities, we write a NeuroLang program that first projects the voxels
26 reported active in each study onto the 1024 functional regions to determine which ones are
27 reported by the study (step 2 in Figure 6B). In this context, the program regards the reporting
28 of a brain region by a study as a probabilistic event rather than a certain one. That is, if a
29 voxel reported active has a normalized weight w on a region \mathbf{r} , then the region is assigned a
30 probability w of being reported by the study. If multiple voxels are reported active within a
31 region, then the union of their locations’ weights is considered the overall probability for the
32 region to be reported by the study. This union is interpreted as the probability that at least
33 one of those peaks is reported active in the region. Intuitively, a region is considered to be not
34 reported by a study, if no activation is reported in any of its constituent voxels.

35 We then infer the conditional probabilities of observing activation in a brain region given the
36 presence, and subsequently given the absence, of activation in a LPFC region. To quantitatively
37 contrast these two hypotheses and get a representative measure of meta-analytic connectivity,
38 we compute the logarithm with base 10 of their odds ratio (LOR). This yields a vector for
39 each LPFC region whose elements represent the amount of evidence (in log-scale) for pairwise
40 meta-analytic connectivity with every brain region. A positive LOR indicates more evidence

- 1 for a brain region to be reported active given activation in a LPFC region, a negative LOR
- 2 implies more evidence for a brain region to be reported active given no activation in the LPFC
- 3 region, and a LOR equal to 0 implies that the evidence is inconclusive for either hypotheses.
- 4 The program that infers the meta-analytic connectivity matrix is as follows:

```
RegionMaxWeight(r, max(w)) :-
    RegionVoxelWeighted(r, x, y, z, w)

RegionVoxel(r, x, y, z) :: w/W :-
    RegionVoxelWeighted(r, x, y, z, w)
    & RegionMaxWeight(r, W)

LateralPFCRegionVoxel(r, x, y, z) :-
    RegionVoxel(r, x, y, z)
    & LateralPFCRegion(r)

LateralPFCRegionActivation(r, study) :-
    VoxelReported(x, y, z, study)
    & LateralPFCRegionVoxel(r, x, y, z)

NotLateralPFCRegionActivation(r, study) :-
    Study(study)
    & LateralPFCRegion(r)
    & ~LateralPFCRegionActivation(r, study)

BrainRegionActivation(r, study) :-
    VoxelReported(x, y, z, study)
    & RegionVoxel(r, x, y, z)

ProbabilityOfCoactivation(r, r2, PROB) :-
    BrainRegionActivation(r, study) //
    (
        LateralPFCRegionActivation(r2, study)
    & SelectedStudy(study)
    )

ProbabilityOfNoCoactivation(r, r2, PROB) :-
    BrainRegionActivation(r, study) //
    (
        NotLateralPFCRegionActivation(r2, study)
    & SelectedStudy(study)
    )

MetaAnalyticConnectivityMatrix(r2, r, LOR) :-
    ProbabilityOfCoactivation(r, r2, p1)
    & ProbabilityOfNoCoactivation(r, r2, p0)
    & LOR = log10(p1/(1-p1))/(p0/(1-p0))

ans(r2, r, LOR) :- MetaAnalyticConnectivityMatrix(r2, r, LOR)
```

- 5 In order for the program to solve the query, we need to declare some useful predicates. First,

1 we get the maximum weight in each DiFuMo brain region in `RegionMaxWeight` using the built-in
2 function `max(w)`. This will be used to declare the probabilistic table `RegionVoxel` which implic-
3 itly incorporates the normalized weight w/W of each voxel (x, y, z) on each region r . This is
4 represented by the $(: : w/W)$ notation after `RegionVoxel(r, x, y, z)`. Second, we define the
5 tables `LateralPFCRegionActivation` and `BrainRegionActivation`. These are probabilistic
6 rule tables, wherein each row is implicitly assigned a probability that a given brain or LPFC re-
7 gion is reported active by a `study`. Likewise, we declare the studies that do not report activation
8 in each LPFC region by using the negation sign “ \sim ” before `LateralPFCRegionActivation`.
9 Each row of this table represents a `study` that does not report activation in a LPFC region with
10 a certain level of uncertainty. To be able to obtain this table in safe range, we must re-assert
11 that the variable `study` comes from the fact table `Study` and the variable r is found in the fact
12 table `LateralPFCRegion`.

13 To infer the conditional probabilities, we use the “//” sign, which means “given”. For
14 instance, `ProbabilityOfCoactivation` is a rule table that encodes the probability (PROB) of
15 activation being reported in brain region r **given** that activation is also reported in LPFC region
16 $r2$. Likewise, `ProbabilityOfNoCoactivation` is another rule table that encodes the probab-
17 ility (PROB) of activation being reported in brain region r **given** that activation is **not** reported
18 in LPFC region $r2$. The `SelectedStudy` table sets the program to assign an equal weight $(1/N,$
19 $N = 14, 370)$ to all the studies in the meta-analysis. Finally, the `MetaAnalyticConnectivityMatrix`
20 rule table is inferred by computing the “LOR” of the two hypotheses as a measure of evidence
21 of meta-analytic connectivity between each LPFC region and every brain region.

22 **4.6 Diffusion map embedding using the BrainSpace toolbox**

23 To recover a low-dimensional embedding of the meta-analytic connectivity matrix, we choose
24 to apply diffusion embedding [45], an unsupervised nonlinear dimensionality reduction method.
25 The low-dimensional embedding reveals the axes of variation in coactivation-based connectivity
26 patterns in the LPFC, and can be recovered with two steps. First, we estimate the similarity
27 between LPFC regions in terms of their coactivation patterns. Here, we quantify similarity
28 between each pair of LPFC regions using the eta-squared coefficient following [69], yielding a
29 square affinity matrix (step 4 in Figure 6B). The eta-squared coefficient represents the fraction
30 of the variance in one meta-analytic connectivity profile that is accounted for by the variance in
31 another, and ranges from 0 (totally dissimilar) to 1 (perfectly similar). Diffusion embedding then
32 represents this similarity structure as an arrangement of regions in an embedding space spanned
33 by 20 components known as “gradients”. Gradients are conceptually similar to the components
34 of principal components analysis and represent unidimensional axes each explaining a fraction
35 of the variance in a given feature [26], in our case, meta-analytic connectivity. In each gradient,
36 regions that have very similar meta-analytic connectivity patterns occupy nearby zones, while
37 regions with dissimilar patterns are situated further apart. The first or principal gradient is
38 the most informative component as it captures the dominant axis of variation in meta-analytic
39 connectivity patterns within the LPFC.

40 **4.7 Inferring whole-brain coactivation patterns of quintile bins along** 41 **the principal gradient using NeuroLang**

42 To be able to infer varying coactivation patterns along the principal gradient in the LPFC,
43 we first create regions-of-interest from successive twenty-percentile bins (i.e. five quintile bins)
44 along the gradient in each hemisphere. Then, we identify the large-scale brain networks that
45 overlap with each quintile bin’s coactivation pattern to characterize the variation of network
46 connectivity along the principal gradient (step 6 in Figure 6B). We represent the regions-of-
47 interest created from quintile bins in each hemisphere as fact tables called `LeftBinVoxel` and

1 `RightBinVoxel` for the left and right LPFC, respectively. Each of these tables includes a row
2 (`bin`, `x`, `y`, `z`) for each voxel at location (`x`, `y`, `z`) in MNI space and belonging to a quintile
3 `bin`. Moreover, we declare another fact table `Bin` whose rows contain only the labels of the
4 quintile bins (i.e., `bin1` to `bin5`).

5 We write a NeuroLang program that infers the conditional probability of a brain region to
6 be reported active given activation reported in a bin as well as when given no bin activation.
7 Specifically, the program infers the LOR of these two hypotheses as a measure of evidence for
8 coactivation between each brain region and each quintile bin along the principal gradient. A
9 cortical coactivation pattern for each quintile bin is then constructed by recovering the brain
10 regions that exhibit at least threefold the evidence (or $LOR > 0.5$) of being reported active
11 when given activation in a bin relative to no bin activation. The NeuroLang program that
12 infers coactivation patterns of quintile bins in the left LPFC is as follows:

```
LeftBinActivation(bin, study) :-
    LeftBinVoxel(bin, x, y, z)
    & PeakReported(x2, y2, z2, study)
    & distance = EUCLIDEAN(x, y, z, x2, y2, z2)
    & distance < 3

NotLeftBinActivation(bin, study) :-
    Study(study)
    & Bin(bin)
    & ~LeftBinActivation(bin, study)

BrainRegionActivation(r, study) :-
    VoxelReported(x, y, z, study)
    & RegionVoxel(r, x, y, z)

ProbabilityOfCoactivation(r, bin, PROB) :-
    BrainRegionActivation(r, study) //
    (
        LeftBinActivation(bin, study)
    & SelectedStudy(study)
    )

ProbabilityOfNoCoactivation(r, bin, PROB) :-
    BrainRegionActivation(r, study) //
    (
        NotLeftBinActivation(bin, study)
    & SelectedStudy(study)
    )

CoactivationPatternOfBin(bin, r) :-
    ProbabilityOfCoactivation(r, bin, p1)
    & ProbabilityOfNoCoactivation(r, bin, p0)
    & LOR = log10(p1/(1 - p1))/(p0/(1 - p0))
    & LOR > 0.5

ans(bin, r) :- CoactivationPatternOfBin(bin, r)
```

13 As in the program of the previous section, we first declare the predicates that will be used
14 to find the answer to our query. We set the program to consider activity in a quintile bin to be
15 reported by a study if at least one peak activation is reported within the bin or within its near

1 vicinity (`distance < 3`). The program stores the results in the rule table `LeftBinActivation`,
2 which includes a row (`bin, study`) for each `bin` in which activation is reported by a `study`. The
3 program then derives the studies that do not report activity within each bin using the negation
4 operator and stores them in another rule table `NotLeftBinActivation`. This rule table includes
5 a row for each `bin` wherein no activation has been reported by a `study`. Similarly as the program
6 in the previous section, the program here considers activation reporting in individual brain
7 regions as a probabilistic rather than deterministic event depending on the location of active
8 voxels within each region, and stores the results in the rule table `BrainRegionActivation`.
9 The program then infers the conditional probabilities of the two hypotheses and stores them
10 in the rule tables `ProbabilityOfCoactivation` and `ProbabilityOfNoCoactivation`. Finally,
11 the answer to our query `CoactivationPatternOfBin` is derived by estimating the “LOR” as a
12 measure of evidence in favor of coactivation between each brain region `r` and each `bin` and
13 thresholding it at `LOR > 0.5`. Below is a similar program that infers coactivation patterns of
14 quintile bins in the right LPFC:

```
RightBinActivation(bin, study) :-
    RightBinVoxel(bin, x, y, z)
    & PeakReported(x2, y2, z2, study)
    & distance = EUCLIDEAN(x, y, z, x2, y2, z2)
    & distance < 3

NotRightBinActivation(bin, study) :-
    Study(study)
    & Bin(bin)
    & ~RightBinActivation(bin, study)

BrainRegionActivation(r, study) :-
    VoxelReported(x, y, z, study)
    & RegionVoxel(r, x, y, z)

ProbabilityOfCoactivation(r, bin, PROB) :-
    BrainRegionActivation(r, study) //
    (
        RightBinActivation(bin, study)
    & SelectedStudy(study)
    )

ProbabilityOfNoCoactivation(r, bin, PROB) :-
    BrainRegionActivation(r, study) //
    (
        NotRightBinActivation(bin, study)
    & SelectedStudy(study)
    )

CoactivationPatternOfBin(bin, r) :-
    ProbabilityOfCoactivation(r, bin, p1)
    & ProbabilityOfNoCoactivation(r, bin, p0)
    & LOR = log10(p1/(1 - p1))/(p0/(1 - p0))
    & LOR > 0.5

ans(bin, r) :- CoactivationPatternOfBin(bin, r)
```

1 4.8 Inferring specific structure-function associations using NeuroLang 2 segregation queries

3 We infer specific structure-function associations by estimating the extent to which a spatially-
4 localized activation along the principal gradient in the LPFC predicts a Neurosynth topic's
5 presence in a study. For this purpose, we write NeuroLang programs (see below) that includes
6 what we call "segregation queries".

7 Intra-hemispheric segregation queries infer "the probability that a topic is present in a study
8 given spatially-constrained activation within a range of quintile bins and the **simultaneous**
9 **absence of activation outside this range within the same hemisphere**". Concurrently,
10 a segregation query infers the probability of the opposite hypothesis: a topic is present given
11 no activation within the range of quintile bins **or** there exists activation outside the range. The
12 LOR of these two hypotheses gives us a measure of evidence in favor of association between a
13 topic and patterns of activity along the principal gradient. The NeuroLang program that infers
14 specific structure-function associations in the left LPFC using segregation queries is as follows:

```
LeftBinActivation(bin, study) :-  
    LeftBinVoxel(bin, x, y, z)  
    & PeakReported(x2, y2, z2, study)  
    & distance = EUCLIDEAN(x, y, z, x2, y2, z2)  
    & distance < 3  
  
SegregationQuery(bin1, bin2, study) :-  
    LeftBinActivation(bin1, study)  
    & LeftBinActivation(bin2, study)  
    & (bin2 >= bin1)  
    & ~exists(bin3;  
        Bin(bin3) & (bin3 < bin1 | bin3 > bin2)  
        & Study(study) & LeftBinActivation(bin3, study))  
  
NotSegregationQuery(bin1, bin2, study) :-  
    Study(study)  
    & Bin(bin1) & Bin(bin2)  
    & ~SegregationQuery(bin1, bin2, study)  
  
TopicPresentGivenSegregationQuery(topic, bin1, bin2, PROB) :-  
    TopicInStudy(topic, study) //  
    (  
        SegregationQuery(bin1, bin2, study)  
    & SelectedStudy(study)  
    )  
  
TopicPresentGivenNotSegregationQuery(topic, bin1, bin2, PROB) :-  
    TopicInStudy(topic, study) //  
    (  
        NotSegregationQuery(bin1, bin2, study)  
    & SelectedStudy(study)  
    )  
  
TopicAssociationMatrix(topic, bin1, bin2, LOR) :-  
    TopicPresentGivenSegregationQuery(topic, bin1, bin2, p1)
```

```
& TopicPresentGivenNotSegregationQuery(topic, bin1, bin2, p0)
& LOR = log10(p1/(1 - p1))/(p0/(1 - p0))
```

```
ans(topic, bin1, bin2, LOR) :- TopicAssociationMatrix(topic, bin1, bin2, LOR)
```

1 We first declare the studies that report activations in each quintile bin of the left LPFC prin-
2 cipal gradient in a rule table `LeftBinActivation`. Then, we declare a segregation query which
3 first identifies the studies that report coactivation between each pair of quintile bins along the
4 principal gradient, `bin1` and `bin2`, under the conditions that (`bin2 >= bin1`) **and there exists**
5 **no** activation reported in any `bin3`, such that (`bin3 < bin1 | bin3 > bin2`). That is, activa-
6 tion in any bin that is outside the range [`bin1`, `bin2`] should not be present, whereas activation
7 in the range between the bins can exist. Here, “**there exists no**” is represented by `~exists`,
8 which is a combination of the negation operator and the existential quantifier. The results are
9 represented in a `SegregationQuery` rule table, which includes a row (`bin1`, `bin2`, `study`)
10 for bins (`bin1`, `bin2`) between which activation is reported in `study` that also satisfies the
11 segregation condition. Concurrently, we declare the studies that do not match the conditions
12 of the segregation query, and represent them in the rule table `NotSegregationQuery`.

13 After defining the useful predicates, the program infers the conditional probability that a
14 `topic` is present in a `study` given the presence as well as absence of the segregation condition.
15 The results are represented in the tables `TopicPresentGivenSegregation` and `TopicPresentGivenNotSegrega`
16 Finally, the answer to our query, represented in the rule table `TopicBinsAssociationMatrix`,
17 is derived by computing the “LOR” of the two hypotheses as a measure of evidence in favor of
18 specific association between each topic `topic` and activation in a quintile range [`bin1`, `bin2`]
19 along the principal gradient. To ensure that the results are not driven by a single choice of stud-
20 ies, we run this NeuroLang program 1000 times using random sub-samples of the Neurosynth
21 database (80% of the dataset) in each run. This procedure creates an empirical distribution for
22 each probability estimation from which we consider the 95th percentile as a point estimate of
23 interest. The NeuroLang program that infers specific topic associations of coactivation patterns
24 within the right LPFC is as follows:

```
RightBinActivation(bin, study) :-
  RightBinVoxel(bin, x, y, z)
  & PeakReported(x2, y2, z2, study)
  & distance = EUCLIDEAN(x, y, z, x2, y2, z2)
  & distance < 3

SegregationQuery(bin1, bin2, study) :-
  RightBinActivation(bin1, study)
  & RightBinActivation(bin2, study)
  & (bin2 >= bin1)
  & ~exists(bin3;
    Bin(bin3) & (bin3 < bin1 | bin3 > bin2)
    & Study(study) & RightBinActivation(bin3, study))

NotSegregationQuery(bin1, bin2, study) :-
  Study(study)
  & Bin(bin1) & Bin(bin2)
  & ~SegregationQuery(bin1, bin2, study)

TopicPresentGivenSegregationQuery(topic, bin1, bin2, PROB) :-
  TopicInStudy(topic, study) //
  (
    SegregationQuery(bin1, bin2, study)
```



```
& SelectedStudy(study)
)
```

```
TopicPresentGivenNotSegregationQuery(topic, bin1, bin2, PROB) :-
  TopicInStudy(topic, study) //
  (
    NotSegregationQuery(bin1, bin2, study)
    & SelectedStudy(study)
  )
```

```
TopicAssociationMatrix(topic, bin1, bin2, LOR) :-
  TopicPresentGivenSegregationQuery(topic, bin1, bin2, p1)
  & TopicPresentGivenNotSegregationQuery(topic, bin1, bin2, p0)
  & LOR = log10(p1/(1 - p1))/(p0/(1 - p0))
```

```
ans(topic, bin1, bin2, LOR) :- TopicAssociationMatrix(topic, bin1, bin2, LOR)
```

1 Finally, we write a program that performs inter-hemispheric segregation queries to infer the
 2 probability “that a topic is present given activation in a right LPFC quintile bin and there exists
 3 no reported activation in the entire left LPFC”. The program also infers the probability of the
 4 opposite hypothesis; “a topic is present given activation in a left LPFC quintile bin and there
 5 exists no reported activation in the entire right LPFC”. The NeuroLang program that infers
 6 hemisphere-specific topic-bin associations is as follows:

```
LeftBinActivation(bin, study) :-
  LeftBinVoxel(bin, x, y, z)
  & PeakReported(x2, y2, z2, study)
  & distance = EUCLIDEAN(x, y, z, x2, y2, z2)
  & distance < 3
```

```
RightBinActivation(bin, study) :-
  RightBinVoxel(bin, x, y, z)
  & PeakReported(x2, y2, z2, study)
  & distance = EUCLIDEAN(x, y, z, x2, y2, z2)
  & distance < 3
```

```
OnlyLeftBinActivation(bin, study) :-
  LeftBinActivation(bin, study)
  & ~exists(bin2;
    Bin(bin2)
    & Study(study) & RightBinActivation(bin2, study)
  )
```

```
OnlyRightBinActivation(bin, study) :-
  RightBinActivation(bin, study)
  & ~exists(bin2;
    Bin(bin2)
    & Study(study) & LeftBinActivation(bin2, study))
```

```
TopicPresentGivenOnlyLeftBinActivation(topic, bin, PROB) :-
  TopicInStudy(topic, study) //
  (
```

```
    OnlyLeftBinActivation(bin, study)
  & SelectedStudy(study)
)

TopicPresentGivenOnlyRightBinActivation(topic, bin, PROB) :-
  TopicInStudy(topic, study) //
  (
    OnlyRightBinActivation(bin, study)
  & SelectedStudy(study)
  )

InterHemisphereTopicBinAssociation(topic, bin, LOR) :-
  TopicPresentGivenOnlyRightBinActivation(topic, bin, p1)
  & TopicPresentGivenOnlyLeftBinActivation(topic, bin, p2)
  & LOR = log10(p1/(1 - p1))/(p2/(1 - p2))

ans(topic, bin, LOR) :- InterHemisphereTopicBinAssociation(topic, bin, LOR)
```

1 In this program, we define the predicates `LeftBinActivation` and `RightBinActivation`
2 that store the studies reporting activation in each quintile bin of the principal gradient in the
3 left and right LPFC, respectively. Then we declare the inter-hemispheric segregation queries
4 using the negation operator and the existential quantifier, `~exists`, and stores the results in
5 `OnlyLeftBinActivation` and `OnlyRightBinActivation`. Subsequently, the program infers the
6 conditional probabilities that a `topic` is present in a `study` when given activation either in a left
7 or a right quintile bin. The final answer, `InterHemisphereTopicBinAssociation` is derived by
8 computing the “LOR” of the two hypotheses. We run this NeuroLang program 1000 times using
9 random sub-samples of the Neurosynth database (80% of the dataset) in each run, which yields
10 an empirical distribution for each conditional probability estimation from which we consider
11 the 95th percentile as the point estimate of interest.

12 5 Data Availability Statement

13 All data and scripts used in this study are openly available to be accessed and freely used
14 by the community. The source code of NeuroLang is freely available on GitHub at <https://github.com/NeuroLang/NeuroLang>.
15

16 6 Acknowledgements

17 This work is funded by the ERC-2017-STG NeuroLang grant. We are grateful to Jonas Renault
18 who worked on optimising NeuroLang’s engine and develop its web interface.

19 7 Competing interests

20 The authors claim no competing interests for this study.

References

- [1] Joaquin Fuster. *The prefrontal cortex*. Academic Press, 2015.

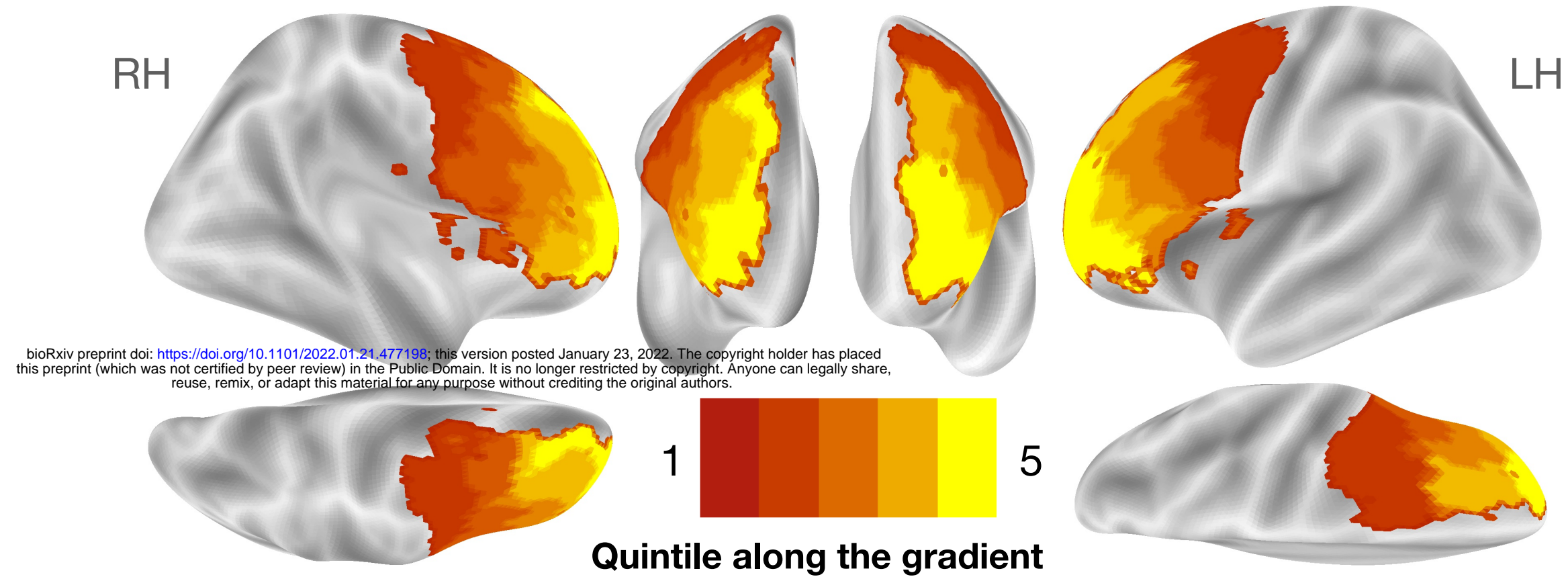
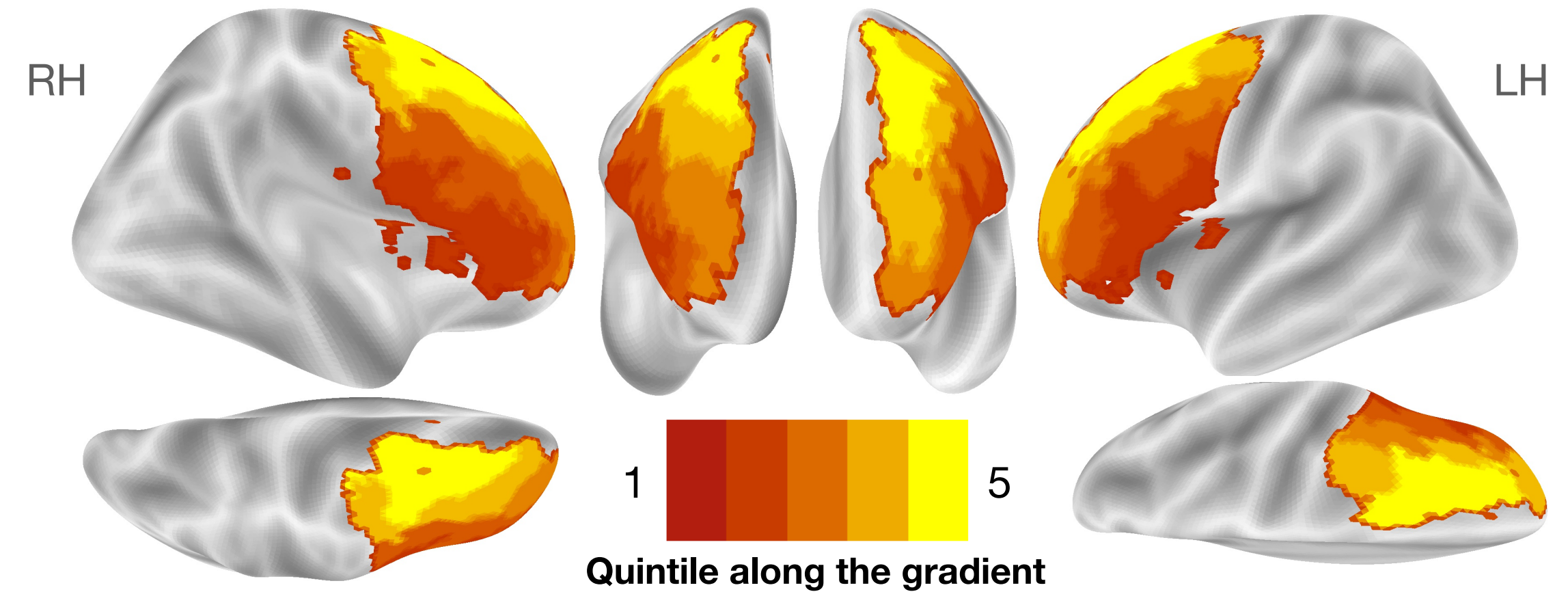
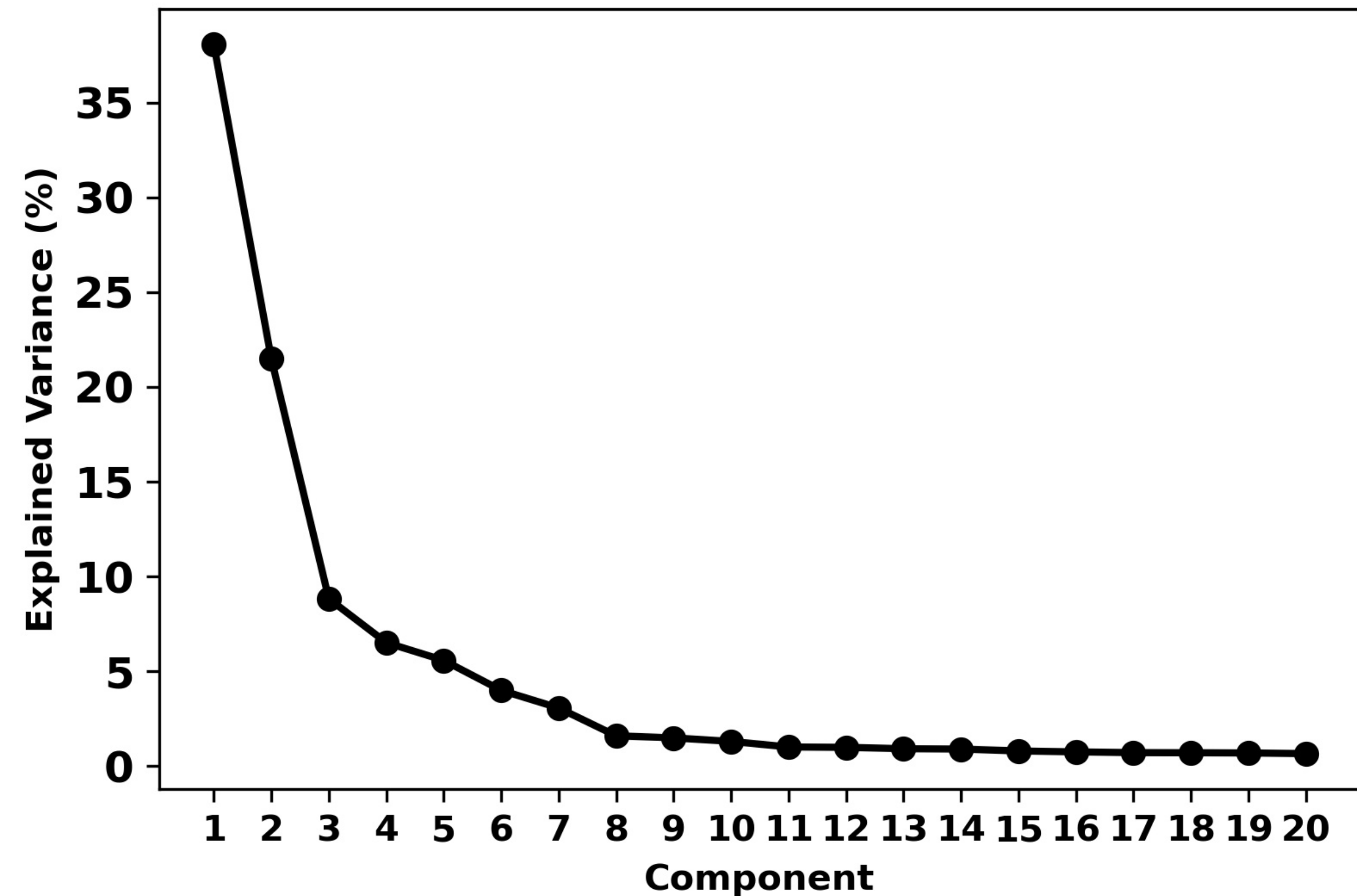
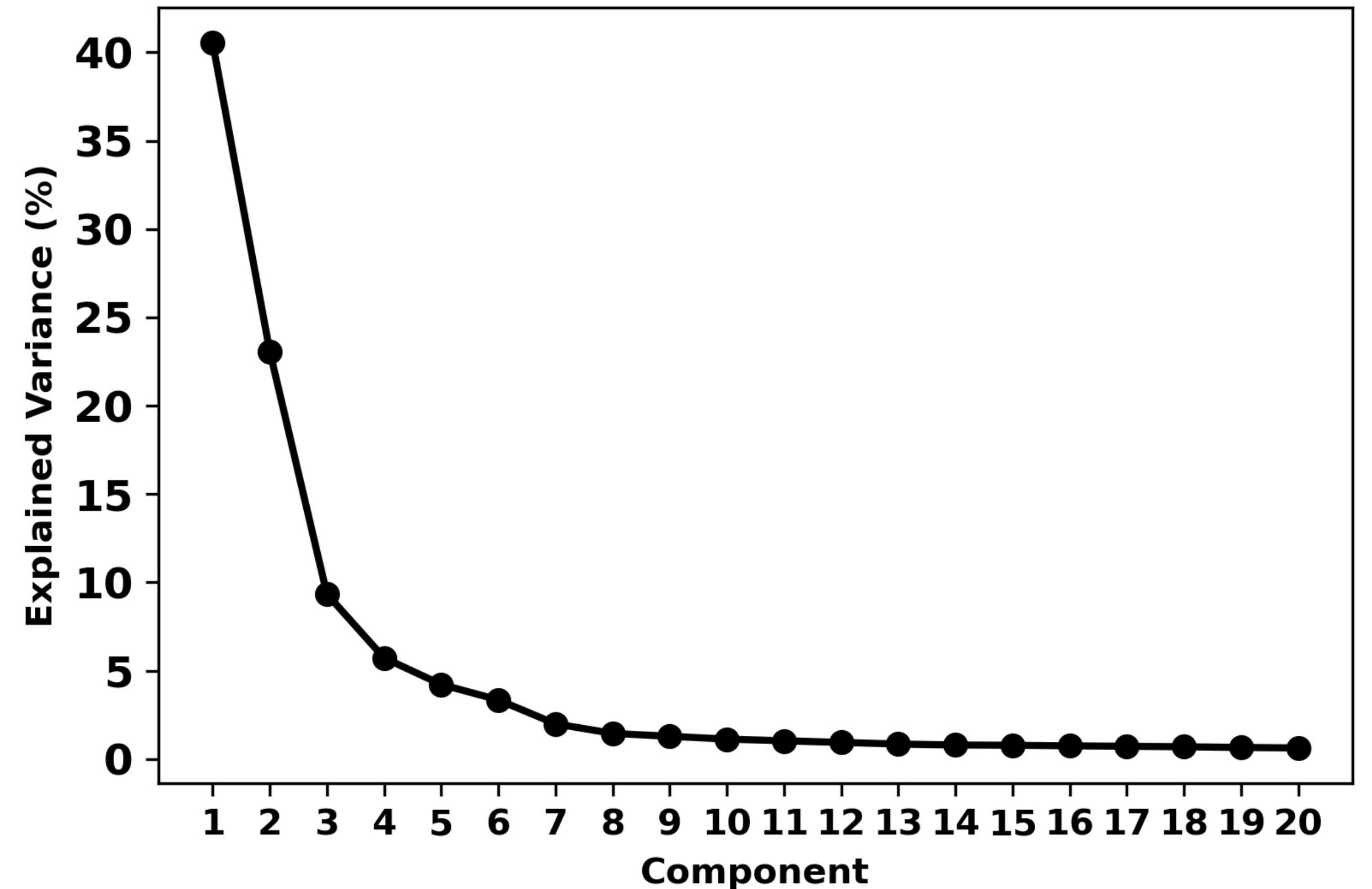
- [2] Michael Petrides. Lateral prefrontal cortex: architectonic and functional organization. *Philosophical Transactions of the Royal Society B: Biological Sciences*, 360(1456):781–795, 2005.
- [3] David Badre and Mark D’Esposito. Is the rostro-caudal axis of the frontal lobe hierarchical? *Nature Reviews Neuroscience*, 10(9):659–669, 2009.
- [4] John Duncan. The multiple-demand (md) system of the primate brain: mental programs for intelligent behaviour. *Trends in cognitive sciences*, 14(4):172–179, 2010.
- [5] Alexandros Goulas, Harry BM Uylings, and Peter Stiers. Unravelling the intrinsic functional organization of the human lateral frontal cortex: a parcellation scheme based on resting state fmri. *Journal of Neuroscience*, 32(30):10238–10252, 2012.
- [6] Derek Evan Nee and Mark D’Esposito. The hierarchical organization of the lateral prefrontal cortex. *Elife*, 5:e12112, 2016.
- [7] Jeremy R Reynolds, Randall C O’Reilly, Jonathan D Cohen, and Todd S Braver. The function and organization of lateral prefrontal cortex: a test of competing hypotheses. *PloS one*, 7(2):e30284, 2012.
- [8] Derek Evan Nee. Integrative frontal-parietal dynamics supporting cognitive control. *Elife*, 10:e57244, 2021.
- [9] Alejandro De La Vega, Tal Yarkoni, Tor D Wager, and Marie T Banich. Large-scale meta-analysis suggests low regional modularity in lateral frontal cortex. *Cerebral cortex*, 28(10):3414–3428, 2018.
- [10] Matthew L Dixon, Alejandro De La Vega, Caitlin Mills, Jessica Andrews-Hanna, R Nathan Spreng, Michael W Cole, and Kalina Christoff. Heterogeneity within the frontoparietal control network and its relationship to the default and dorsal attention networks. *Proceedings of the National Academy of Sciences*, 115(7):E1598–E1607, 2018.
- [11] Etienne Koechlin, Chrystele Ody, and Frédérique Kouneiher. The architecture of cognitive control in the human prefrontal cortex. *Science*, 302(5648):1181–1185, 2003.
- [12] Carole Azuar, Pablo Reyes, Andrea Slachevsky, Emmanuelle Volle, Serge Kinkingnehun, Frédérique Kouneiher, Eduardo Bravo, Bruno Dubois, Etienne Koechlin, and Richard Levy. Testing the model of caudo-rostral organization of cognitive control in the human with frontal lesions. *Neuroimage*, 84:1053–1060, 2014.
- [13] David Badre. Cognitive control, hierarchy, and the rostro-caudal organization of the frontal lobes. *Trends in cognitive sciences*, 12(5):193–200, 2008.
- [14] Matthew M Botvinick. Hierarchical models of behavior and prefrontal function. *Trends in cognitive sciences*, 12(5):201–208, 2008.
- [15] Kalina Christoff and John DE Gabrieli. The frontopolar cortex and human cognition: Evidence for a rostrocaudal hierarchical organization within the human prefrontal cortex. *Psychobiology*, 28(2):168–186, 2000.
- [16] Hyeon-Ae Jeon and Angela D Friederici. Two principles of organization in the prefrontal cortex are cognitive hierarchy and degree of automaticity. *Nature Communications*, 4(1):1–8, 2013.

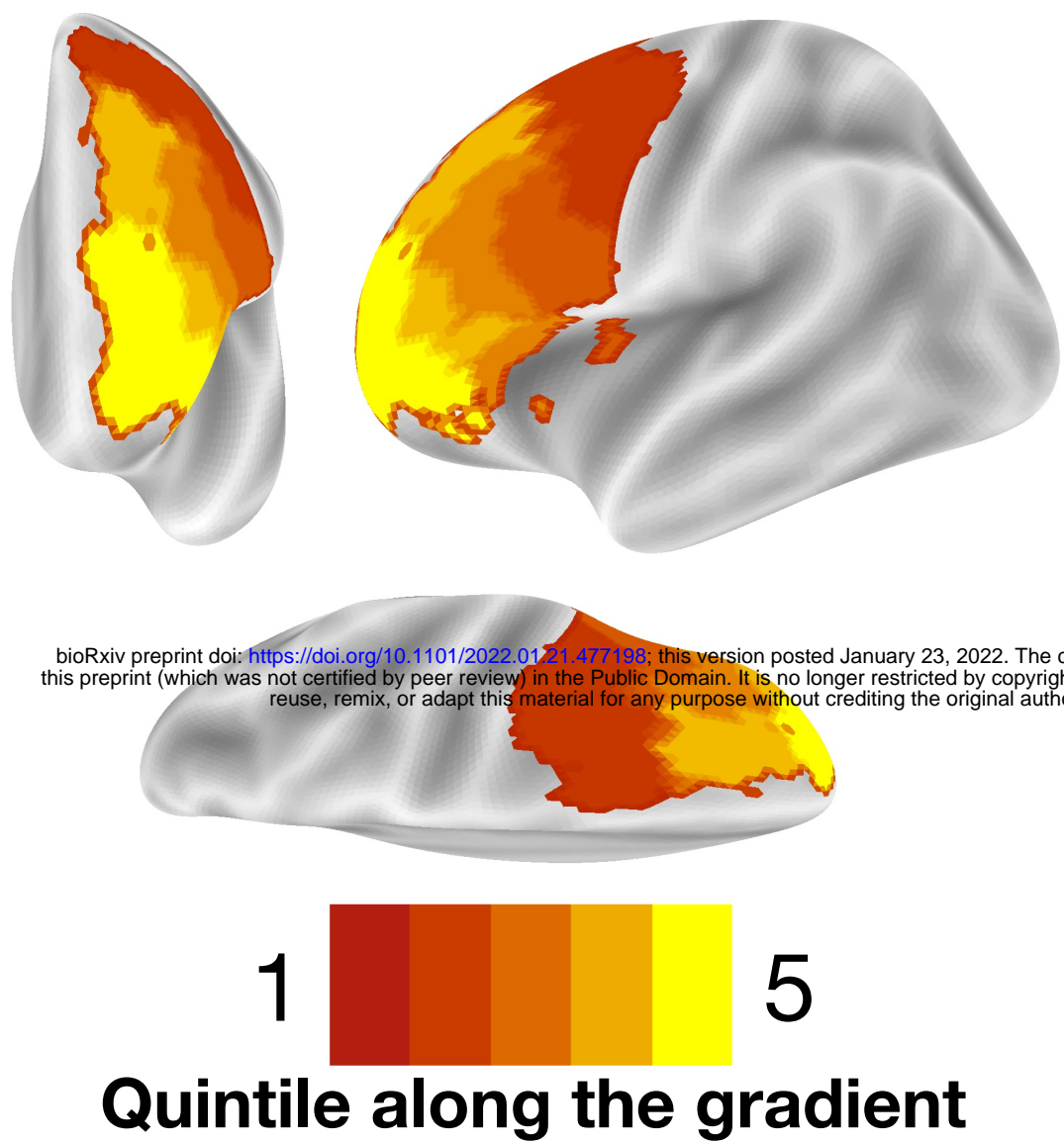
- [17] Christoffer Rahm, Benny Liberg, Maria Wiberg-Kristoffersen, Peter Aspelin, and Mussie Msghina. Rostro-caudal and dorso-ventral gradients in medial and lateral prefrontal cortex during cognitive control of affective and cognitive interference. *Scandinavian journal of psychology*, 54(2):66–71, 2013.
- [18] Valeria Parlatini, Joaquim Radua, Flavio Dell’Acqua, Anoushka Leslie, Andy Simmons, Declan G Murphy, Marco Catani, and Michel Thiebaut de Schotten. Functional segregation and integration within fronto-parietal networks. *Neuroimage*, 146:367–375, 2017.
- [19] Jörg Bahlmann, Robert S Blumenfeld, and Mark D’Esposito. The rostro-caudal axis of frontal cortex is sensitive to the domain of stimulus information. *Cerebral cortex*, 25(7):1815–1826, 2015.
- [20] Robert S Blumenfeld, Emi M Nomura, Caterina Gratton, and Mark D’Esposito. Lateral prefrontal cortex is organized into parallel dorsal and ventral streams along the rostro-caudal axis. *Cerebral Cortex*, 23(10):2457–2466, 2013.
- [21] Michael W Cole, Grega Repovš, and Alan Anticevic. The frontoparietal control system: a central role in mental health. *The Neuroscientist*, 20(6):652–664, 2014.
- [22] Evelina Fedorenko, Michael K Behr, and Nancy Kanwisher. Functional specificity for high-level linguistic processing in the human brain. *Proceedings of the National Academy of Sciences*, 108(39):16428–16433, 2011.
- [23] Scott Marek and Nico UF Dosenbach. The frontoparietal network: function, electrophysiology, and importance of individual precision mapping. *Dialogues in clinical neuroscience*, 20(2):133, 2018.
- [24] BT Thomas Yeo, Fenna M Krienen, Jorge Sepulcre, Mert R Sabuncu, Danial Lashkari, Marisa Hollinshead, Joshua L Roffman, Jordan W Smoller, Lilla Zöllei, Jonathan R Polimeni, et al. The organization of the human cerebral cortex estimated by intrinsic functional connectivity. *Journal of neurophysiology*, 2011.
- [25] Julia M Huntenburg, Pierre-Louis Bazin, and Daniel S Margulies. Large-scale gradients in human cortical organization. *Trends in cognitive sciences*, 22(1):21–31, 2018.
- [26] Daniel S Margulies, Satrajit S Ghosh, Alexandros Goulas, Marcel Falkiewicz, Julia M Huntenburg, Georg Langs, Gleb Bezgin, Simon B Eickhoff, F Xavier Castellanos, Michael Petrides, et al. Situating the default-mode network along a principal gradient of macroscale cortical organization. *Proceedings of the National Academy of Sciences*, 113(44):12574–12579, 2016.
- [27] Danilo Bzdok, Gaël Varoquaux, Olivier Grisel, Michael Eickenberg, Cyril Poupon, and Bertrand Thirion. Formal models of the network co-occurrence underlying mental operations. *PLoS computational biology*, 12(6):e1004994, 2016.
- [28] Derek Evan Nee and Mark D’Esposito. Causal evidence for lateral prefrontal cortex dynamics supporting cognitive control. *Elife*, 6:e28040, 2017.
- [29] David Badre and Derek Evan Nee. Frontal cortex and the hierarchical control of behavior. *Trends in cognitive sciences*, 22(2):170–188, 2018.
- [30] David F Abbott, Anthony B Waites, Leasha M Lillywhite, and Graeme D Jackson. fmri assessment of language lateralization: an objective approach. *Neuroimage*, 50(4):1446–1455, 2010.

- [31] H Garavan, TJ Ross, and EA Stein. Right hemispheric dominance of inhibitory control: an event-related functional mri study. *Proceedings of the National Academy of Sciences*, 96(14):8301–8306, 1999.
- [32] Adam R Aron. The neural basis of inhibition in cognitive control. *The neuroscientist*, 13(3):214–228, 2007.
- [33] Gesa Hartwigsen, Nicole E Neef, Julia A Camilleri, Daniel S Margulies, and Simon B Eickhoff. Functional segregation of the right inferior frontal gyrus: evidence from coactivation-based parcellation. *Cerebral Cortex*, 29(4):1532–1546, 2019.
- [34] Tirso Rene del Jesus Gonzalez Alam, Brontë LA Mckeown, Zhiyao Gao, Boris Bernhardt, Reinder Vos de Wael, Daniel S Margulies, Jonathan Smallwood, and Elizabeth Jefferies. A tale of two gradients: differences between the left and right hemispheres predict semantic cognition. *Brain Structure and Function*, pages 1–24, 2021.
- [35] Rotem Botvinik-Nezer, Felix Holzmeister, Colin F Camerer, Anna Dreber, Juergen Huber, Magnus Johannesson, Michael Kirchler, Roni Iwanir, Jeanette A Mumford, R Alison Adcock, et al. Variability in the analysis of a single neuroimaging dataset by many teams. *Nature*, 582(7810):84–88, 2020.
- [36] Robin G Jennings and John D Van Horn. Publication bias in neuroimaging research: implications for meta-analyses. *Neuroinformatics*, 10(1):67–80, 2012.
- [37] Benjamin O Turner, Erick J Paul, Michael B Miller, and Aron K Barbey. Small sample sizes reduce the replicability of task-based fmri studies. *Communications Biology*, 1(1): 1–10, 2018.
- [38] Peter T Fox, Jack L Lancaster, Angela R Laird, and Simon B Eickhoff. Meta-analysis in human neuroimaging: computational modeling of large-scale databases. *Annual review of neuroscience*, 37:409–434, 2014.
- [39] Veronika I Müller, Edna C Cieslik, Angela R Laird, Peter T Fox, Joaquim Radua, David Mataix-Cols, Christopher R Tench, Tal Yarkoni, Thomas E Nichols, Peter E Turkeltaub, et al. Ten simple rules for neuroimaging meta-analysis. *Neuroscience & Biobehavioral Reviews*, 84:151–161, 2018.
- [40] Tal Yarkoni, Russell A Poldrack, Thomas E Nichols, David C Van Essen, and Tor D Wager. Large-scale automated synthesis of human functional neuroimaging data. *Nature methods*, 8(8):665–670, 2011.
- [41] Derek Evan Nee, Joshua W Brown, Mary K Askren, Marc G Berman, Emre Demiralp, Adam Krawitz, and John Jonides. A meta-analysis of executive components of working memory. *Cerebral cortex*, 23(2):264–282, 2013.
- [42] Valentin Iovene and Demian Wassermann. Probabilistic programming in neurolang: Bridging the gap between cognitive science and statistical modeling. In *2020 OHBM-Annual Meeting of Organization for Human Brain Mapping*, 2020.
- [43] Kamalaker Dadi, Gaël Varoquaux, Antonia Machlouzardes-Shalit, Krzysztof J Gorgolewski, Demian Wassermann, Bertrand Thirion, and Arthur Mensch. Fine-grain atlases of functional modes for fmri analysis. *NeuroImage*, 221:117126, 2020.

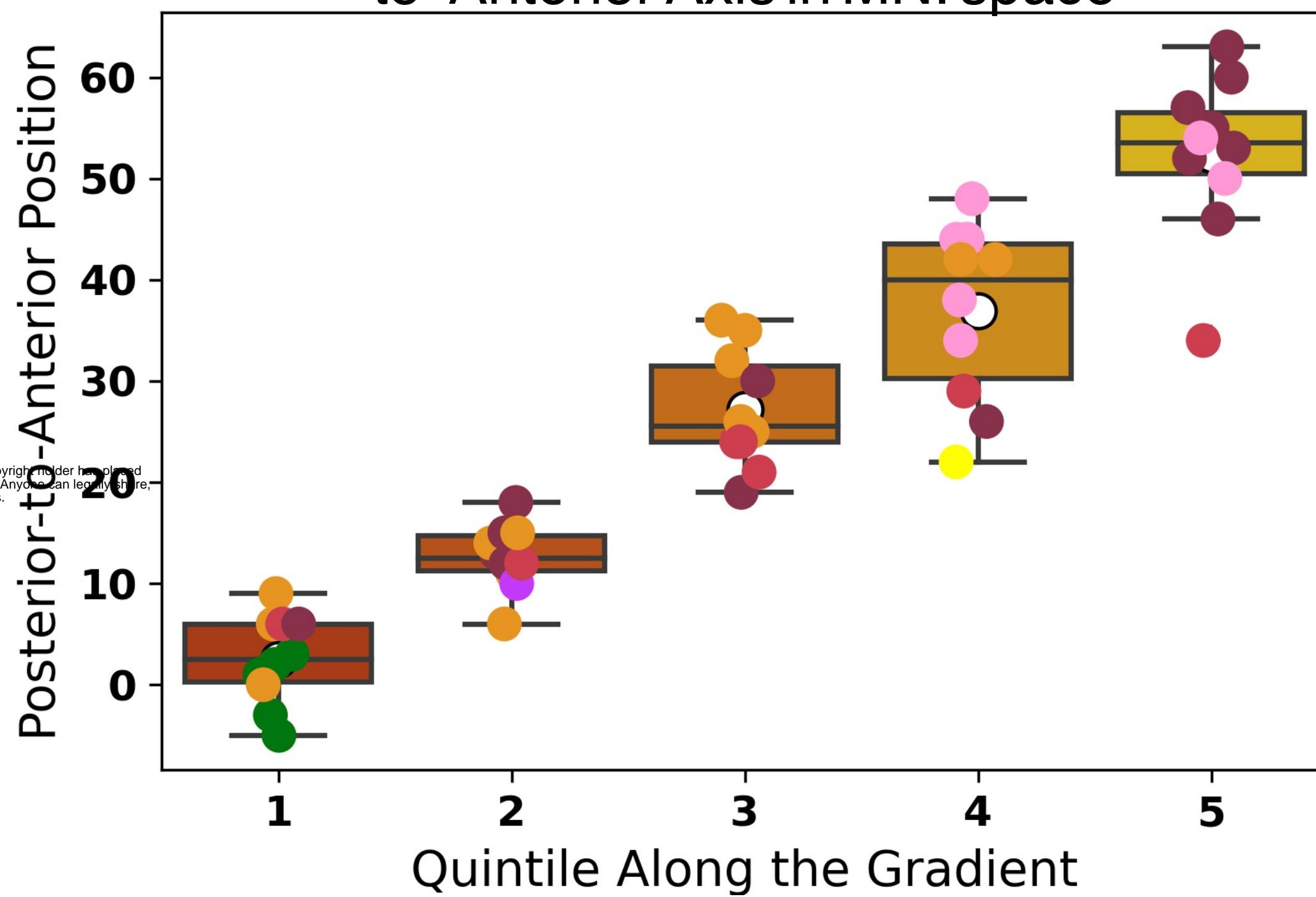
- [44] Christopher J Markiewicz, Krzysztof J Gorgolewski, Franklin Feingold, Ross Blair, Yaroslav O Halchenko, Eric Miller, Nell Hardcastle, Joe Wexler, Oscar Esteban, Mathias Goncavles, et al. The openneuro resource for sharing of neuroscience data. *Elife*, 10: e71774, 2021.
- [45] Ronald R Coifman, Stephane Lafon, Ann B Lee, Mauro Maggioni, Boaz Nadler, Frederick Warner, and Steven W Zucker. Geometric diffusions as a tool for harmonic analysis and structure definition of data: Diffusion maps. *Proceedings of the national academy of sciences*, 102(21):7426–7431, 2005.
- [46] Reinder Vos de Wael, Oualid Benkarim, Casey Paquola, Sara Lariviere, Jessica Royer, Shahin Tavakol, Ting Xu, Seok-Jun Hong, Georg Langs, Sofie Valk, et al. Brainspace: a toolbox for the analysis of macroscale gradients in neuroimaging and connectomics datasets. *Communications biology*, 3(1):1–10, 2020.
- [47] Tor D Wager, Martin Lindquist, and Lauren Kaplan. Meta-analysis of functional neuroimaging data: current and future directions. *Social cognitive and affective neuroscience*, 2(2):150–158, 2007.
- [48] Russell A Poldrack, Aniket Kittur, Donald Kalar, Eric Miller, Christian Seppa, Yolanda Gil, D Stott Parker, Fred W Sabb, and Robert M Bilder. The cognitive atlas: toward a knowledge foundation for cognitive neuroscience. *Frontiers in neuroinformatics*, 5:17, 2011.
- [49] Russell A Poldrack, Jeanette A Mumford, Tom Schonberg, Donald Kalar, Bishal Barman, and Tal Yarkoni. Discovering relations between mind, brain, and mental disorders using topic mapping. 2012.
- [50] Stephen J Gotts, Hang Joon Jo, Gregory L Wallace, Ziad S Saad, Robert W Cox, and Alex Martin. Two distinct forms of functional lateralization in the human brain. *Proceedings of the National Academy of Sciences*, 110(36):E3435–E3444, 2013.
- [51] John DE Gabrieli, Russell A Poldrack, and John E Desmond. The role of left prefrontal cortex in language and memory. *Proceedings of the national Academy of Sciences*, 95(3): 906–913, 1998.
- [52] Paolo Bartolomeo and Tal Seidel Malkinson. Hemispheric lateralization of attention processes in the human brain. *Current opinion in psychology*, 29:90–96, 2019.
- [53] Michel Thiebaut De Schotten, Flavio Dell’Acqua, Stephanie Forkel, Andrew Simmons, Francesco Vergani, Declan GM Murphy, and Marco Catani. A lateralized brain network for visuo-spatial attention. *Nature Precedings*, pages 1–1, 2011.
- [54] Carter Wendelken, David Chung, and Silvia A Bunge. Rostrolateral prefrontal cortex: Domain-general or domain-sensitive? *Human brain mapping*, 33(8):1952–1963, 2012.
- [55] Vinod Menon and Lucina Q Uddin. Saliency, switching, attention and control: a network model of insula function. *Brain structure and function*, 214(5-6):655–667, 2010.
- [56] M-Marsel Mesulam. From sensation to cognition. *Brain: a journal of neurology*, 121(6): 1013–1052, 1998.
- [57] Sabine Oligschläger, Julia M Huntenburg, Johannes Golchert, Mark E Lauckner, Tyler Bonnen, and Daniel S Margulies. Gradients of connectivity distance are anchored in primary cortex. *Brain Structure and Function*, 222(5):2173–2182, 2017.

- [58] Jonathan Smallwood, Boris C Bernhardt, Robert Leech, Danilo Bzdok, Elizabeth Jefferies, and Daniel S Margulies. The default mode network in cognition: a topographical perspective. *Nature Reviews Neuroscience*, pages 1–11, 2021.
- [59] Randy L Buckner and Fenna M Krienen. The evolution of distributed association networks in the human brain. *Trends in cognitive sciences*, 17(12):648–665, 2013.
- [60] Andrew J Westphal, Nicco Reggente, Kaori L Ito, and Jesse Rissman. Shared and distinct contributions of rostrolateral prefrontal cortex to analogical reasoning and episodic memory retrieval. *Human brain mapping*, 37(3):896–912, 2016.
- [61] Vyacheslav R Karolis, Maurizio Corbetta, and Michel Thiebaut de Schotten. The architecture of functional lateralisation and its relationship to callosal connectivity in the human brain. *Nature communications*, 10(1):1–9, 2019.
- [62] Mehraveh Salehi, Amin Karbasi, Daniel S Barron, Dustin Scheinost, and R Todd Constable. Individualized functional networks reconfigure with cognitive state. *NeuroImage*, 206:116233, 2020.
- [63] Gholamreza Salimi-Khorshidi, Stephen M Smith, John R Keltner, Tor D Wager, and Thomas E Nichols. Meta-analysis of neuroimaging data: a comparison of image-based and coordinate-based pooling of studies. *Neuroimage*, 45(3):810–823, 2009.
- [64] Krzysztof J Gorgolewski, Gael Varoquaux, Gabriel Rivera, Yannick Schwarz, Satrajit S Ghosh, Camille Maumet, Vanessa V Sochat, Thomas E Nichols, Russell A Poldrack, Jean-Baptiste Poline, et al. Neurovault. org: a web-based repository for collecting and sharing unthresholded statistical maps of the human brain. *Frontiers in neuroinformatics*, 9:8, 2015.
- [65] Russell A Poldrack and Tal Yarkoni. From brain maps to cognitive ontologies: informatics and the search for mental structure. *Annual review of psychology*, 67:587–612, 2016.
- [66] Arthur Mensch, Julien Mairal, Bertrand Thirion, and Gaël Varoquaux. Dictionary learning for massive matrix factorization. In *International Conference on Machine Learning*, pages 1737–1746. PMLR, 2016.
- [67] Guy Van den Broeck and Dan Suciu. Query processing on probabilistic data: A survey. *Foundations and Trends® in Databases*, 7(3-4), 2015.
- [68] S. Abiteboul, Richard Hull, and Victor Vianu. *Foundations of databases*. Addison-Wesley, Reading, Mass, 1995. ISBN 978-0-201-53771-0.
- [69] Koen V Haak, Andre F Marquand, and Christian F Beckmann. Connectopic mapping with resting-state fmri. *Neuroimage*, 170:83–94, 2018.

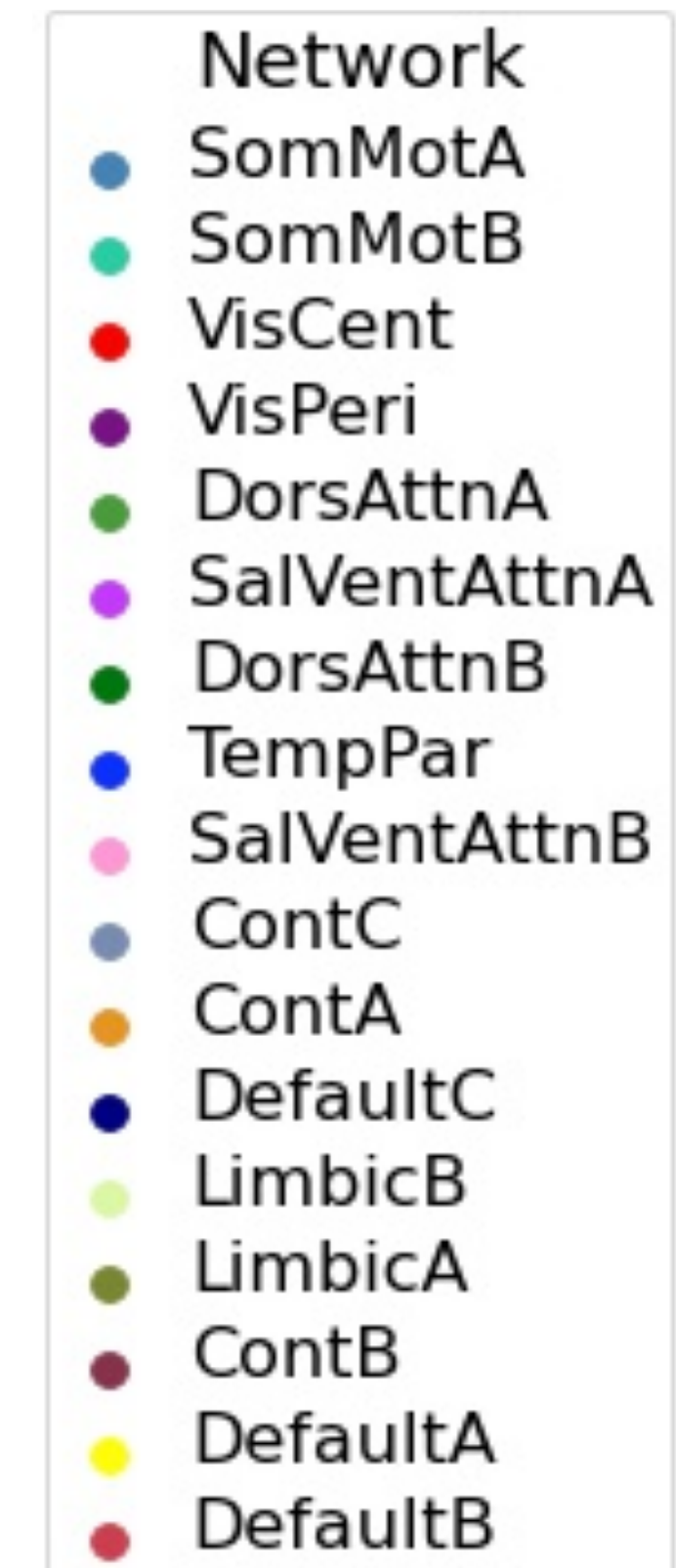
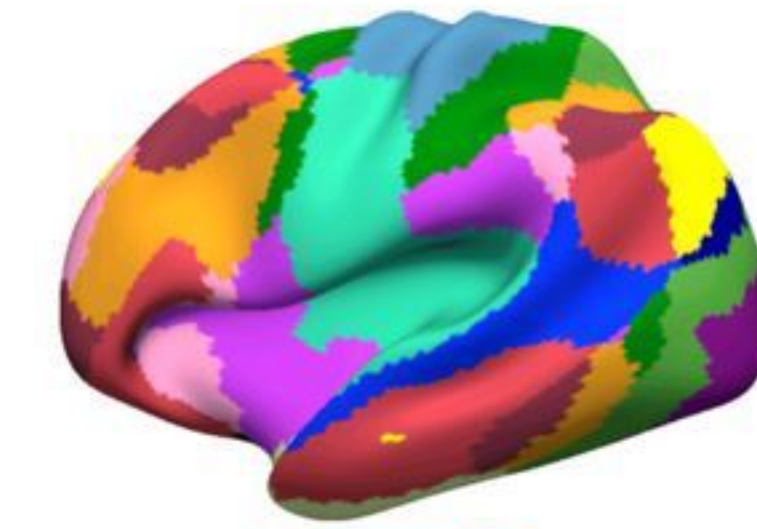
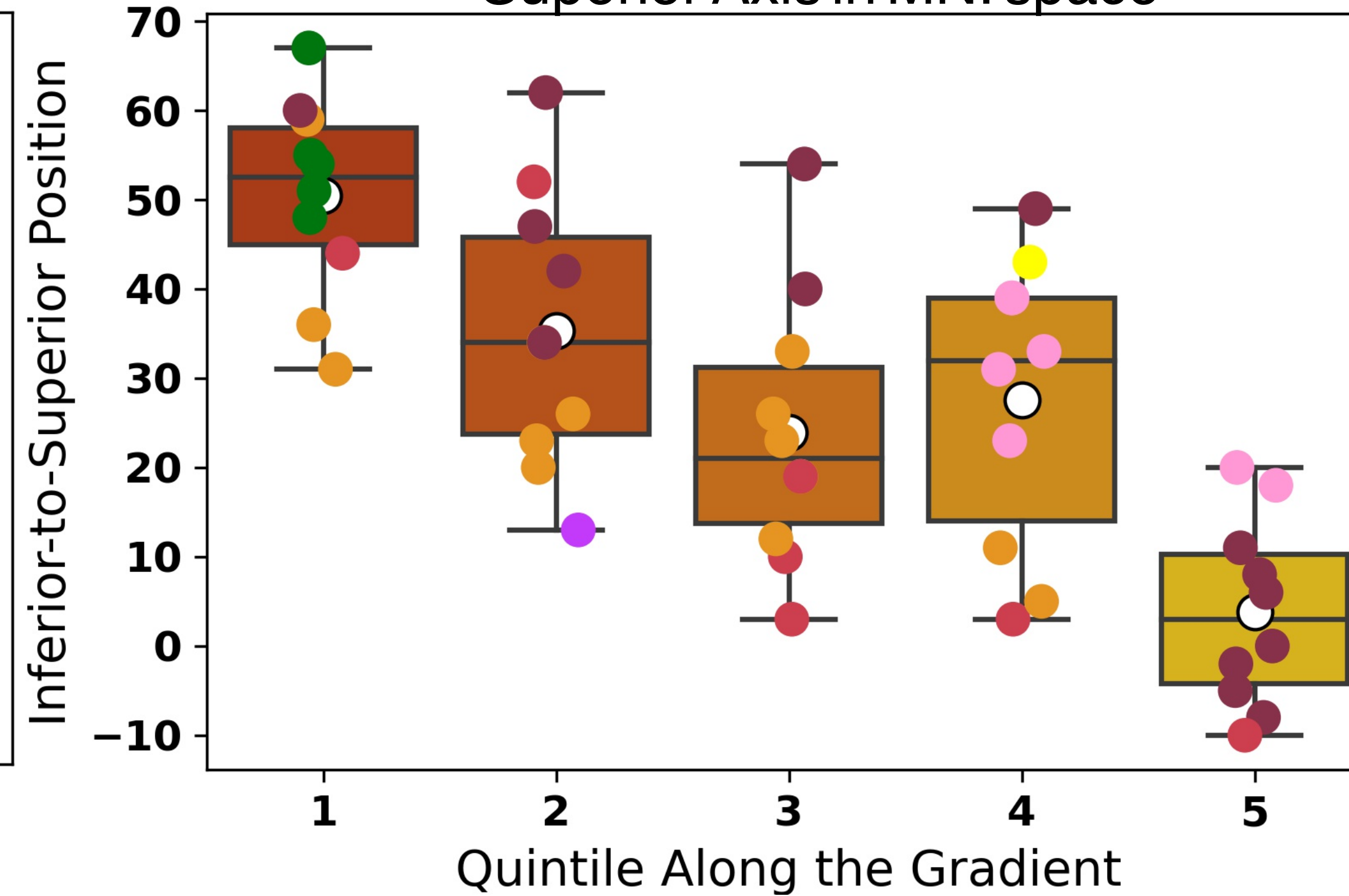
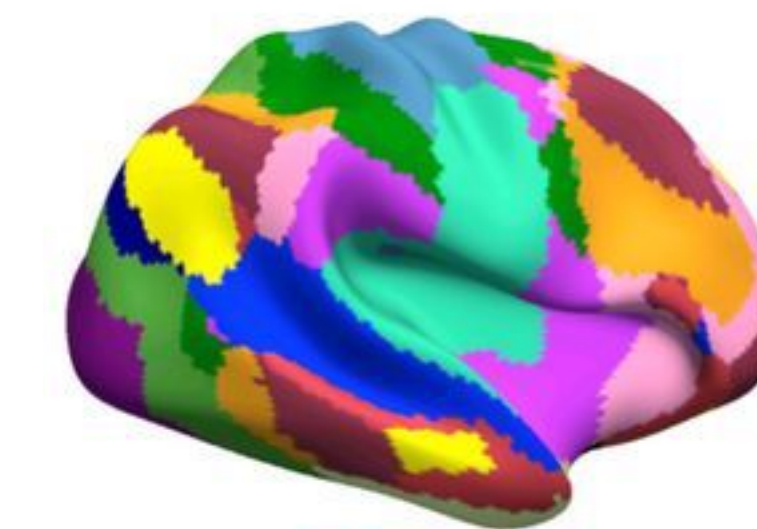
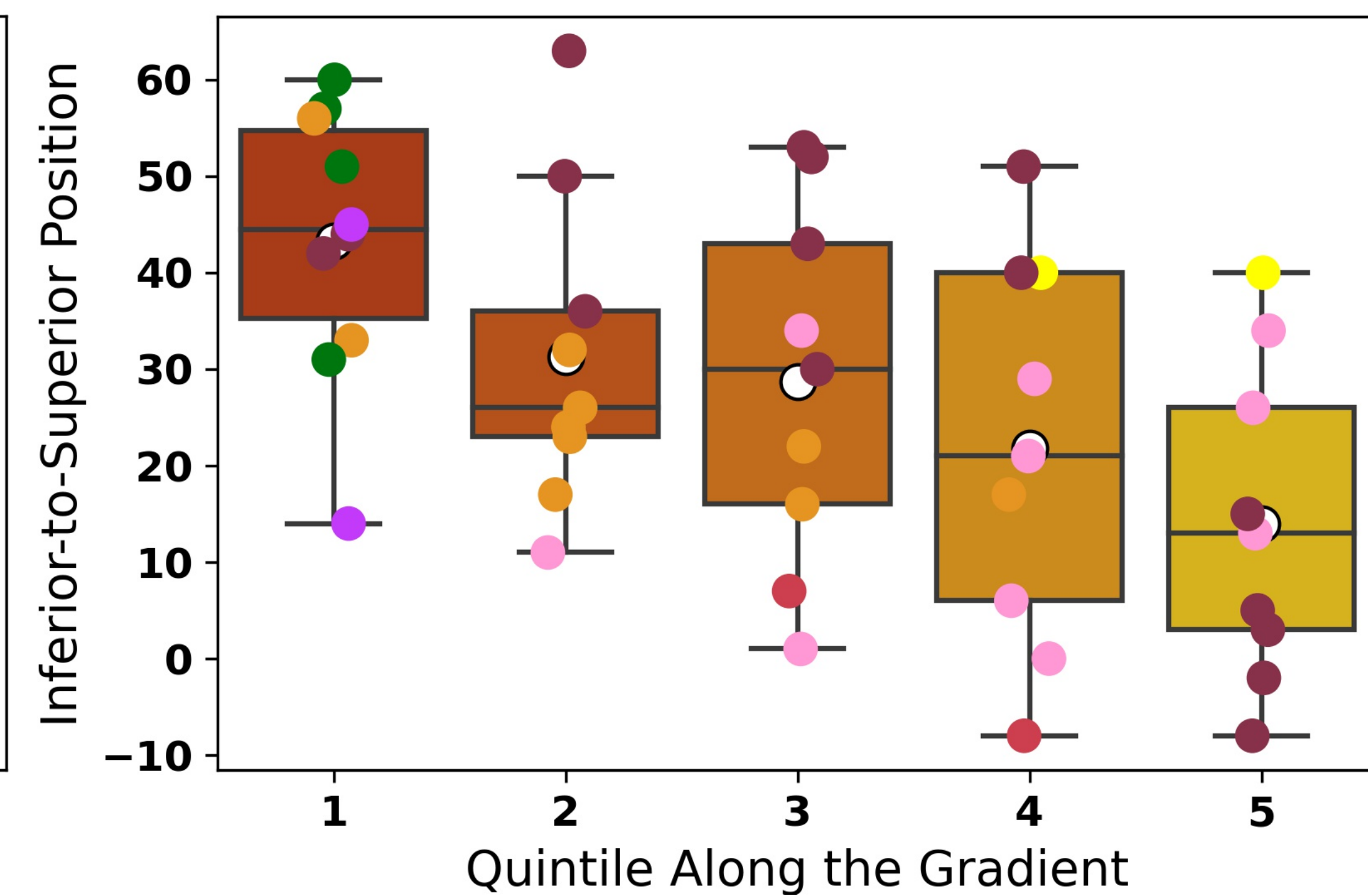
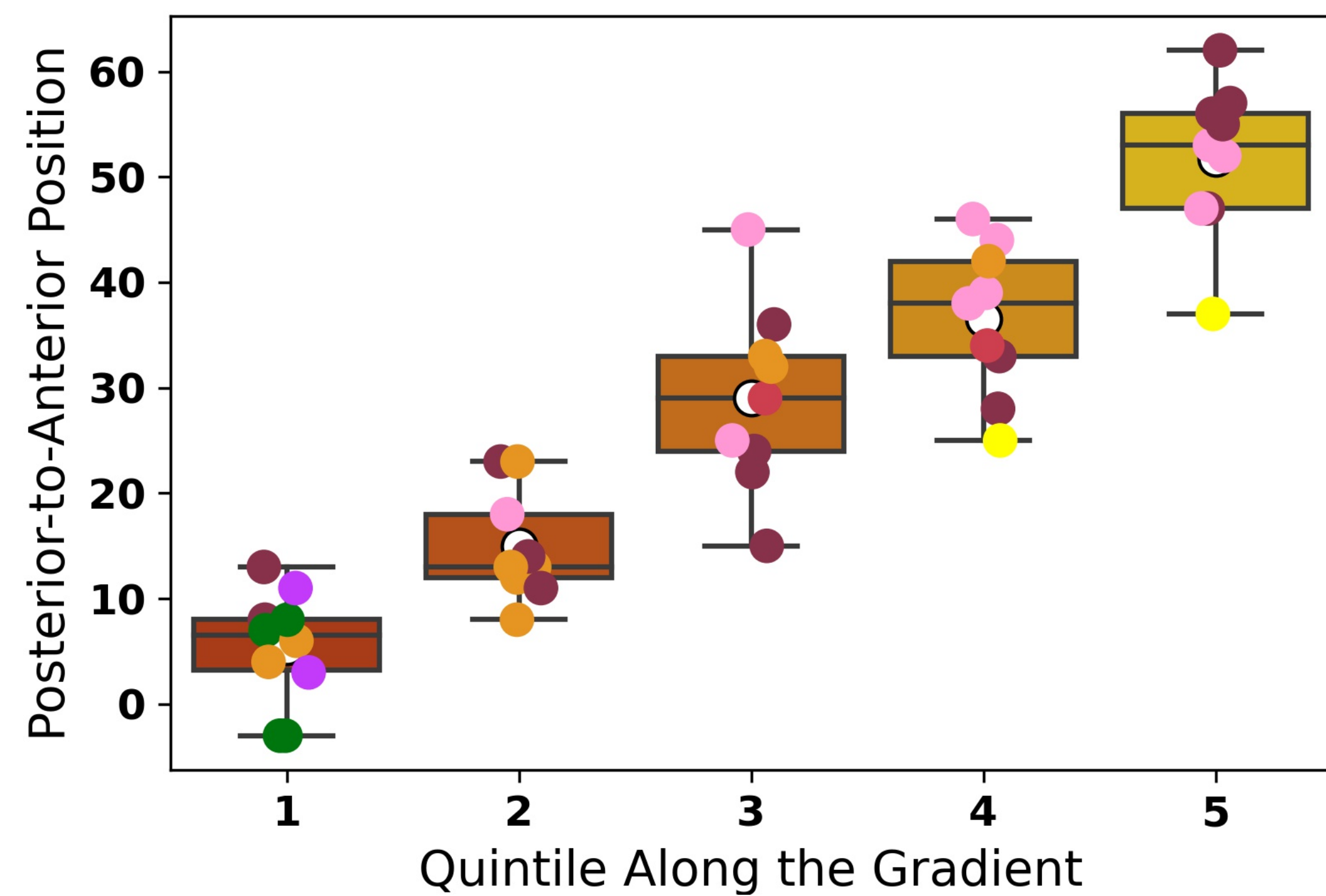
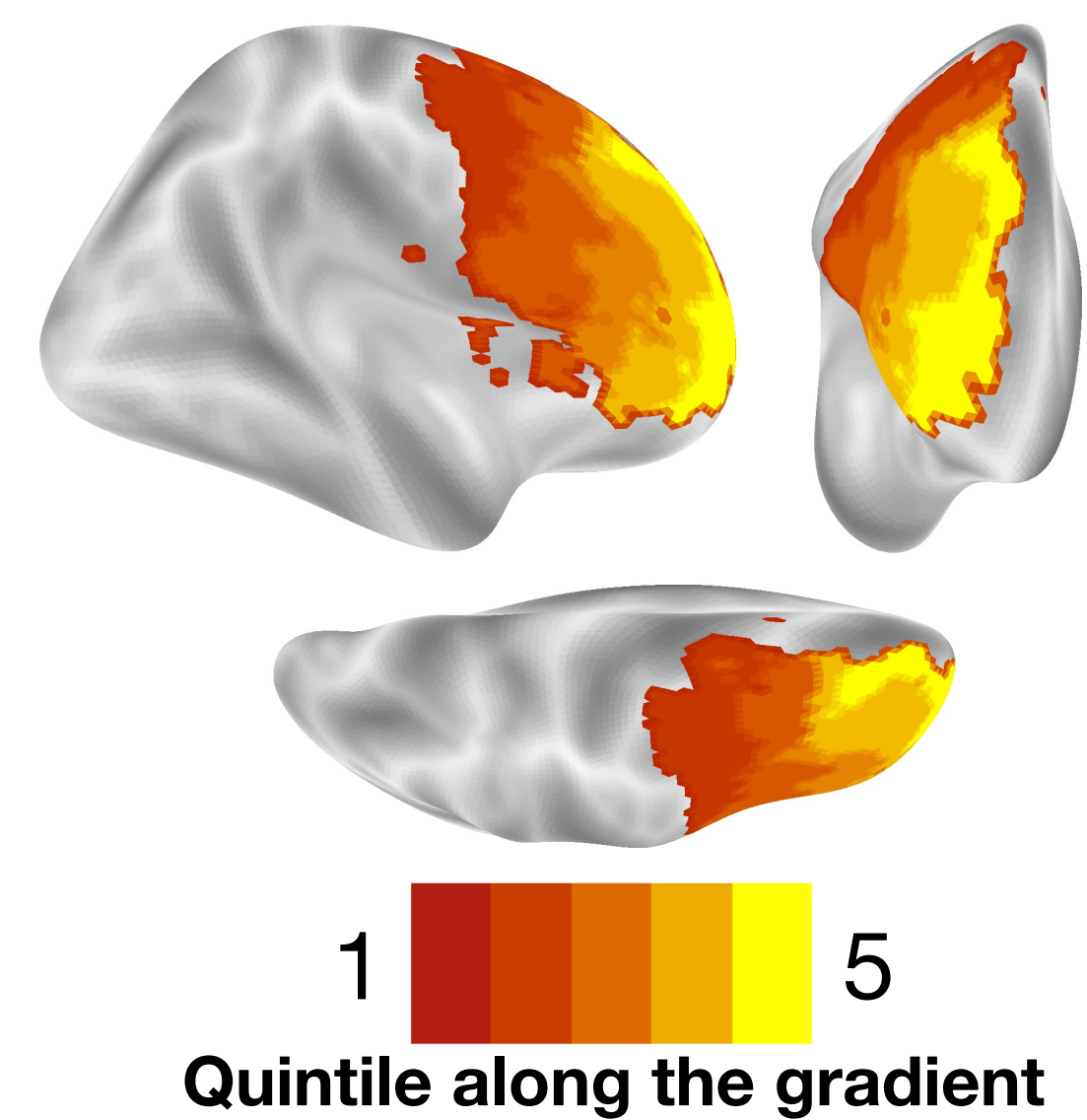
A Principal Gradient of Coactivation-based Connectivity in the LPFC**B** Second Gradient of Coactivation-based Connectivity in the LPFC**C** Percentage of Variance Explained by Diffusion Embedding Components in the Right Hemisphere**D** Percentage of Variance Explained by Diffusion Embedding Components in the Left Hemisphere

A Left Hemisphere

Positions of Quintiles Along the Posterior-to-Anterior Axis in MNI space

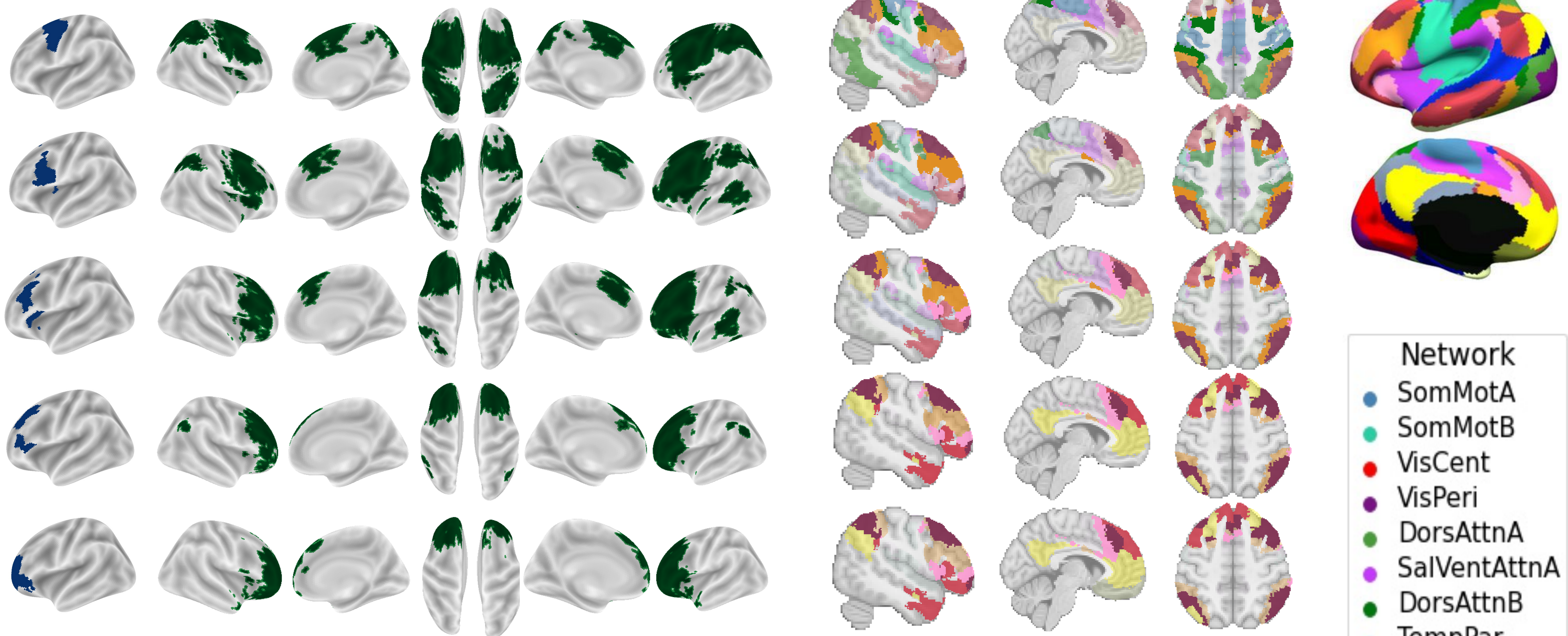


Positions of Quintiles Along the Inferior-to-Superior Axis in MNI space

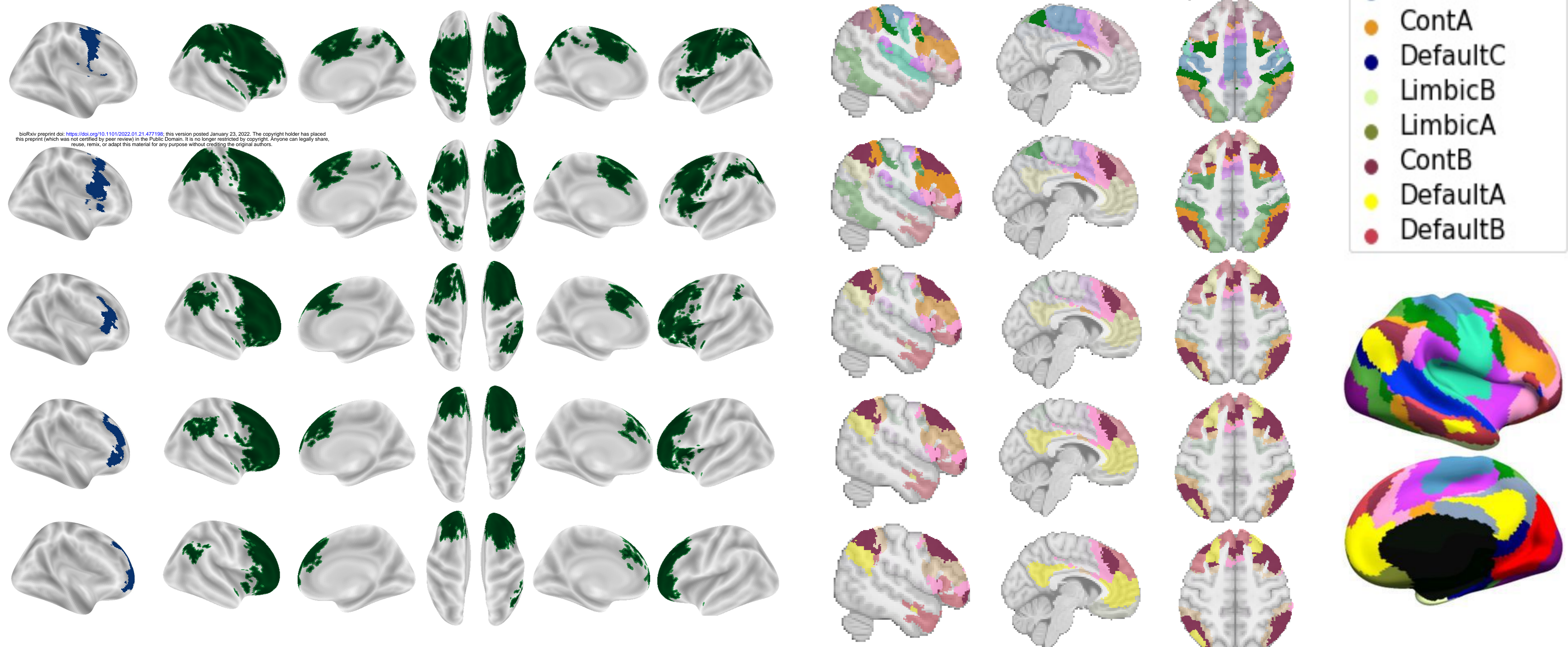
**B** Right Hemisphere

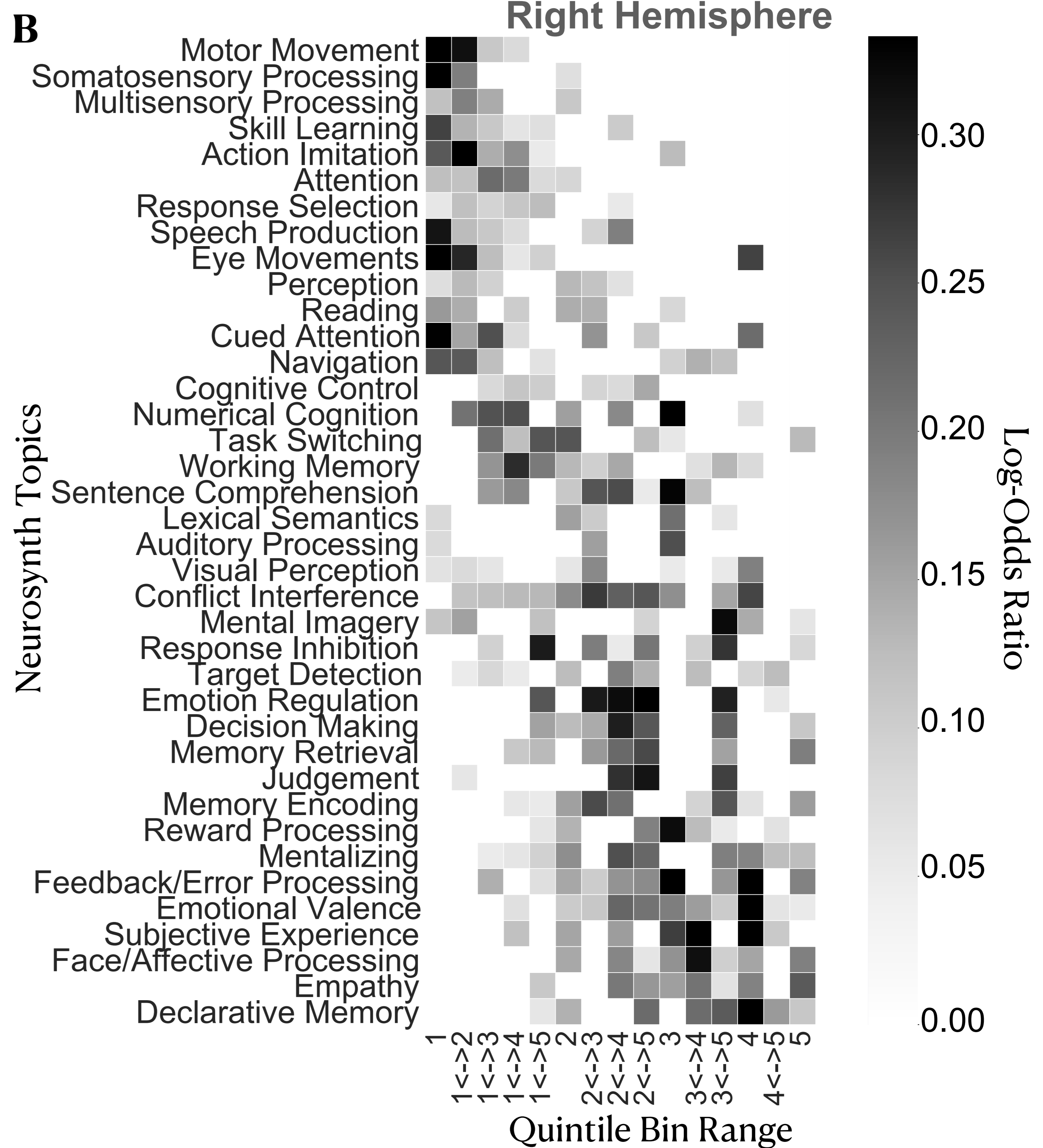
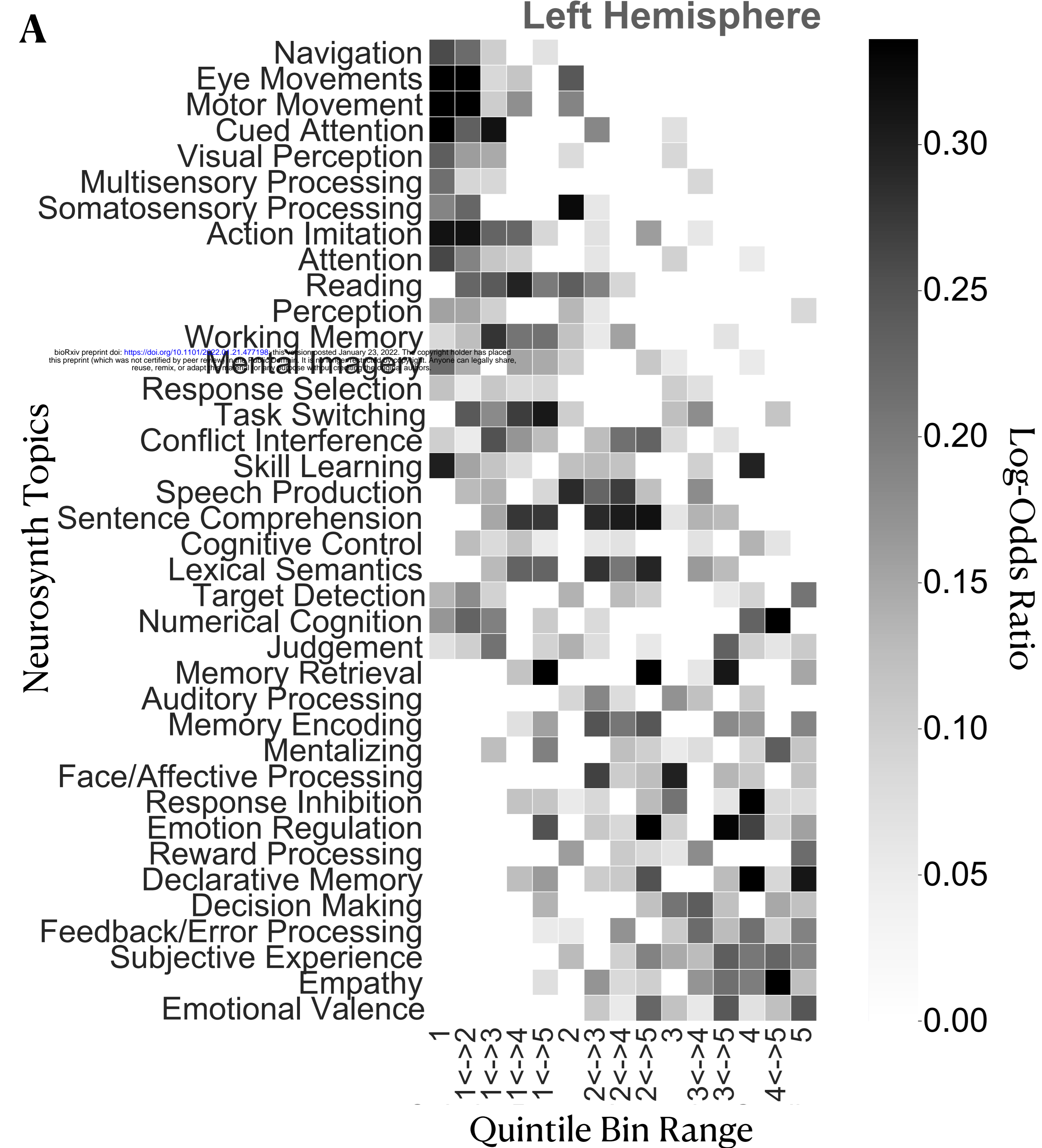
A**Bins 1-5****Left Hemisphere**
Coactivation Patterns

Network Overlap

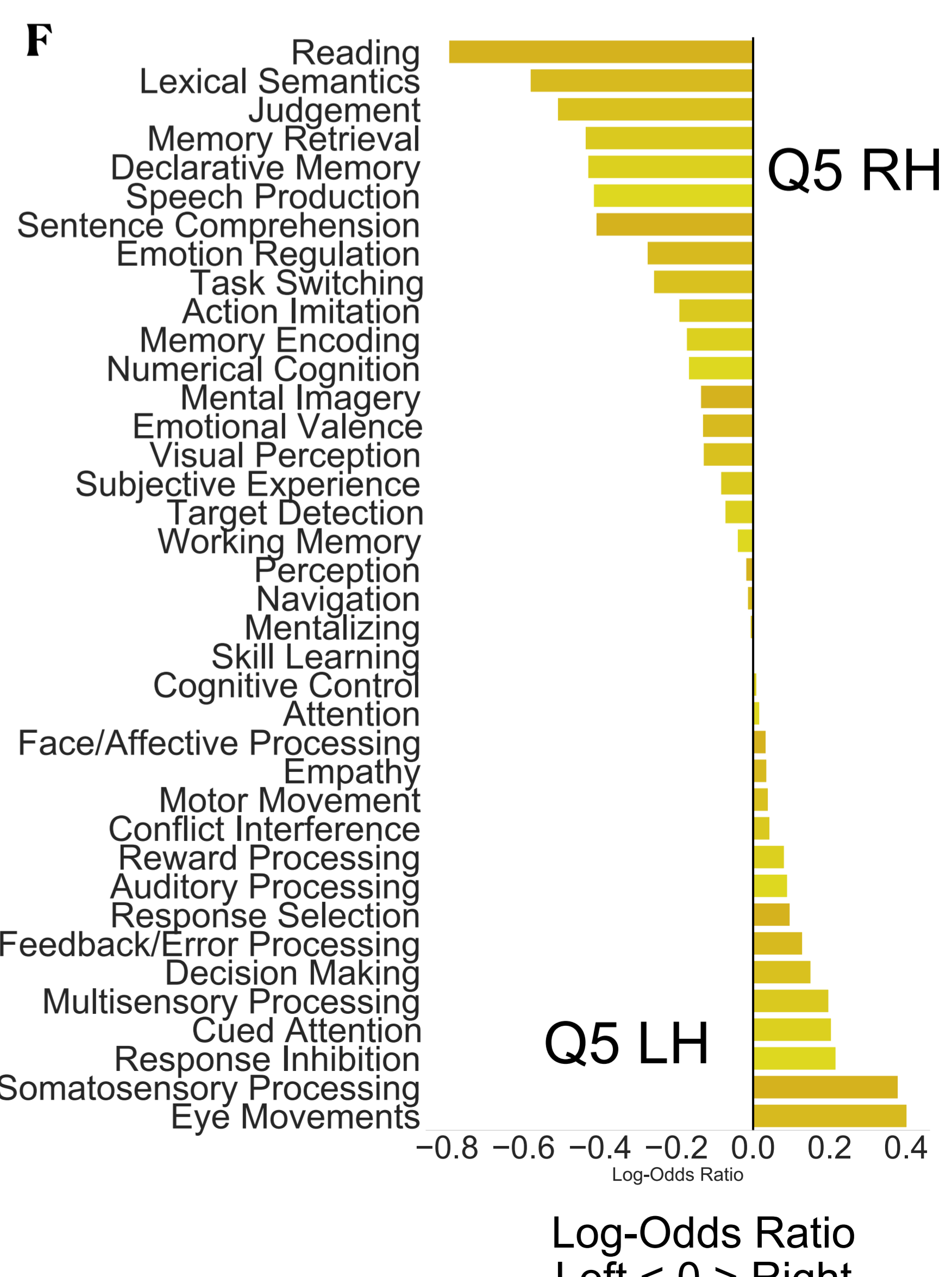
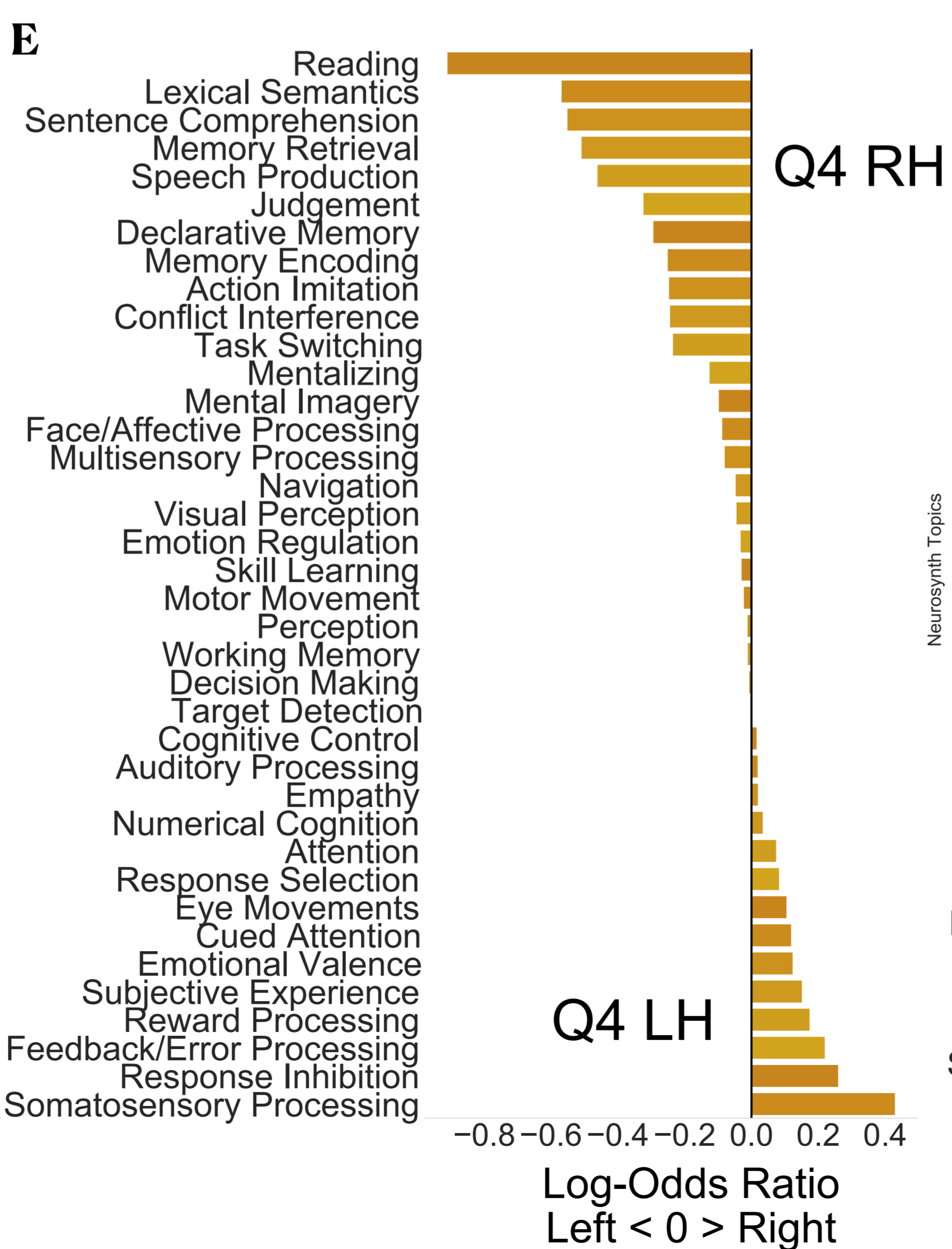
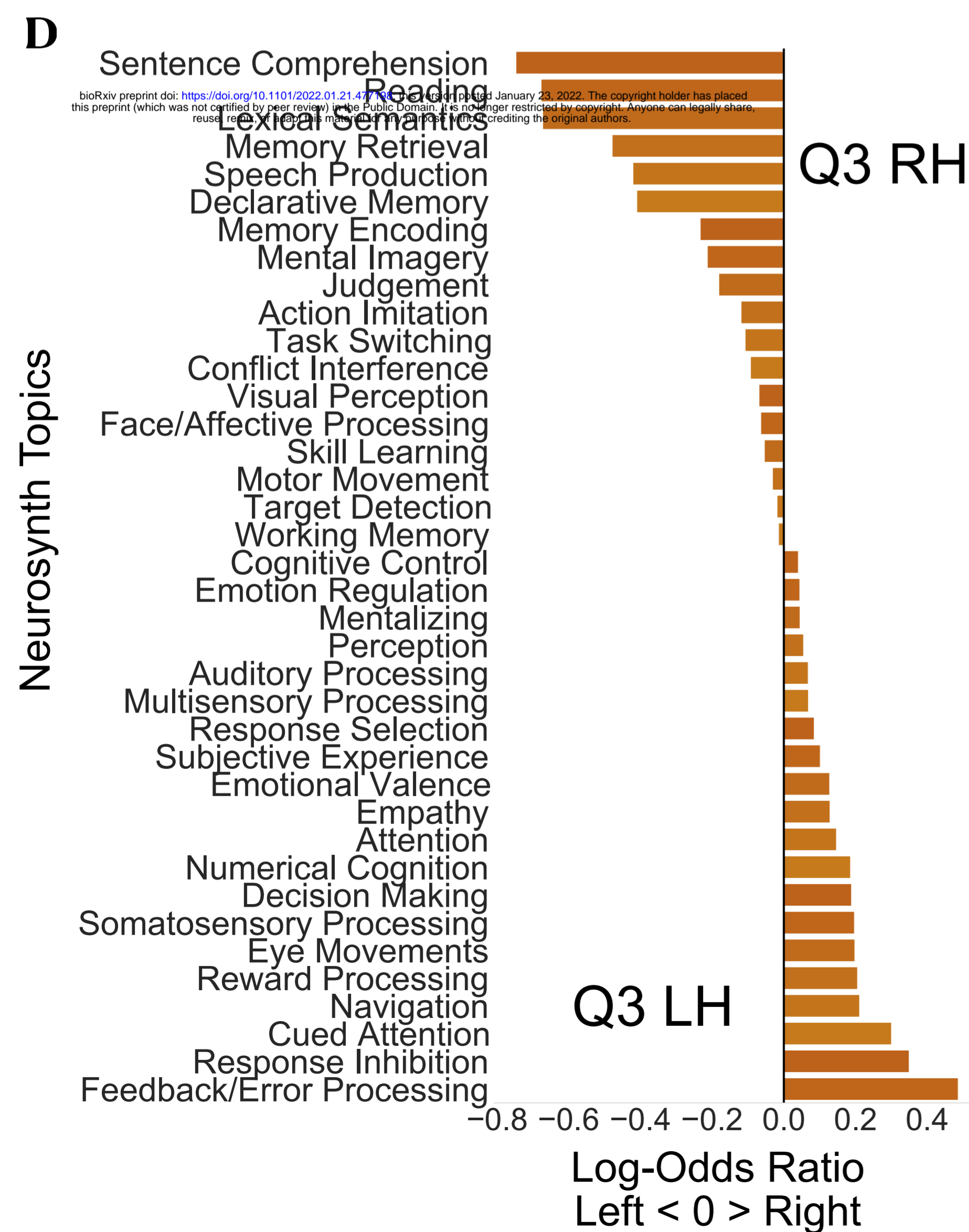
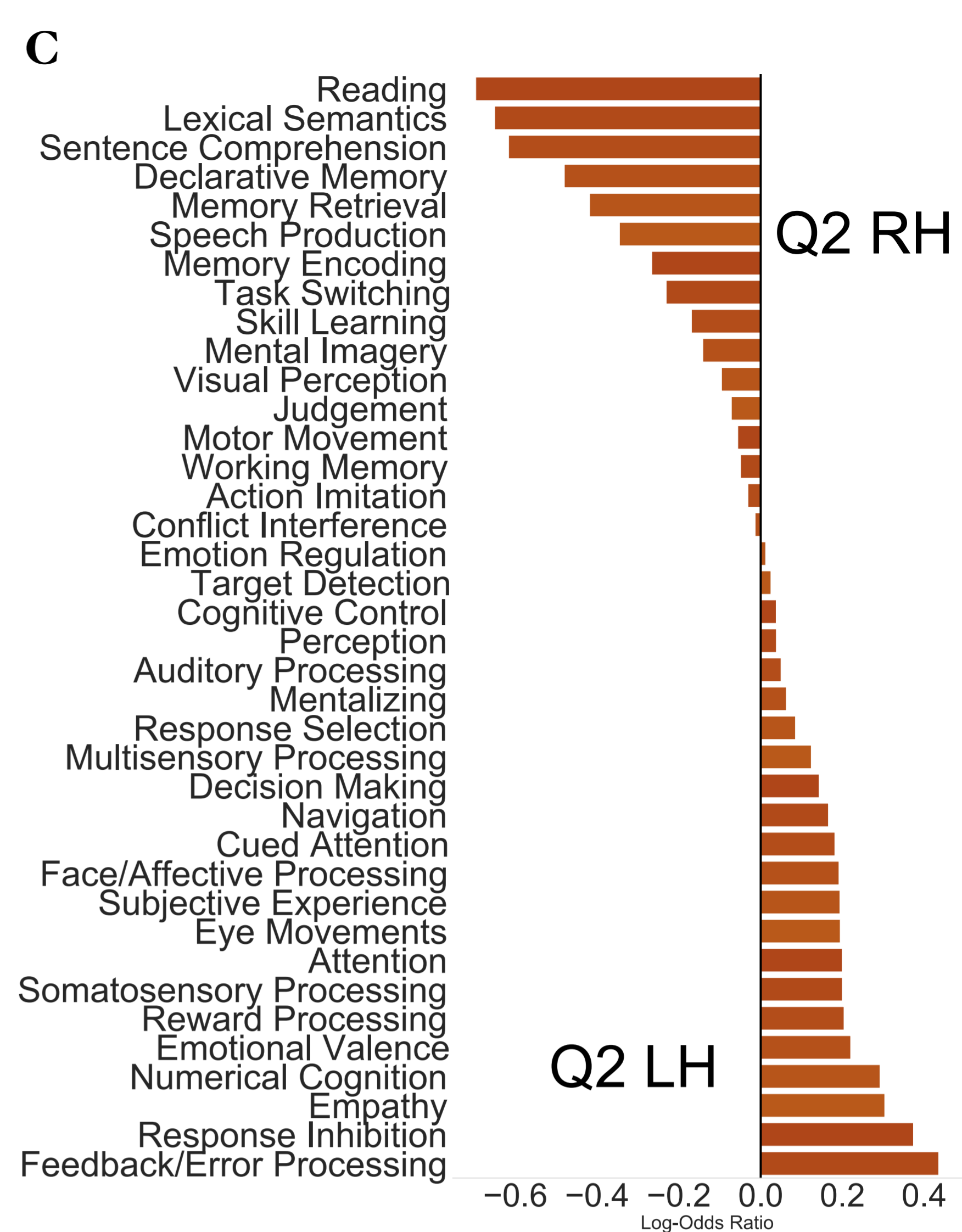
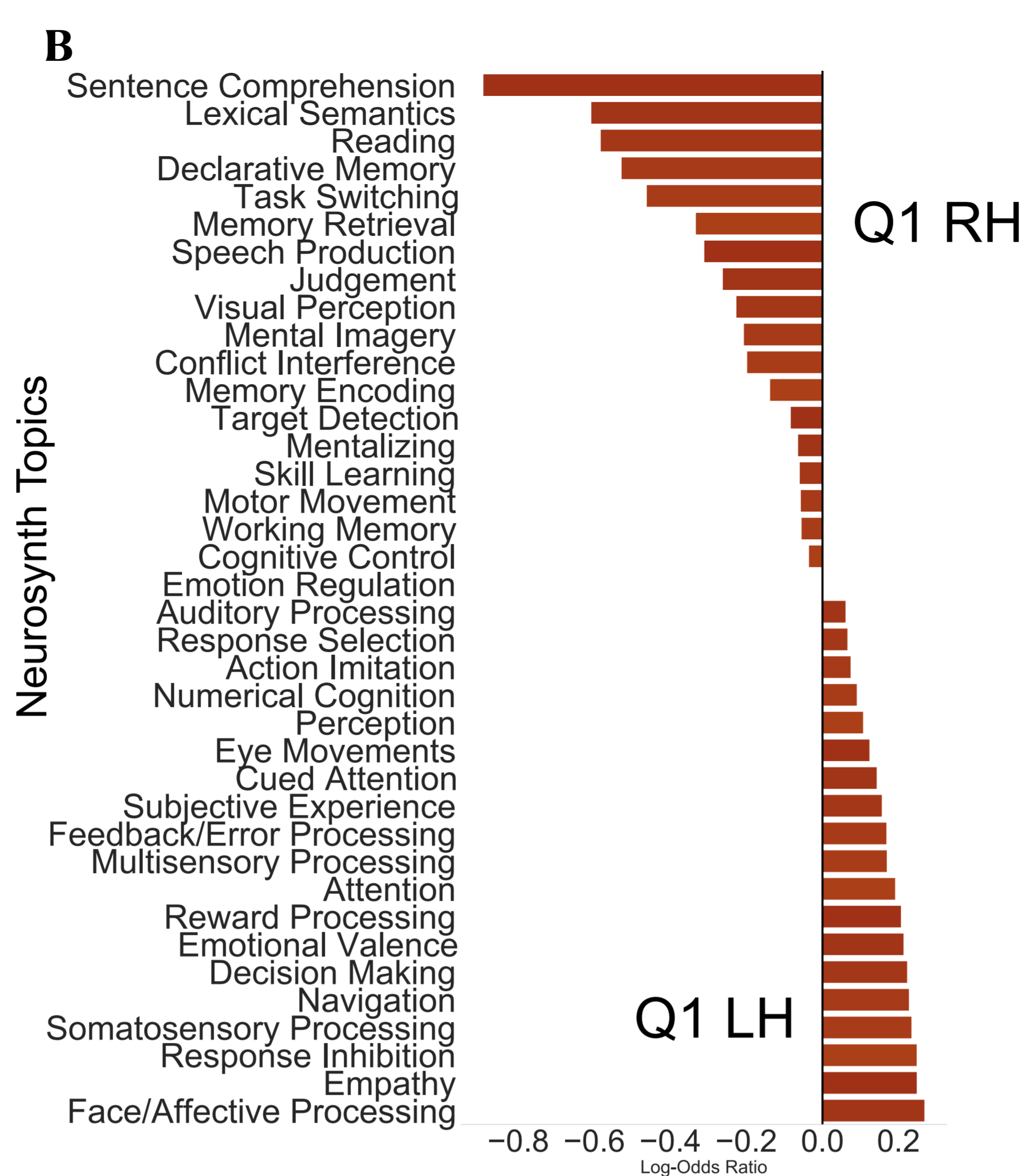
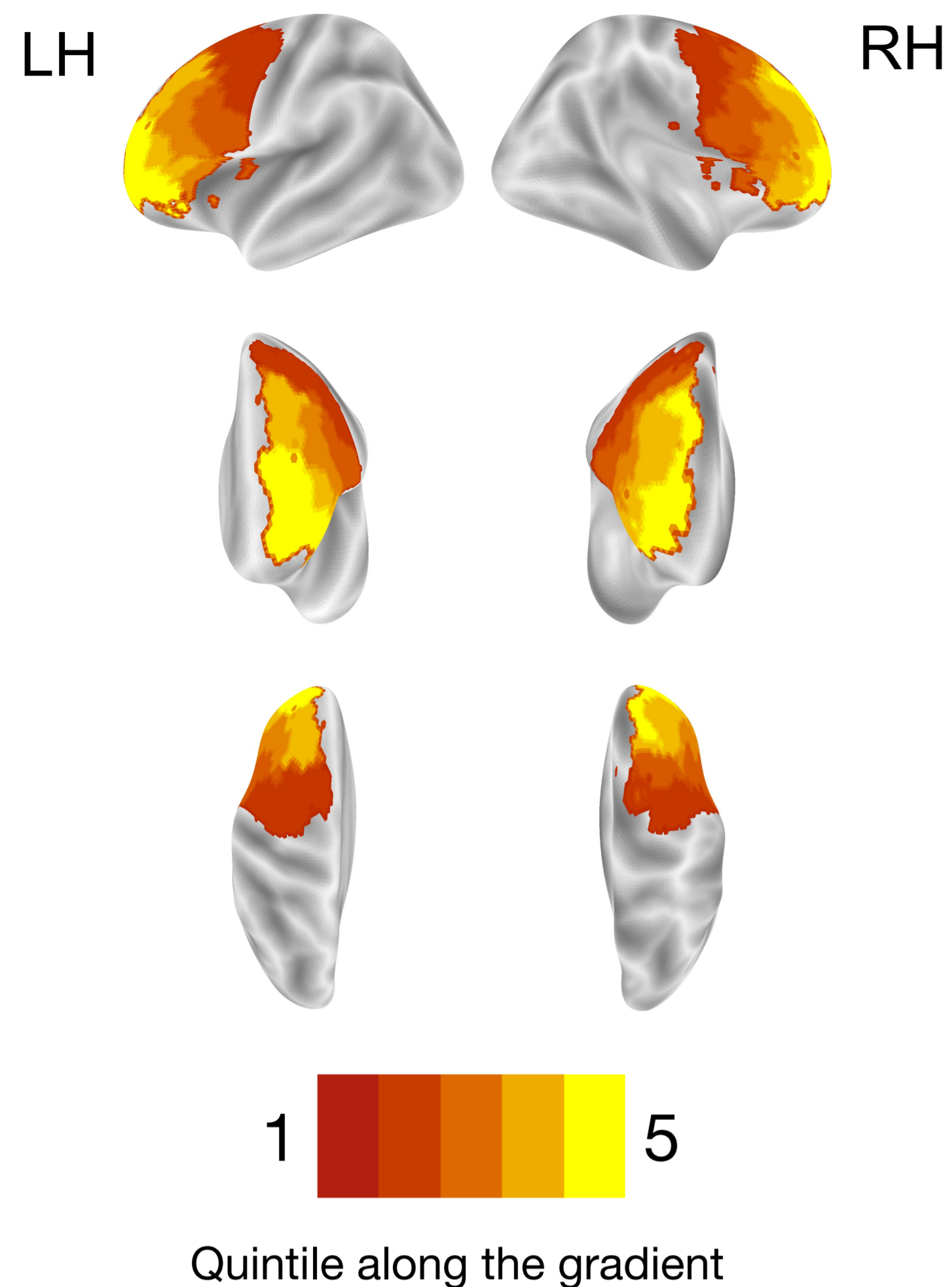
**B****Bins 1-5****Right Hemisphere**
Coactivation Patterns

Network Overlap

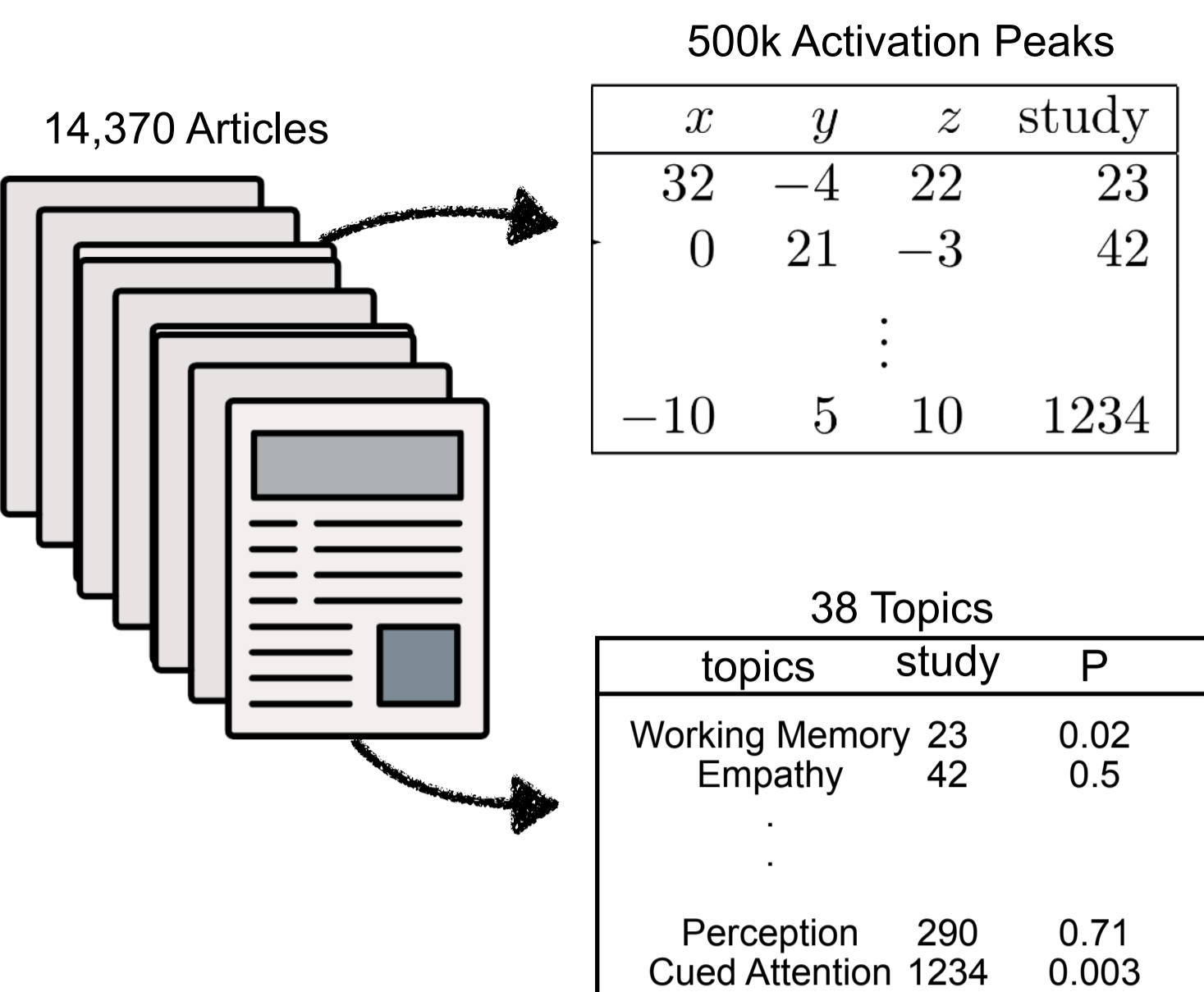




A Rostro-Caudal LPFC Gradient



A Neurosynth database



PeakReported

LateralPFCVoxel

NeuroLang

LateralPFCRegion

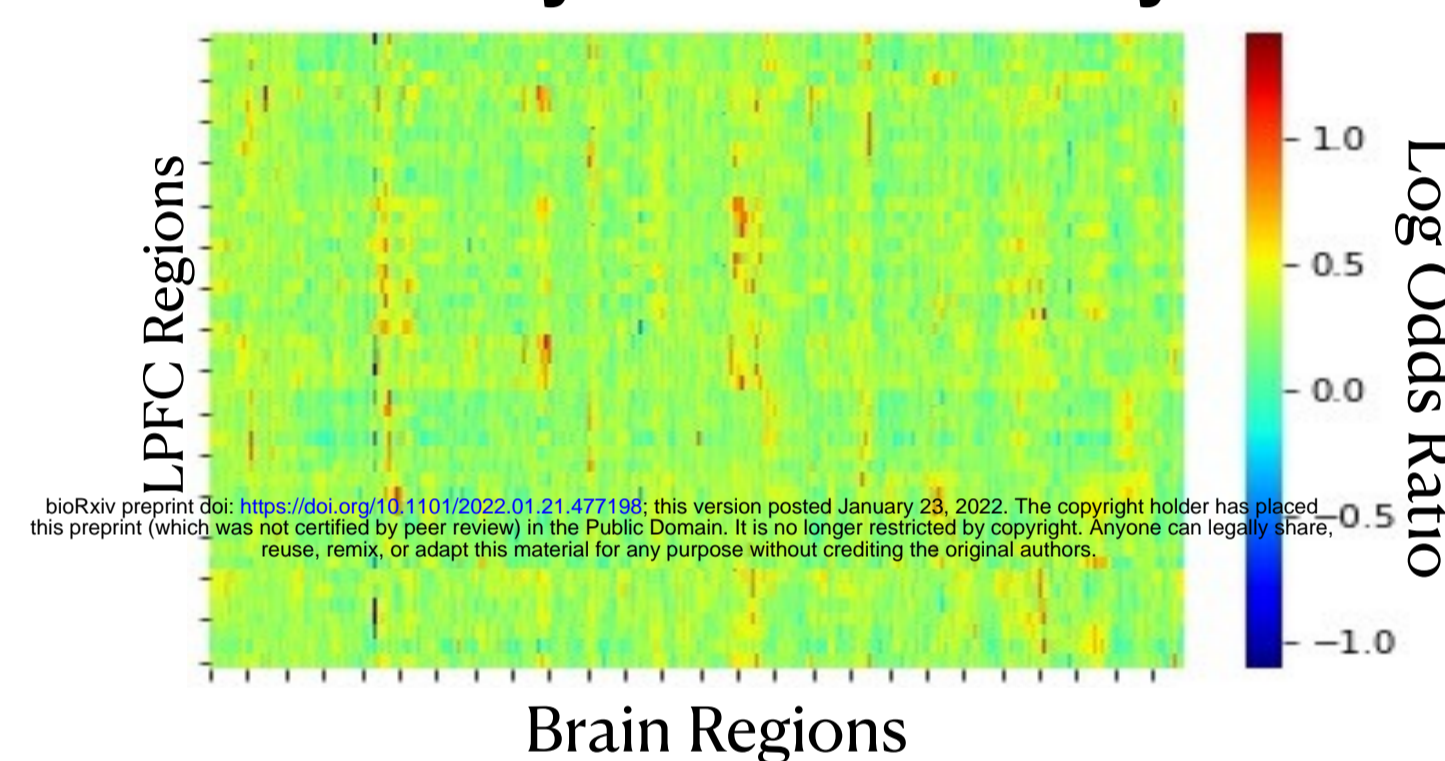
RegionVoxel

TopicInStudy

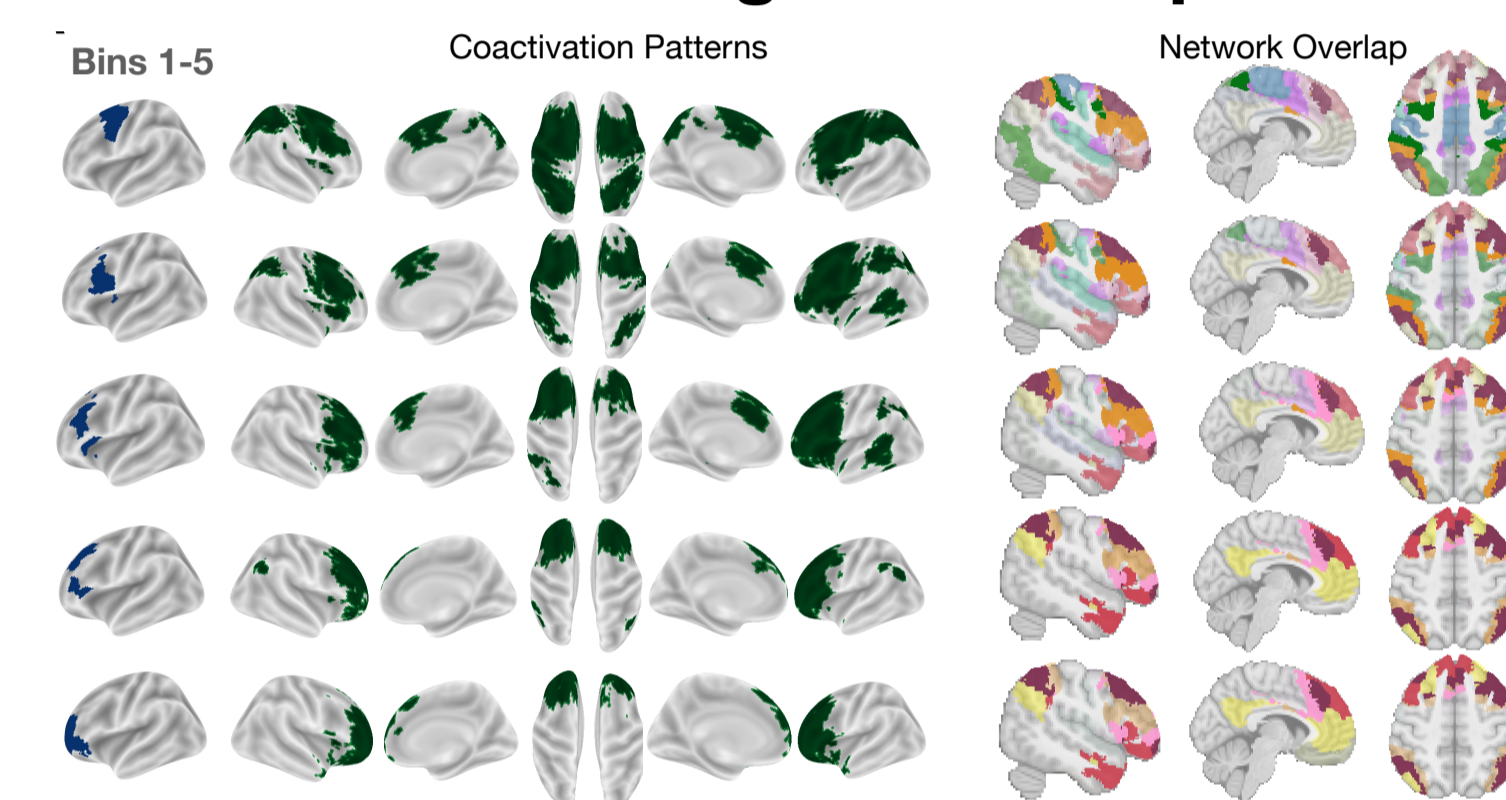
Functional Atlas

1024 Regions

Meta-Analytic Connectivity Matrix



Coactivation Patterns Along the Principal Gradient

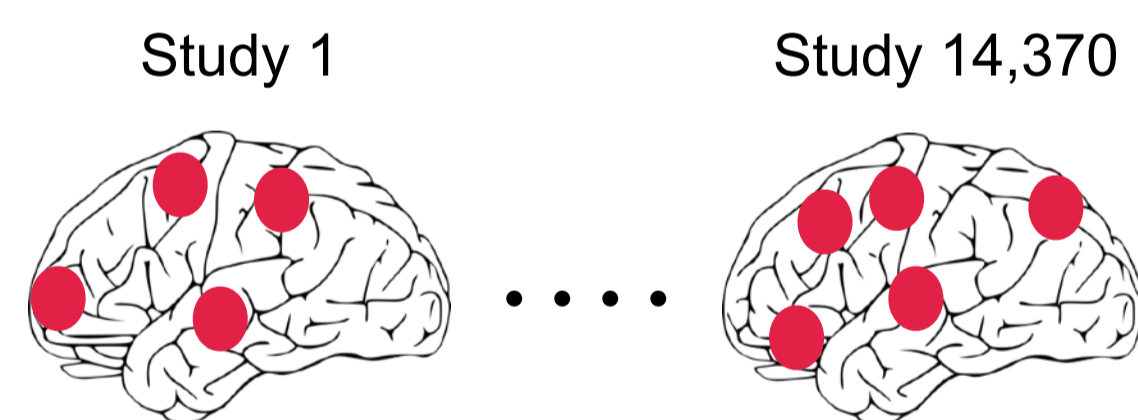


CoactivationPatternLeftBin

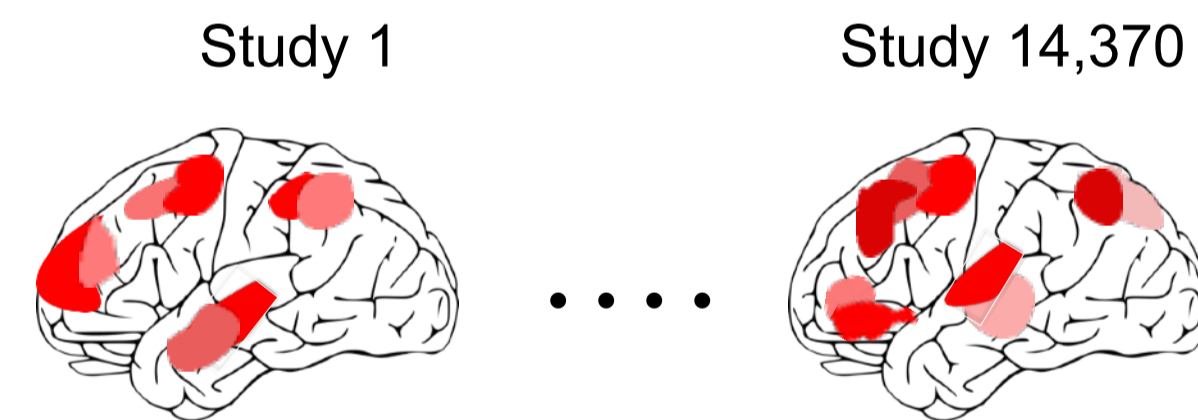
MetaAnalyticConnectivityMatrix

B

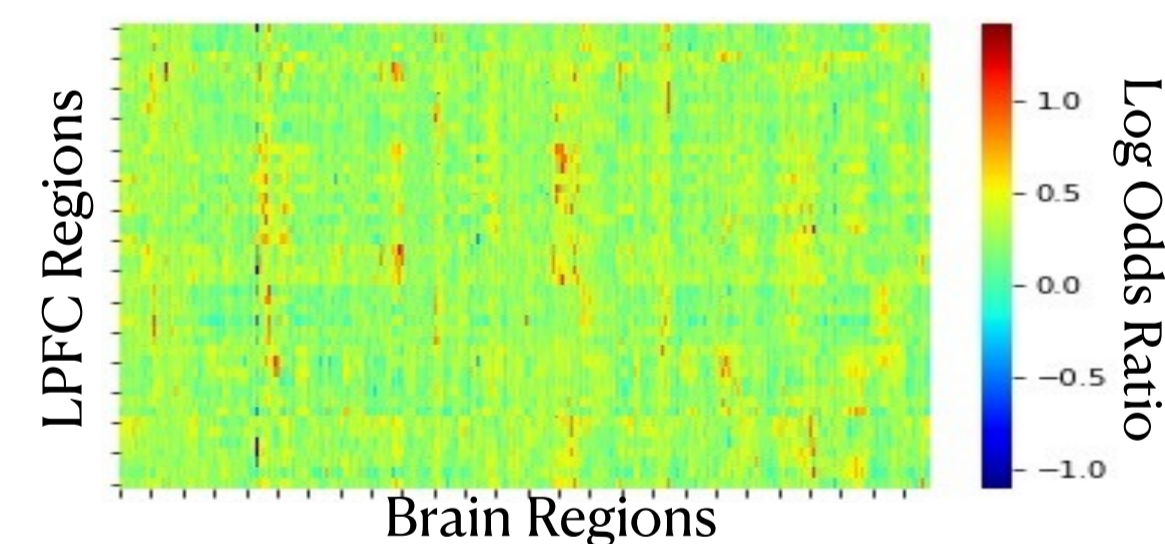
1 MKDA (radius = 10 mm)



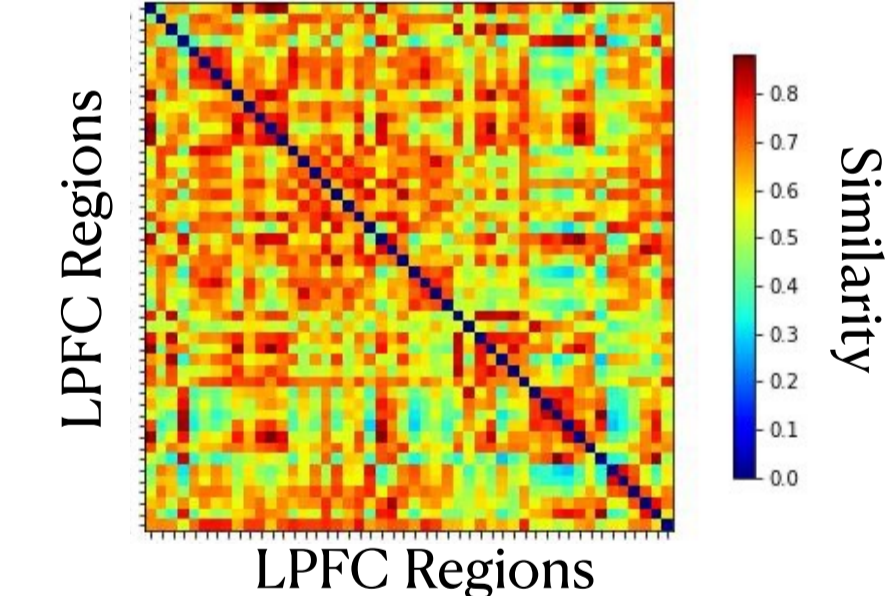
2 Projection onto 1024 Regions



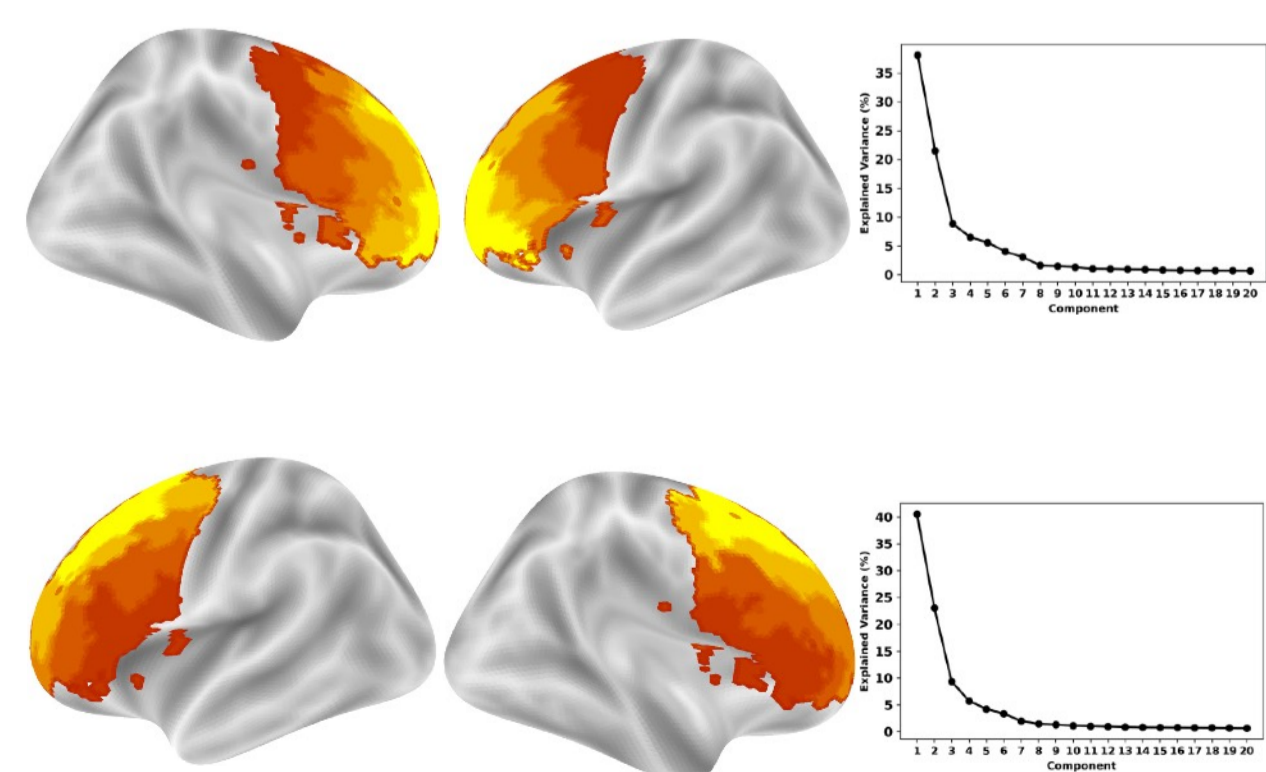
3 Meta-Analytic Connectivity Matrix



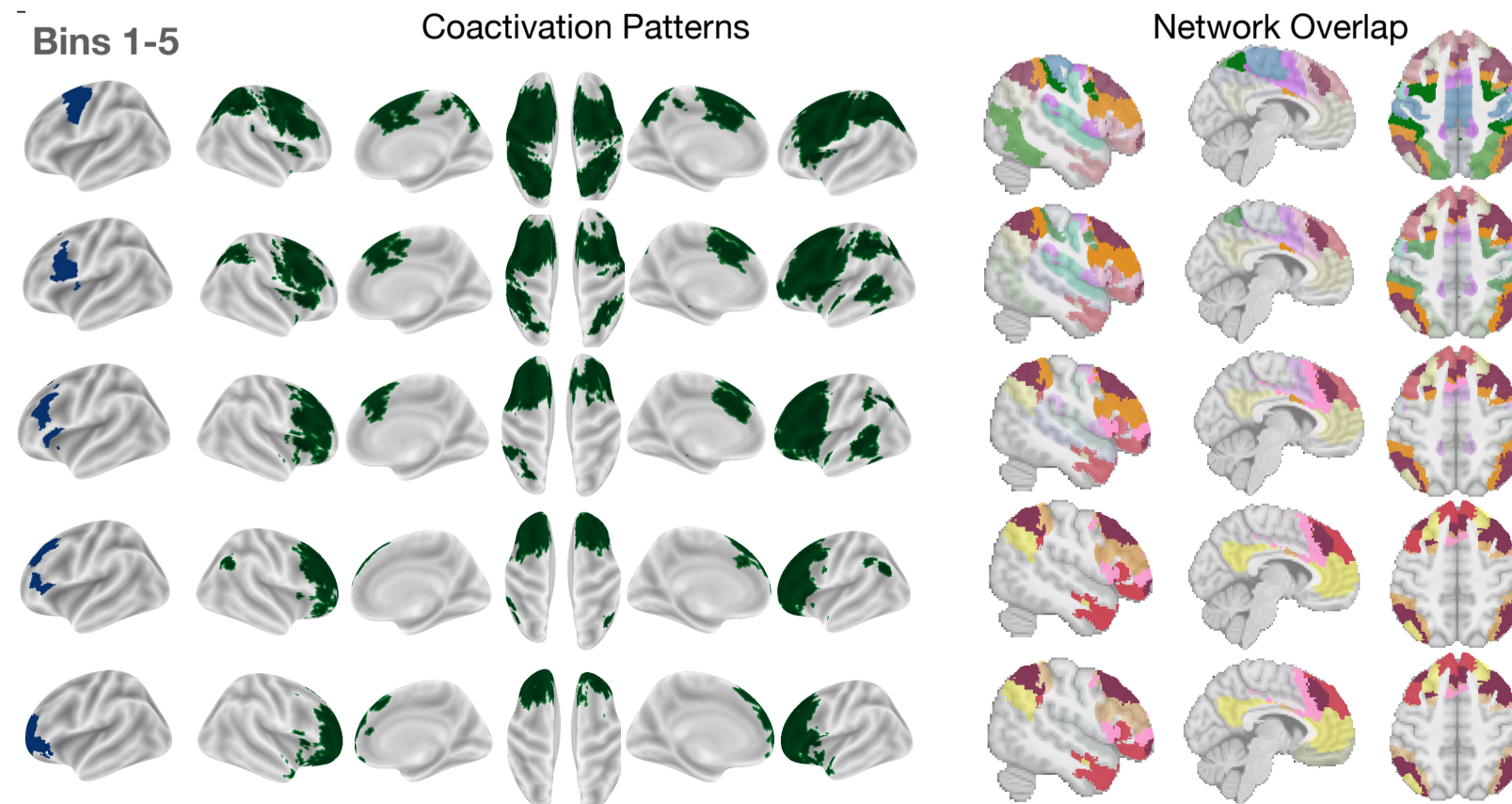
4 Eta-Squared Similarity Matrix



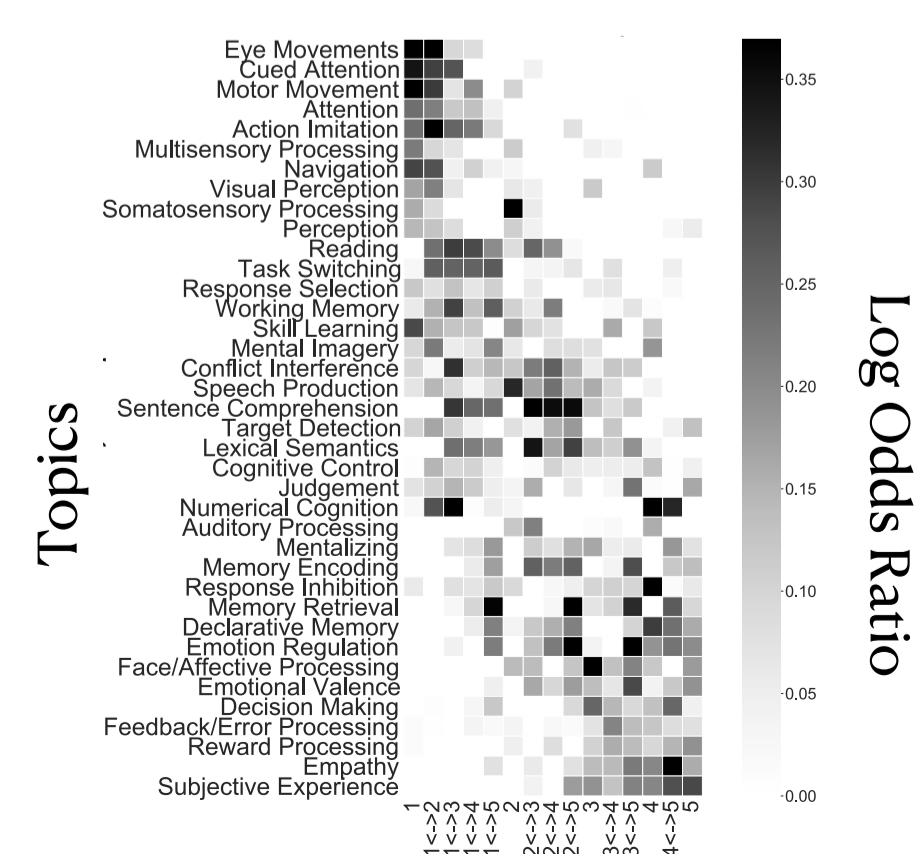
5 Gradients Extraction with Diffusion Embedding



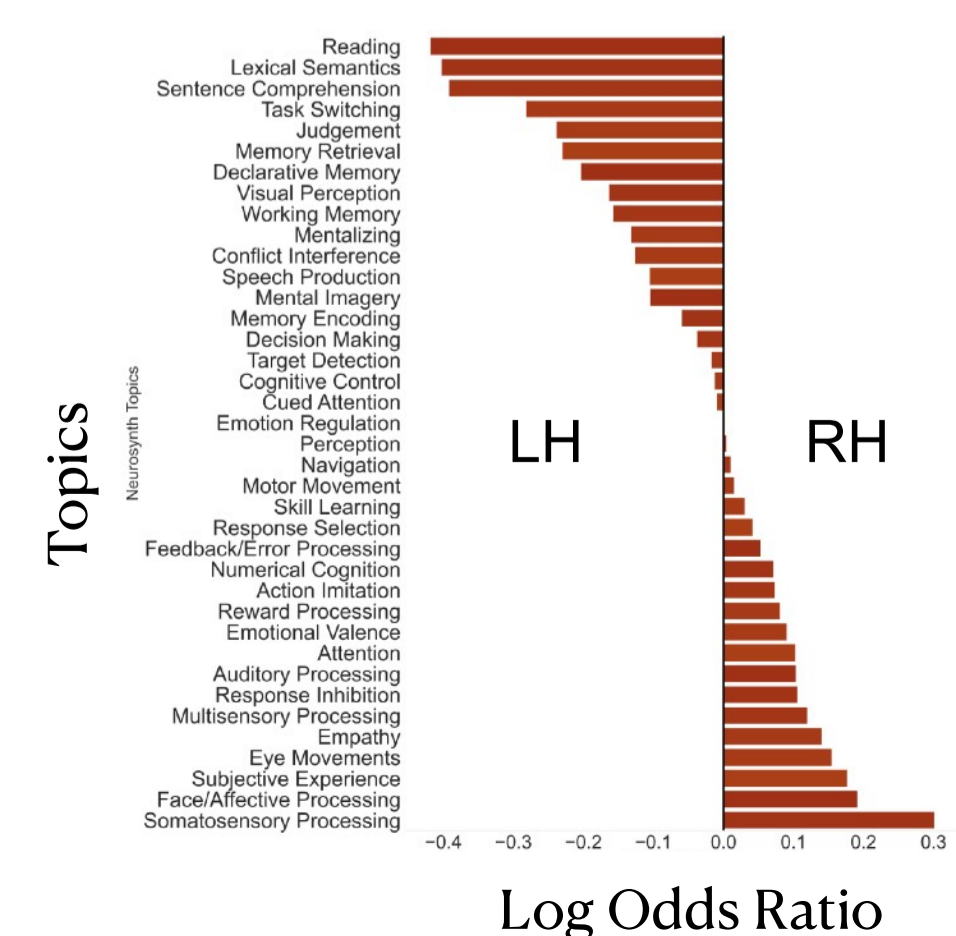
6 Coactivation Patterns Along the Principal Gradient



7 Topic Associations Along the Principal Gradient



8 Gradient-based Hemispheric Asymmetries



Activation Pattern Along the Gradient